



# Characterizing Interwoven Materials:

## Testing and Modeling Textile Roots

# Characterizing Interwoven: Testing and Modeling Root-Based Textiles

## Chair:

Prof. dr. Elvin Karana  
Sustainable Design Engineering

## Mentor:

Dr. Sepideh Ghodrat  
Sustainable Design Engineering

## Collaborators

### *Interwoven Creator*

Diana Scherer | <http://dianascherer.nl>

### *Materials Science Consultant*

Prof.dr.ir. Leo Kestens  
Department of Electromechanical, Systems  
and Metals Engineering  
University of Ghent, Belgium

Submission Date:

08 July 2021

## Author:

Israel Carrete

This project is a collaboration between Diana Scherer, creator of Interwoven and the Materials Experience Lab at the Technische Universiteit Delft. It is under a non-disclosure agreement with Diana Scherer, so some results and processes are only included in a confidential appendix.

## Acknowledgments

This project would not have been possible without the permission of Diana Scherer, whose creativity and passion for both nature and textiles led to the creation of Interwoven. I would like to thank her, first and foremost, for allowing me to take part in such an interesting journey and dip my feet into the world of characterizing grown materials. Next, I would like to thank my supervisory team, Elvin Karana and Sepideh Ghodrat. The support and guidance given throughout the project was more than I could wish for. I really enjoyed working with both of you.

My gratitude to Damien and Jiwei, as well, for guiding me through the Interwoven process and giving me tips along the way. Finally, I want to thank my support network, without whom this journey would not have been possible. Thanks to my friends, old and new, that all contributed in one way or another.

Más que a nadie, gracias a mi familia: por el esfuerzo común que me trajo hasta acá y todos los sacrificios que me abrieron el camino. Gracias

**Gracias a mi Tío Beto. Por ayudar a cumplir el sueño de ser diseñador.**

Dedicado a Pedro...

## Executive Summary

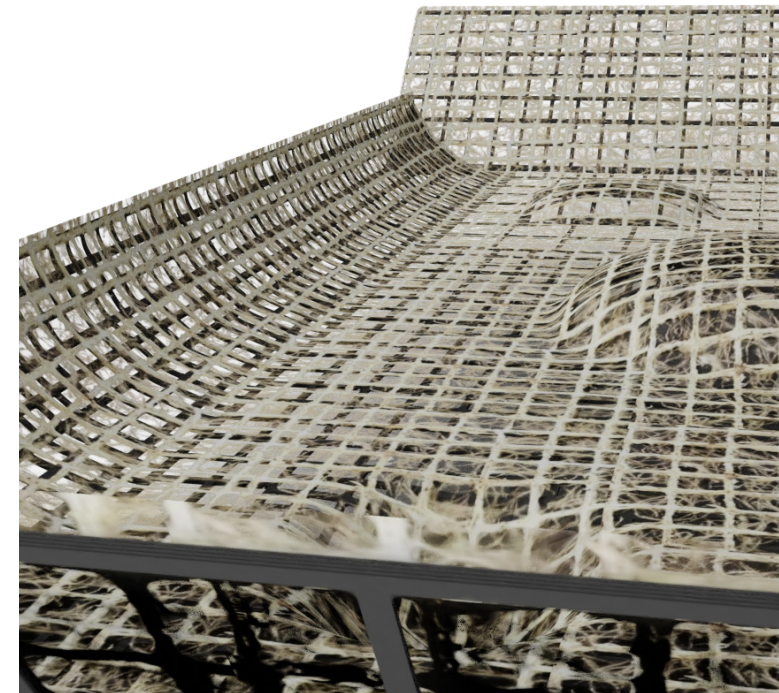
Interwoven refers to material structures made by growing plant roots into man-made patterns. Originally developed as an art piece to demonstrate root intelligence and bring attention to human-nature relations, Interwoven shows the potential to disrupt various commercial industries, especially as textile-based natural fiber reinforcements for composite materials. The artist that created Interwoven, Amsterdam-based Diana Scherer, started a collaboration with the TU Delft Faculty of Industrial Design Engineering to help further develop Interwoven from an art piece to a sustainable material for products design. Following the Material Driven Design method (Karana, et al., 2015), two students have identified materials experience opportunities created by Interwoven materials, the mechanical properties and internal structure of Interwoven are still not fully understood.

This study tackles the challenge of performing a technical characterization on Interwoven structures in an effort to correlate processing parameters to its structure, properties, and performance. It is known from past works that Interwoven is fragile and “weak”, but a quantified value for these terms serves as a point of comparison with other materials in the market. To determine these values, a series of tensile tests were performed

on grids with a simple square pattern. Dynamic Mechanical Analysis (DMA) tests performed on single roots proved that the amalgamation of roots that make up an Interwoven structure do not efficiently transfer tensile loads since the tensile strength and elastic moduli of Interwoven samples were nearly two orders of magnitude lower than those of a single root. Load transfer between roots was improved through the design of natural fiber-reinforced composites (NFRCs). The (bio)-polymer matrix used for these NFRCs was made up of agar gel, which improved the tensile properties of Interwoven samples, but was still lower than the single root.

A full characterization of a material correlates the observed properties to the structure of the material, which is done through the use of microscopy. Microscopic analyses were performed on all the tested samples to find any correlation between the observed tensile properties and the structure of Interwoven samples. In addition to providing insight about the complex interactions of roots as they form the patterns that they grow into, the microscopy also revealed that there is a direct correlation between the number of root tips (root endings) present at the intersection of squares in the grid and the mechanical properties of the sample.

With further research, this result can be tied to a parameter that the designer has direct control of, giving them better control of the properties of their Interwoven structures. Varying cell size in square patterns also allows designers to create structures with locally varying properties. The correlations between design parameters and material strength are summarized in the **Guidelines to Designing with Interwoven** booklet. A material demonstrator was also designed to showcase the locally variable mechanical properties in one structure while summarizing the test results in a way that is accessible and easy to understand.



# Contents

Executive Summary	iv	Composite Design	29
<b>1 - Project Description</b>	<b>1</b>	Matrix Composition	30
Introduction	2	<b>Fabrication Parameters</b>	<b>31</b>
Interwoven	2	Pre - Processing	32
Root Intelligence	5	Post-Processing	33
<b>Project Scope</b>	<b>7</b>	<b>4 - Characterization</b>	<b>34</b>
<b>Approach</b>	<b>8</b>	<b>The Importance of Characterization</b>	<b>35</b>
<b>2 - Literature Review</b>	<b>10</b>	Overview	35
Material Taxonomy	11	What is Characterization?	35
Growing Design	12	<b>Understanding Mechanical Properties</b>	<b>36</b>
Textiles	14	<b>Root Orientation Tests</b>	<b>38</b>
Composite Materials	17	Purpose	38
3D Printed Specimens	19	Testing Procedure	39
Characterization	20	Results	39
Literature Review Takeaways	22	<b>Experiential Characterization</b>	<b>48</b>
<b>3 -Tinkering with Parameters</b>	<b>23</b>	Setup	49
Material Parameters	24	Results	51
Design Parameters	26	<b>Interwoven Composites</b>	<b>54</b>
Template Pattern	27	Chosen Parameters	54
Template Design (abridged)	28	<b>Grid Cell Size Tests</b>	<b>55</b>
		Results	57
		Conclusion	58

## Root-Agar Composites

Purpose

Procedure

Results

Discussion

Conclusions

## 5 - Material Demonstrator 68

### Parameter Overview

Material Demonstrator

Designing the Demonstrator

## 6 - Conclusions 76

### Conclusions

Recommendations for Future Works

Final (Personal) Reflections

### References

## 7 - Appendices 83

59 Appendix A: Interwoven

59 Parameters (Full) 84

62 Appendix B: Technical

65 Characterization Tests 88

67

B-1 Dimensional Calibration Test 88

B-2 Tensile Tests on Control Group 95

B-3 Grid Cell Tests (Extended) 103

B- 4 Single Roots Tests (DMA) 107

### B-5 Root-Agar Tests 115

Procedure 115

Results 118

Comparison Across All Sample Sets 120

### Appendix E: Project Brief 123

# **1 - Project Description**

# Introduction

Humans' ability to transform natural resources to better serve their needs has led to the innovation of materials, tools, and products throughout history (Kozlowski et al., 2009). However, the presence of nature within modern products is hardly evident anymore. Oil-based plastics synthesized from fossil fuels are so out of the natural that bacteria cannot decompose them easily (Liboiron 2016). This is one of the reasons discarded plastics have accumulated and made their way into the oceans (Jambeck et al. 2015).

Concerns for the environment's health have entered the public conscience over the last decades in such a way that scientists and artists alike are finding ways to get involved. Diana Scherer, an Amsterdam-based artist, is giving human-nature collaborations a modern spin with Interwoven. Interwoven (seen below) is a textile-like material structure grown from oat roots in a method developed by Scherer.

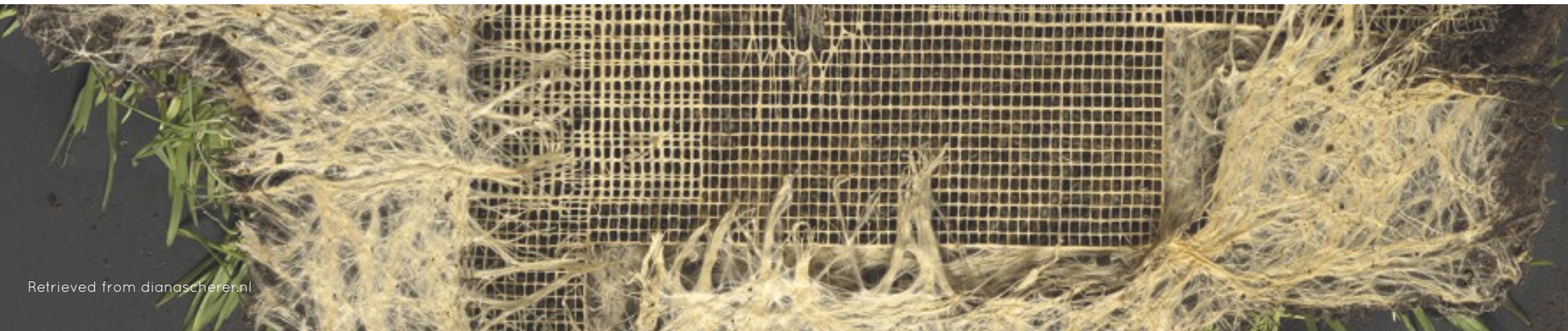
Interwoven manipulates the path in which roots grow into digitally designed patterns. Yet despite any manipulations from Diana, there is always some ambiguity with the product's growth, which makes the product more of a collaboration with nature. In fact, the presence nature is evidenced completely considering the leaves that are still seen on the material.

## Interwoven

Though it started as an artistic piece meant to begin a dialogue about humans' manipulative relationship with nature, Interwoven has the potential to disrupt various industries as a sustainable alternative to other materials. Scherer understands this potential and wishes to turn Interwoven into a marketable product, which is why she started a collaboration with TU Delft in 2019.

Previous works under this collaboration have explored Interwoven's potential to create structural hybrids/composites (Zhou, et al., 2021; Ford, 2019), but its properties are not yet fully understood. If a scale-up is to successfully introduce Interwoven as a viable material alternative, it is important to understand what these structures really are and how they function first.

Figure [1.1]: Interwoven mat with grids



## Rootsystem Domestication

Interwoven is a textile-like material structure grown out of plant roots. Diana Scherer, an Amsterdam-based artist, developed the method for domesticating roots and growing them into patterns that she designs. The development of Interwoven started with the photography collection, **Nurture Studies** (Fig. 1.2) in 2012, where Scherer noted the way in which plant roots took the shape of the container they were in. Through experimentation, she developed a process in which the same principle is applied to manipulate roots into growing in the shape of a mold.



Figure [1.2]: Nurture Studies (2012) (Scherer et al., 2012)

This root domestication process became what is now known as Interwoven by 2016. An early example of Interwoven was a dress: the Rootbound: Exercises in Rootsystem Domestications series (Fig. 1.3), which was exhibited at the *Fashioned from Nature* exhibition in Victoria & Albert Museum. The interest that placed Interwoven in that museum is only a taste of the potential that Interwoven has to disrupt various industries as a sustainable alternative.



Figure [1.3]: Rootbound #2 for the exhibition *Fashioned from Nature* Victoria & Albert Museum (retrieved from [dianascherer.nl](http://dianascherer.nl))

## Root Functions and Systems

For a material that is made up of roots, a basic understanding of roots' functions and anatomy is imperative. Roots serve multiple purposes for plant organisms - anchoring, water absorption, mineral absorption and storage, and transportation of minerals to other parts of the roots. Although the purposes are the same for different plants, there are two different root systems depending on whether the plant is a monocotyledon (grasses) or dicotyledon (flowers, etc) - a fibrous root system, and a taproot system, respectively. (Root - Definition, Types, Morphology, & Functions, n.d.)

Fibrous root systems are closer to the soil surface and form a dense network of roots with equal diameters, while taproots have one large root from which roots of a smaller diameter branch off (Smith & De Smet, 2012). For interwoven materials to have a somewhat uniform composition, the former root system is most relevant. More specifically, this work focuses on oat plants,

which are monocots and give dense root networks (Zhou, 2019b). Regardless, the root anatomy seen in **Fig. 1.4** applies.

### Root Anatomy and Growth

Root growth begins with the germination of a plant from a seed and does not necessarily have a termination point. Growth occurs at the bottom of the stem and is driven by the division of cells in root apical meristems. Roots are composed of concentric cylindrical tissues systems. From the outside in, these are the dermis system, ground system, and vascular systems (Hillis et al., 2013b).

The tip of the root has the root cap, which protects the apical meristem and lubricates the advancement of the root through soil. Above this section, the length of the root can be divided into the zone of cell division, zone of cell elongation, and zone of cell maturation. (**Fig. 1.4 - right**) The zone of cell elongation is above the root apical meristem and is the cause for the root pushing through soil, while the zone of cell maturation is where cells complete their differentiation. (Hillis et al., 2013a)

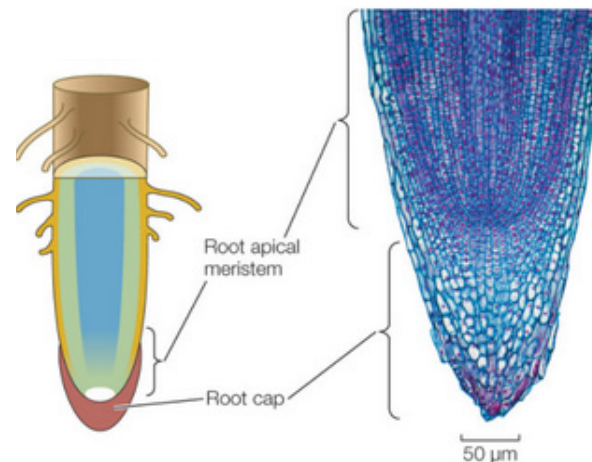


Figure [1.5] Structure of a root (left) and cell zones during growth (right) (Hillis, et al., 2013, Chapter 24.2)

zone of cell maturation

zone of cell elongation

zone of cell division

## Root Intelligence

The successful design of Interwoven molds (henceforth “**templates**”) is dependent on the typical behavior seen in roots when they come across an obstacle. In 2015, a study by Tan et al. found that roots actively seek for a way around an obstacle in the direction of gravity with a grow-and-switch response (Tan et al., 2015). Though gravity may define the main growth direction of a root, it is not the only stimulus that roots respond to.

Mancuso & Viola elaborate on this plant intelligence by identifying the nearly 20 “senses” that plants have which all uniquely influence growth direction in what is known as a tropism, or plant movement toward or away from a stimulus such as light (phototropism), gravity (gravitropism), water, and nutrients) (Mancuso & Viola, 2015). An example of two tropisms is seen in **Fig.1.6** where the roots grow in the direction of gravity and the plant grows towards a light source.

Many other studies suggest that, though they lack a central nervous system like animals, plants do respond to threats for the sake of survival (Trewavas, 2003; Trewavas, 2017). Scientists as far back as Charles Darwin hypothesised that the plant root behaves like the brain because growth decisions were made here in the search for nutrients (Baluska et al., 2009; “Root Apex Transition Zone: A Signalling–response Nexus in the Root,” 2010; Hodge, 2009).

The internal processes that a root undergoes to respond to external stimuli or search for nutrients is not yet fully understood, but it is clear that their function is both passive (in anchoring and internal nutrient transportation), as well as active (in the growth search of roots by extending through soil). These characteristics of roots give Interwoven materials a unique set of characteristics that was explored in previous projects that used the Material Driven Design (MDD) method.

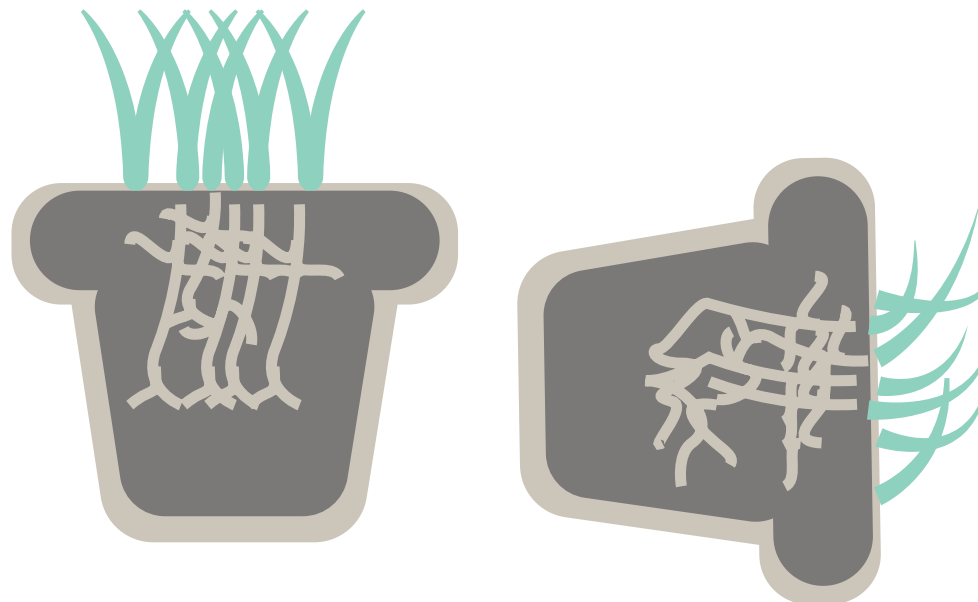


Figure [1.6]: Example of gravitropism and phototropism.

## Material Driven Design (MDD)

This work is a continuation of two projects performed under Scherer's collaboration with TU Delft. Both of these projects used the Material Driven Design (MDD) method seen in **Fig. 1.7** to explore the material experiences available with Interwoven structures.

The MDD method facilitates the design of innovative products with novel materials as the starting point. With this method, enables designers to design a material experience by incorporating technical characterizations, as well as experiential characterization, which is composed of sensorial qualities, emotions, interpretations, and the performative aspects (E. Karana et al., 2015).

The figure shows the four main steps of the MDD process: (1) Understanding the Material, (2) Creating Materials Experience Vision, (3) Manifesting Materials Experience Patterns, and (4) Designing Material/Product Concepts. Ford and Zhou followed the entire process and concluded that Interwoven invokes a connection to nature and sustainability, but from a technical standpoint, the root material on its own is too weak for application in product design (Ford, 2019; Zhou, 2019).

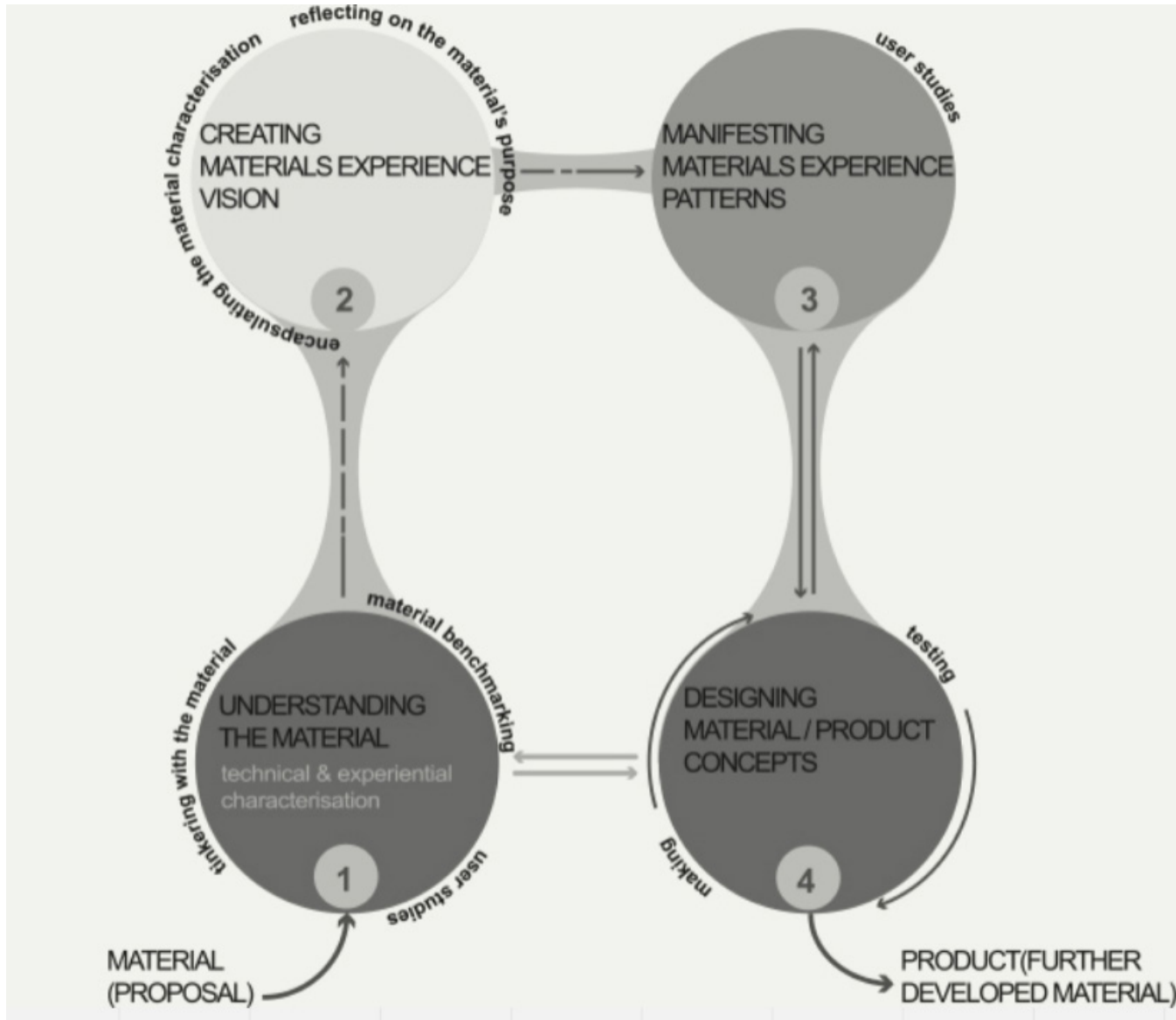


Figure [1.7]: Material Driven Design Steps (Karana, et al., 2015)

# Project Scope

This project continues the previous efforts to fully map the design space available when designing with Interwoven structures by focusing on the first step of the MDD method - Understanding the Material. More specifically, the technical characterization is the focal point. Some tinkering takes place and a preliminary experiential characterization is performed, but the aim of this study is to conduct a thorough technical characterization of Interwoven to identify ways of strengthening its inherent weaknesses.

If Interwoven is to become a feasible substitute for any existing materials in the market (whether this be limited to textiles or other sectors), its properties must be understood enough to be objectively compared with other materials. While the experiential qualities of Interwoven were explored by Zhou and Ford, the technical properties are not yet fully understood. With this in mind, the following goal was defined for this project:

*The goal of this project is to **characterize** the mechanical properties of Interwoven structures to facilitate practical applications in design.*

In this case, the definition of characterization is taken from its use in materials science. Characterization makes use of techniques such as mechanical tests, microscopy, among others, to make connections between a material's processing, structure, properties, and performance.

**Figure 1.8** demonstrates the relationship between these four elements and adds a fifth one to include the experiential characteristics found with the MDD method - elicitation.

For a technical characterization to be successfully performed on Interwoven, the mechanical tests performed must be standardized. Because Interwoven is a novel material, there are no existing standards for testing yet. However, these structures share some properties with other materials that can be considered analogous, and the testing methods for those can be used for guidance.

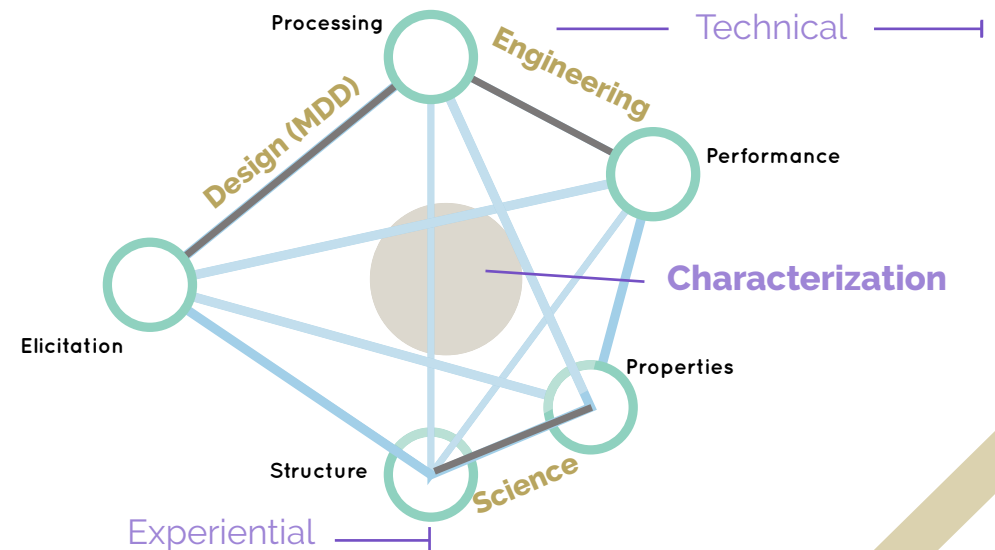


Figure [1.8]: Characterization Pentahedron

# Approach

Characterization correlates a material's processing, structure, properties, and performance. Processing refers to the design decisions made at the fabrication stage. For Interwoven, this includes the type of plant used and the growing process. The structure closely follows fabrication and includes root interactions and the pattern they grow into. The structure is usually identified with microscopy and is used to understand material properties (i.e. what is the typical response to an applied load? what are the limitations of the structure, etc.). Performance can be defined in many ways, but for the purposes of this report, it involves an Interwoven structure's response to tensile loads.

Interwoven is a collaboration with nature, meaning that there are some parameters that the designer cannot alter, such as plant growth rate. An abridged list of parameters under the designer's control are summarized in **Fig. 1.9**. The full list can be seen in Appendix A: Interwoven Parameters (full). They are divided into three categories: Material, Design, and Fabrication.

These parameters were used as the starting point for investigating the relevant literature and benchmarking Interwoven.

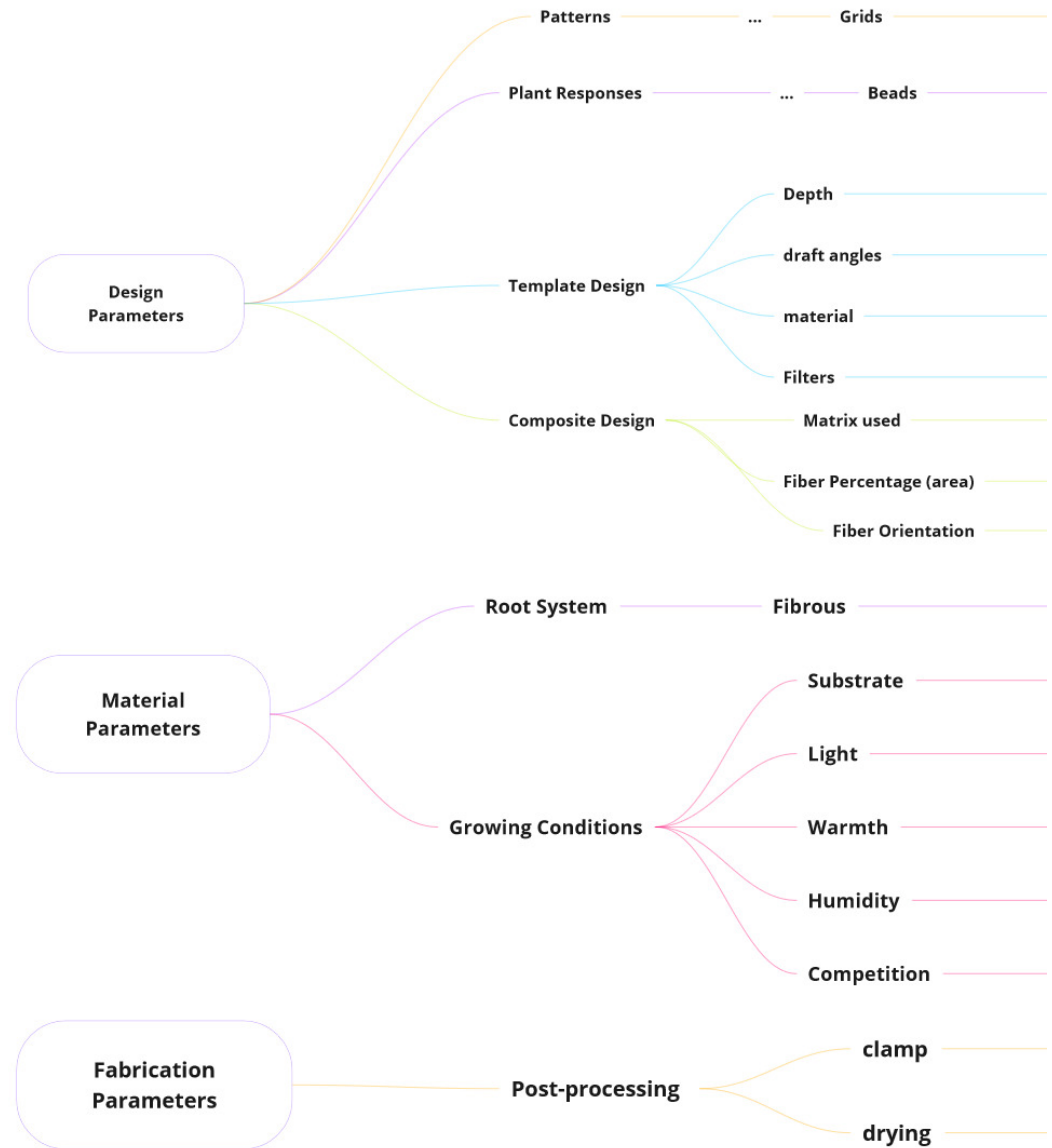


Figure [1.9]: Interwoven Parameters (abridged)

The scope of this project was decided based on the list of parameters in the previous figure. The works of Zhou and Ford served as a foundation and determined most of the material parameters. This work focuses mainly on the effects of *design parameters* on the properties, structure, and performance of Interwoven samples, given that this category of parameters is the one that the designer has most control over. From there, the approach

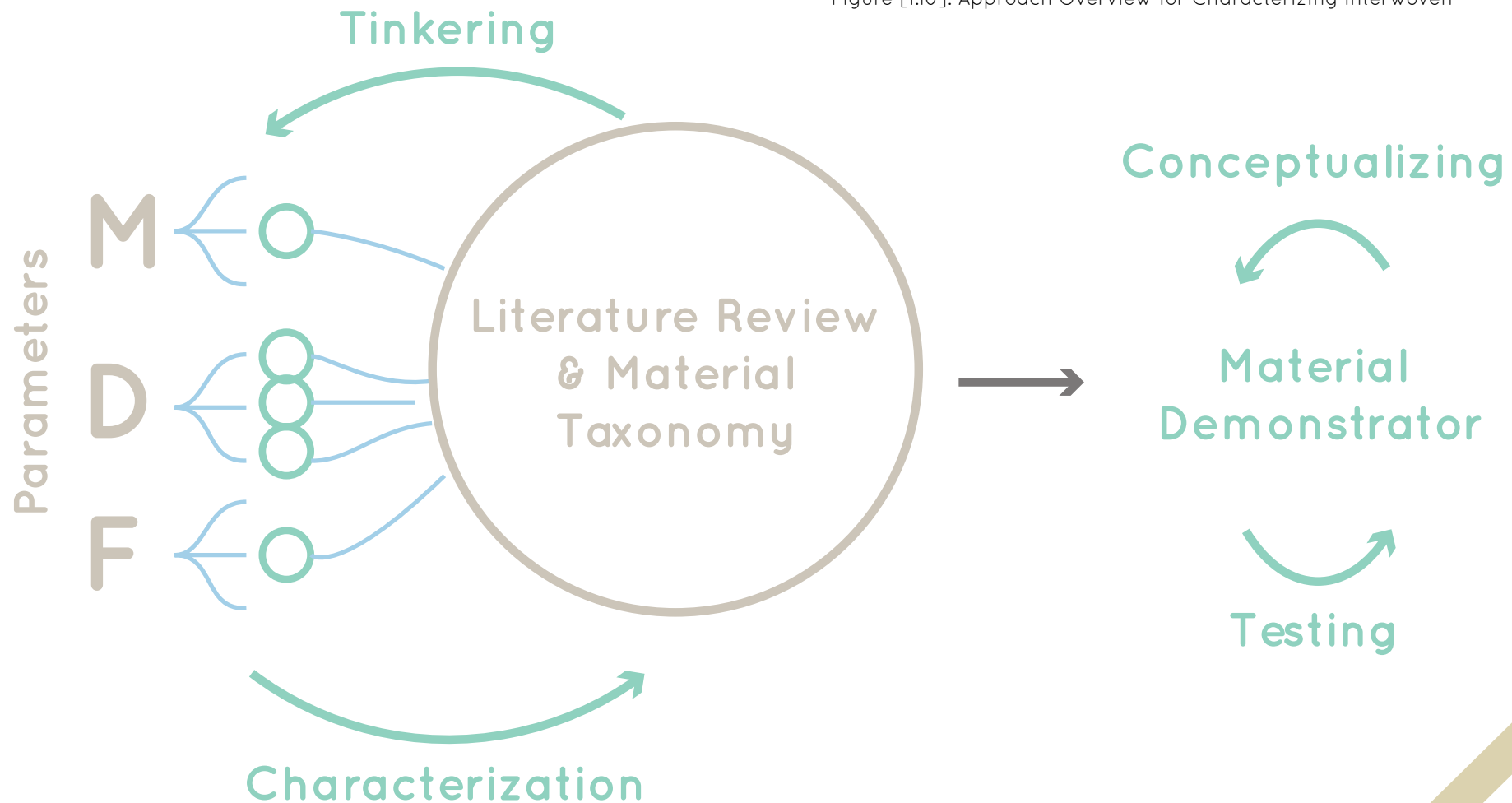
summarized in **Fig. 1.10** was used to characterize the mechanical properties of Interwoven and design a material Demonstrator.

The approach can be summed up by three interconnected stages: (1) Literature Review, (2) Tinkering and Exploration, and (3) Characterization (microscopy and tensile testing). Any identified characteristics that are unique to

Interwoven structures are then exhibited in a material demonstrator.

The initial stage of the approach - Literature Review revolves around the fact that Interwoven is a novel material, but it is reminiscent of various material classes. In an attempt to find a suitable testing method for Interwoven, these material classes are explored with some detail.

Figure [1.10]: Approach Overview for Characterizing Interwoven



# **2 - Literature Review**

# Material Taxonomy

If interwoven is to enter a market as a potential sustainable alternative, it must provide benefits that favor it over existing materials. At the time, the potential of Interwoven has not been fully explored, especially because it shares characteristics with various material classes.

At conception, Interwoven was used as a textile, so it can be compared to other **natural fiber textiles** like hemp or jute. Its nature-based production process places it in the category of **bio-fabricated materials**. The root patterns resemble fibered mats used in fiber reinforced composites, especially natural fiber-reinforced composites (**NFRCs**). The patterning of these structures lends itself to digital fabrication, so even parts that are 3D printed through fused deposition modeling (**FDM**) resemble Interwoven. An overview of the relations between each class and Interwoven are seen in **Fig. 2.1**.

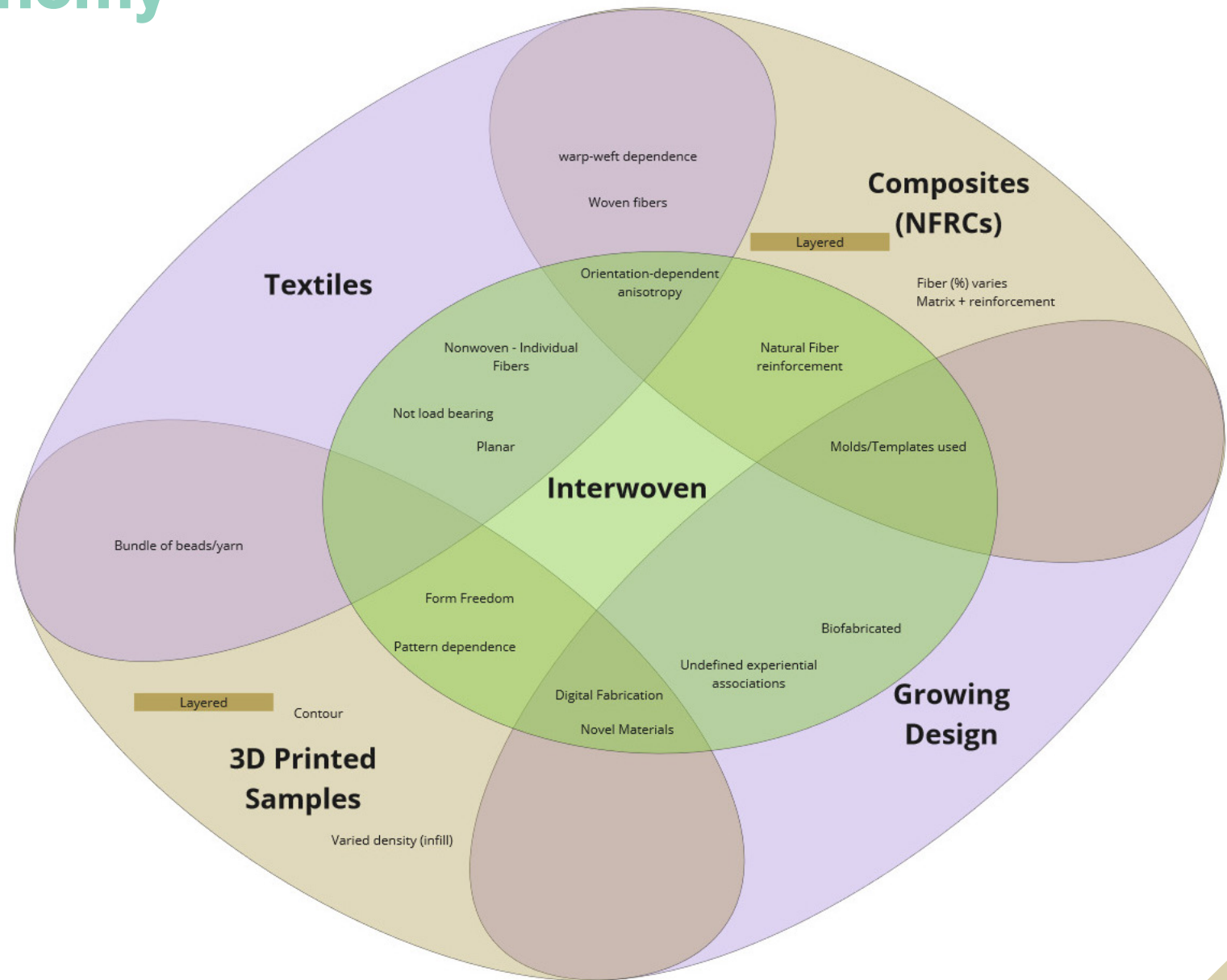


Figure [2.1] Similarities between Interwoven and other materials

## Growing Design

Out of the materials shown in the taxonomy above, there are two classes that are most obviously similar to Interwoven: bio-fabricated materials. The collaborative nature of Interwoven's production process classifies it under the umbrella of **biodesign**, which uses a combination of biology, design, and engineering to produce an artefact (Myers, 2012). A subsection of biodesign includes the direct growth of a material from a living organism, known as **Growing Design**, which offers a sustainable alternative to product design fabrication that uses synthetically

produced materials (Camere & Karana, 2018; Silvia-DforDesign, 2019).

An example of a bio-designed material that is successfully disrupting the industry is Ecovative's MycoComposite, which is a mycelium-based composite that was used to create a Styrofoam alternative with their Mushroom Packaging line seen in **Fig 2.2** (Saint, 2021). Since the production process of these composites entails growing mycelium components, it falls under the umbrella of Growing Design. While using a different material, the processing of this

product line largely resembles Interwoven and there is ample literature detailing the technical characterization of these mycelium composites (Appels et al., 2019; Ziegler et al., 2016).

That being said, mycelium-based biomaterials are not the only ones that exist. There are also products grown from algae, bacteria, or even a tree that was grown into an end product, like the chair seen below from the company Fullgrown.



Figure [2.2]: Ecovative's Mushroom Packaging (Saint, 2021)



Figure [2.3]: Ecovative's Mushroom Packaging (Front Page - Full Grown 2014)

The MIT Media Lab in the United States has also created a grown pavilion using living organisms. In this case, however, the organisms were not bacteria or vegetable-based, they were silkworms. In this Silk Pavilion (**Fig. 2.4**), a structure was digitally designed and silkworms were allowed to grow between into the structure, guided by the original scaffolding (Oxman et al., 2017). The resulting pavilion was a collaboration between designers and nature, much like Interwoven is. Biofabrication is something that the architect behind the Silk Pavilion has explored in various ways (Oxman 2015), but the ethos behind such structures is the potential to decrease carbon emissions from construction (Kirdök et al. 2019).

Beside being impressive to look at, designs like the Silk Pavilion or Ecovative's MycoComposites have been thoroughly tested for various conditions (Su 2015), clearly defining the areas in which these materials and structures can be successfully scaled up. One of the previous works followed a similar path and sought to explore the capabilities of Interwoven as a structural hybrid composite (Zhou et al., 2021).



Figure [2.4]: MIT Media Lab - Silk Pavilion (Oxman et al., 2017)

## Textiles

Given its original inspiration, the most obvious material class that Interwoven resembles is textiles. The inspiration behind Interwoven came from Scherer's background in fashion, so the connection to textiles is evident (Fig. 2.5). There are various classifications for textiles, depending on the type of fibers and yarn used to produce the fabric (T. Rowe, 2009). For the purposes of this text, the main distinction that will be made is that of woven and non-woven fabrics since these two are the ones used in natural fiber composites as well (Peças et al., 2018).

### Woven Fabrics

Woven fabrics use two sets of yarn (each composed of twined fibers) that go in directions perpendicular to each other - the warp and weft directions. Common examples of woven fabrics include denim and corduroy. The yarn types in these fabrics is defined by the way in which the fibers are aligned in the loom during the production of the textile, as

seen in Fig. 2.6. Yarn oriented in the warp direction is pulled under tension in the loom, while the weft fibers are woven and pressed into place.

The different treatment methods of each fiber gives rise to different mechanical properties. For example, fibers in the warp direction are taut in the direction of the loom, so pulling on them will not extend much more, while the fibers in the weft direction still has more room for deformation when pulled along the weft axis. The specifics of tensile testing for textiles will be detailed in the Characterization section of this report, but fibers in this category typically follow ASTM D5035 methods for determining breaking force and elongation.



Figure [2.5]: Rootbound for the exhibition *Fashioned from Nature* Victoria & Albert Museum

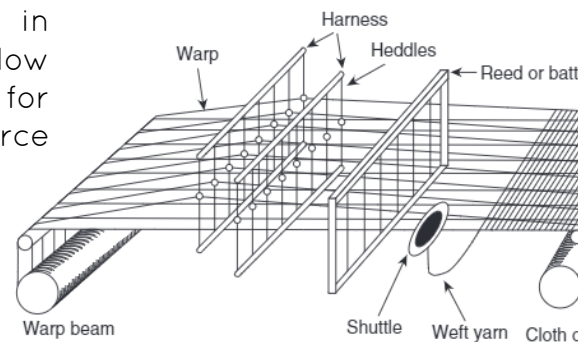
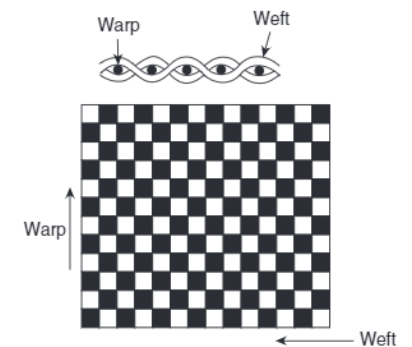


Figure [2.6]: Structure of woven fabrics (Adolph, 2009)



## Non-woven Fabrics

Non-woven fabrics (also known as fiberwebs) are made directly from fibers with uniform or random orientations that are bound together by mechanical needling, polymer adhesives, or heat (Adolph, 2009). Examples of these fiberwebs include cleaning wipes, dust cloths, and disposable bed sheets.

Unlike woven fabrics that have a network of yarn going in perpendicular directions that are tightly interconnected, non-woven fabrics' adhesion is dependent on whatever the binding mechanism is. As such, the mechanical properties of these will be very different, as is the testing method for finding these. Non-woven fabrics typically follow ASTM D5034 methods for finding the tensile breaking force and elongation. The procedures these methods and those of woven textiles are similar, save for the testing of both warp and weft directions seen in woven textiles. Non-woven textiles are often oriented in only one direction, or randomly, meaning that tensile tests focus on only one load orientation.

In Interwoven structures, roots maintain the patterned shape because of roots hairs that create friction between fibers (Hillis et al., 2013, Chapter 24.2). This friction acts as its own binding mechanism, similar to what is typically seen in non-woven fabrics. **Figure 2.8** shows a closeup of an Interwoven sample with aligned roots. Note that, despite weaving displayed by the roots to create the pattern seen, the definition given in the previous section does not apply. The lack of a clear warp and weft direction make the testing methods for non-woven fabrics more applicable for Interwoven structures.



Figure [2.7]: A common example of a non-woven fabric is seen in hospital bedsheets

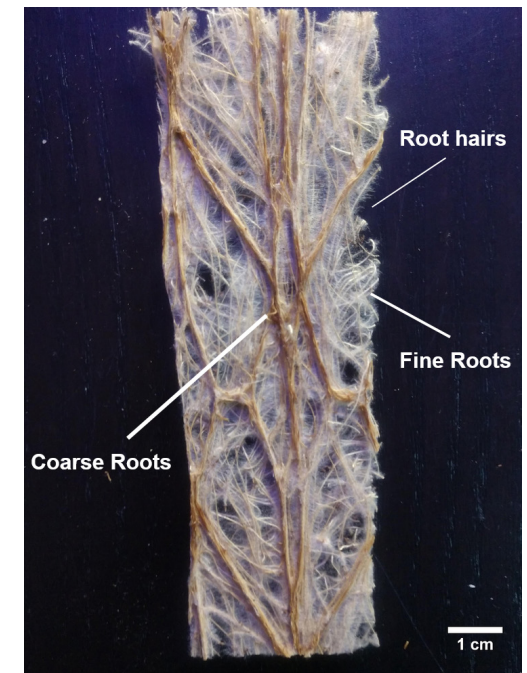


Figure [2.8] Interwoven structure that resembles non-woven fabrics.

## Electrospun Fabrics

Electrospun fabrics are another subsection of non-woven fabrics that resembles Interwoven structures. Recent years have seen the growth of the electrospinning methods to manufacture textiles at a nanoscale. Electrospun textiles are processed from a polymer solution that is spun with an electric field and collected on a substrate. A schematic of this is seen in **Fig. 2.9**. The result is a fabric composed of randomly oriented nanoscale fibers (**Fig. 2.10**), which makes it ideal for medical applications like scaffolding in tissue engineering or high efficiency filtration (H. Li & Yang, 2016). Advances in electrospinning technology has seen the introduction of natural fibers polymer-based fibers made from proteins or even

cellulose into tissue engineering due to biocompatibility (Haghi & Akbari, 2007; Vineis & Varesano, 2018). However, natural polymers are not easily formed at such a small scale, so they are often paired with synthetic polymers for processing.

Interwoven has structures have an irregular root formation that largely resembles these electrospun textiles. The combination of natural fibers with some sort of synthetic polymer for processing could also give rise to a new field of applications for Interwoven-based materials, such as composites. The following section delves into natural fiber-reinforced composites (NFRCs) to explore these possibilities.

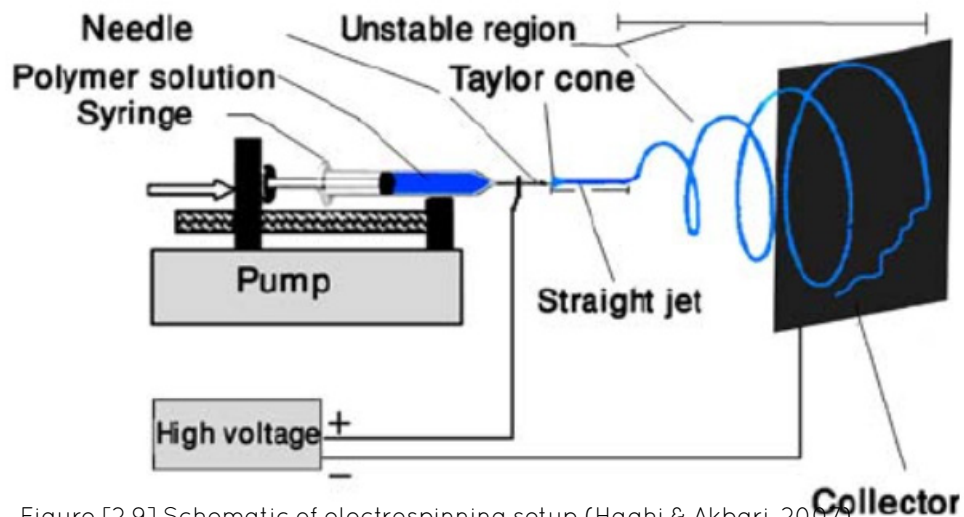


Figure [2.9] Schematic of electrospinning setup (Haghi & Akbari, 2007)

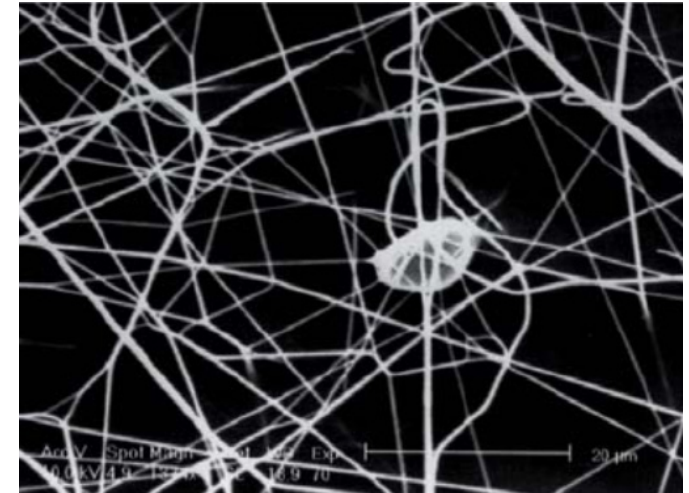


Figure [2.10] Electron micrograph of electrospun fibers (Haghi & Akbari, 2007)

## Composite Materials

Composite materials are those that use a combination of engineering materials (i.e. a metal and a ceramic, a polymer and a ceramic, etc). In these composites, there is usually a matrix and a reinforcing phase. The reinforcing component is typically a particle or a fiber that is embedded into the matrix, which binds the fibers in place. A schematic illustration of this is seen in **Fig. 2.11**. Reinforcements are often much smaller and stiffer than the matrix, but they have a lower density, whereas the matrix has good shear density and is able to distribute a load to the fibers efficiently. The combined properties of both result in more favorable properties than either of the two individual constituents (Courtney, 2005; Khumar, Y.K. & Singh Lohchab, D., 2016). An example of a composite is seen in **Fig. 2.12**, where a carbon fiber mat was molded into the desired shape in a polymeric resin matrix.

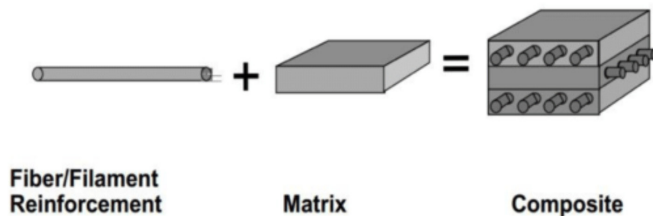


Figure [2.11] Schematic of the phases in a fiber-reinforced composite (Khumar, Y.K and Singh Lohchab, D., 2016)

## Natural Fiber Reinforced Composites (NFRCs)

Many polymer composites use ceramic reinforcers (such as glass fibers) to increase stiffness, but natural fibers are becoming an attractive alternative due to their reduced environmental impact (Bernava et al., 2015). The advantages of natural fibers as reinforcements are the biodegradability, abundance, low density, and CO<sub>2</sub> neutrality (in the case of cellulose-based fibers) (Carrete et al., 2020). Depending on the nature of the matrix, natural fiber reinforced composites (NFRCs) can be classified as a partly eco-friendly composite (if the matrix is not made from a bio-based or biodegradable material), or a green composite (if both constituents are derived from renewable resources). The source of the fiber also impacts the properties of the reinforcement. Natural fibers are classified into animal, plant (cellulose), or mineral fibers, but they can also be considered naturally occurring composites - especially plant fibers that are composed of cellulose fibrils embedded in a lignin matrix (John & Thomas, 2008; Kozlowski et al., 2009).



Figure [2.12] Carbon fiber-reinforced polymer.

The performance of NFRCs depends on many factors, including the relative amounts of each constituent (in %), fiber length, fiber orientation, and the compatibility of both constituents, known as the interfacial adhesion. (Peças et al., 2018; Ku et al., 2011). A common problem with interfacial adhesion (**Fig. 2.13**) stems from the hydrophilic tendencies of natural fibers and the hydrophobic tendencies of the matrix, whose properties could deteriorate in the presence of moisture (Malkapuram et al., 2009).

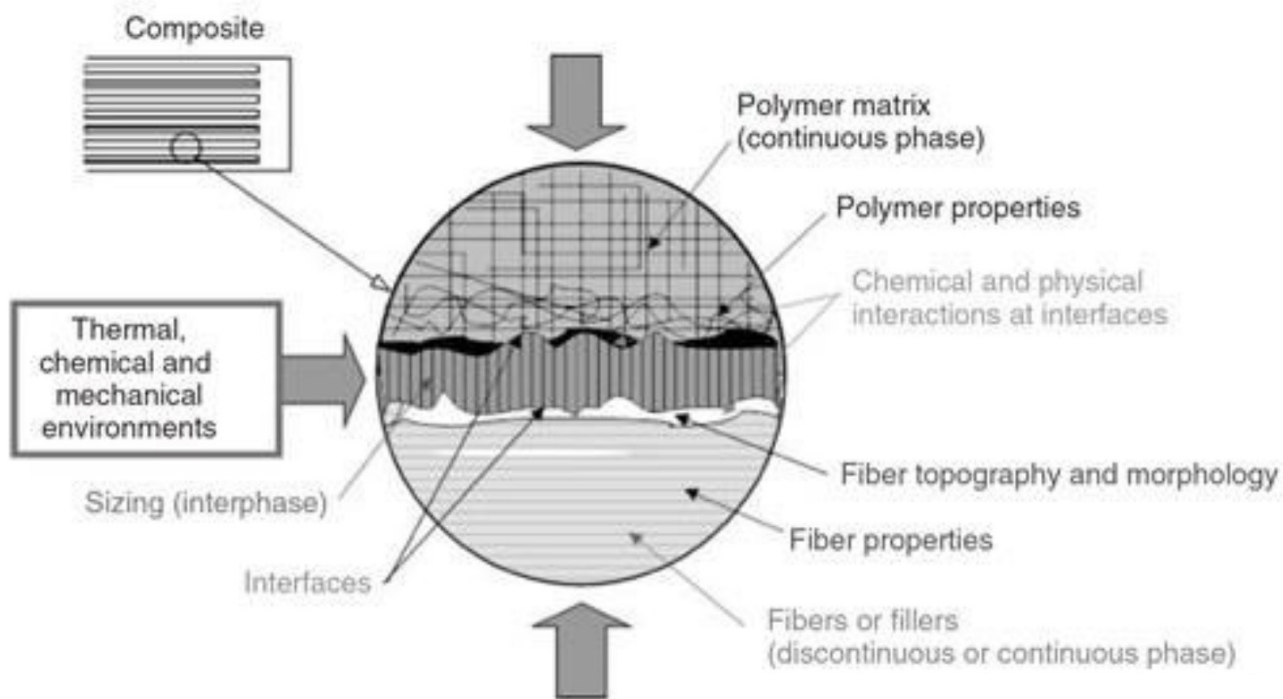


Figure [2.13] Example of what is meant by interfaces and interfacial adhesion. (Zuraida et al. 2018)

Another version of this same problem is seen when these composites are layered in laminates that do not bond to each other properly and delaminate in use (Chermoshentseva et al., 2016). Though continuous fibers (long fibers that run along the length of the matrix that are homogeneously oriented) increase mechanical properties in one direction, the material is left weak if the loading condition is not along the orientation of the fibers. This anisotropy of the aligned fibers is often avoided with short, discontinuous fibers that yield more uniform properties (AL-Oqla & Sapuan, 2014). Although

they are advantageous when regarding environmental impact, NFRCs are not as strong as those reinforced with glass fibers. Because of this, NFRCs are preferred for non-structural products, such as the interior of cars and other similar products in the automotive industry. (Cicala et al., 201

The roots in Interwoven structures can be used like reinforcing fibers in NFRCs. A compatible (bio)polymer matrix can improve the mechanical properties of Interwoven structures, while optimizing their potential as green NFRCs.

In the same way that textiles and grown biomaterials provide a starting point for testing the mechanical properties of Interwoven structures, NFRCs provide an important basis for understanding the behavior of natural fibers, such as the roots in Interwoven structures. The details of this are explored more in Part 4 - Characterization, but it is important to mention that similar composites exist with cellulose-based reinforcements. For example, Ramadan et al. developed laminated jute fibers that were infused in resin, and the properties of both the fibers as and the composite were compared (Ramadan et al., 2015). The jute fibers were characterized by following the standards for nonwoven fabrics (ASTM D5035), so it is safe to assume that this method is appropriate for testing Interwoven structures as well.

## 3D Printed Specimens

The previous section touched on the anisotropy of composites induced by fiber orientation. In composites, fiber orientation is limited to either being completely alignment or misaligned. Interwoven structures are not limited to these two options. The patterns that the roots grow into can be found anywhere in the spectrum of alignment to misalignment. The free-form orientation of these patterns is only replicated by other digitally produced products, such as additively manufactured products. Though not a class of materials on their own, additively manufactured specimens can be anywhere in the alignment spectrum, just as Interwoven structures.

3D printed specimens are built up on a layer-by-layer basis to make a solid object. The contour of each layer is determined with a slicer program that converts a CAD model into a series of layers. However, the infill of each layer can be made up of a variety of patterns like the ones in **Fig. 2.13** (Dudescu & Racz, 2017). The infill orientation and pattern also lead to anisotropy in 3D printed parts, and the effects of this have been extensively analyzed in literature, and it was concluded that the orientation of the infill pattern with respect to the loading direction has a large impact on the recorded mechanical response. In other words, the distribution of a load pulling in only one direction was more effective for some patterns

than others. (Ahn et al., 2002; Es-Said et al., 2000; "On Reducing Anisotropy in 3D Printed Polymers via Ionizing Radiation," 2014; Torrado & Roberson, 2016).

Following this line of reasoning, it is hypothesized that there is a correlation between the orientation of Interwoven patterns with respect to the load they experience and the observed mechanical properties. Specimens printed through fused deposition modeling (FDM) are thus another analogous material that helps when considering the possible applications of Interwoven structures and the possible anisotropic effects that the root patterns may have on the structure.

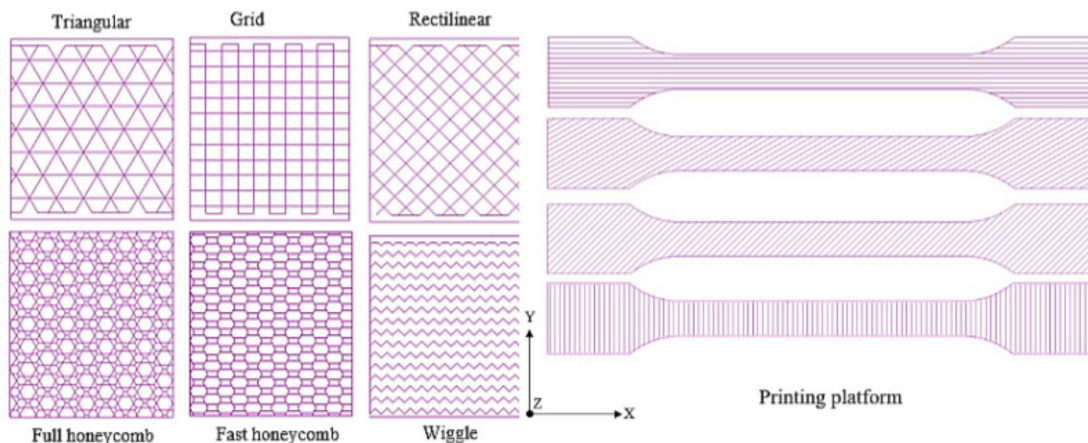


Figure [2.13]: Examples of infill pattern alignment in 3D printed samples. (Dudescu & Racz, 2017)

## Characterization

Part 4 is dedicated to the characterization of Interwoven materials and explains the importance of this in detail, but an introduction to characterization is in order at this point. Recall the characterization pentahedron introduced in **Fig 1.8** and how it is used to relate the processing, structure, properties, and performance of a material. Characterization (and especially technical characterization) is an umbrella term for the multitude of techniques used to correlate these four elements to each other. Some of the available techniques used in the materials science industry include non-destructive methods, such as spectroscopy and microscopy, as well as methods that rely on the destruction of samples to analyze the material behavior. Mechanical testing and fractography are examples of the latter categories.

### Spectroscopy

For a fundamental understanding of a material's properties and structure to be fully developed, it is often necessary to delve into the molecular interactions that occur in a material of interest. Spectroscopy is usually used in these interactions and it refers to the interactions between electromagnetic waves and matter. In other words, it covers methods that use infrared (FTIR), x-ray (XRD), or other forms of energy to identify components

of a material at a molecular level. These methods offer the advantage of being non-destructive and obtaining highly accurate information about a material sample's structure and/or composition, which makes them especially common for identifying the presence of certain elements or phases in a sample (Kafle 2020).

### Microscopy

Microscopy is another category of techniques that has multiple uses and benefits. Most notably, the uses are related to the resolution of microscopes, or the size of the smallest objects that can be detected, which ranges from the macroscopic to the nanometer scale. Despite resolution differences, the theory behind microscopy is the same - a source of energy (photons, electrons, etc) is shot at a target sample in the form of a beam, and an image is produced as a result. **Figure 2.14** shows the same metal particles on a fiber support as they appear under different microscopes - a light microscope, scanning electron microscope (SEM), transmission electron microscope (TEM), and scanning transmission electron microscope (STEM) (Schumacher, 2014).

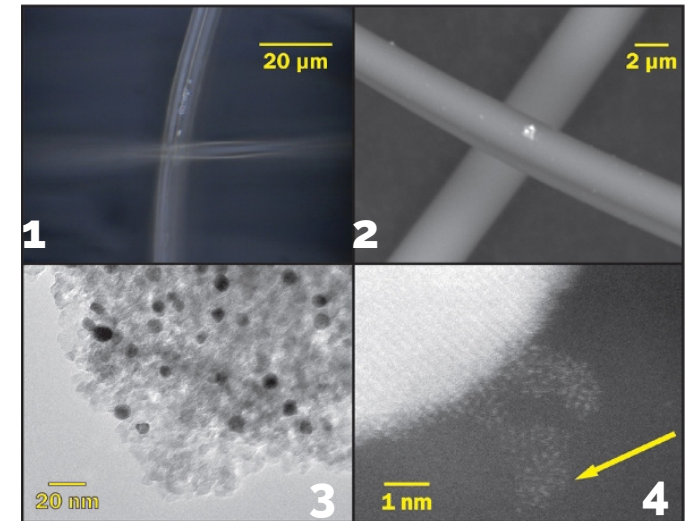


Figure [2.14]: Microscopic images produced on a light microscope (1), SEM (2), TEM (3), STEM (4) (Schumacher, 2014)

## Fractography

Microscopy also allows scientists to closely study the structure of a material, as well as any changes in structure that occur as a result of fracture. Failure analysis refers to a field of study whose aim is to understand the mechanisms that lead to failure in engineered products, and fractography is a method of failure analysis by which the the fracture surface of a failed sample is studied (Jobbins 2018). Failure of engineered products can be a result of a variety of conditions, ranging from processing to environmental conditions in use, and fractography is a form of forensic analysis that helps determine the root of a failed product.

Fractographic images differ for every material structure and class, but failure conditions leave witness marks in all samples. Take the fracture surface of the NFRC in **Fig. 2.15** as an example. In the image, the white arrow points to a strain field that formed in the matrix around a reinforcement fiber before rupture, and the smooth lines across the surface are indicative of brittle behavior. Furthermore, the closeup seen in **Fig. 2.15b** exhibits a single cellulose reinforcement fiber where adequate interfacial adhesion is evident due to a lack of a strain field around the fiber (Carrete, et al., 2020).

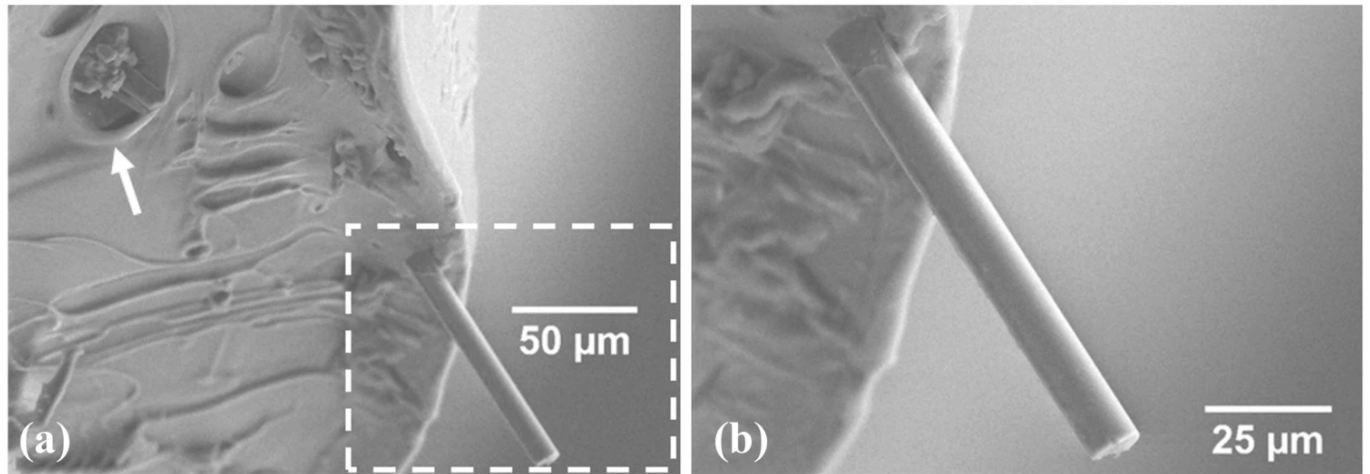


Figure [2.15]: Electron micrograph of a filament for FDM printing made from a recycled PET-cellulose-reinforced NFRC (Carrete, et al., 2020).

## Mechanical Testing

Mechanical testing has been mentioned the most as a characterization method throughout this report. This is largely due to the fact that it encompasses a straightforward method of understanding a material's response to an expected use case. There are many tests that can be performed depending on the use that is most relevant for a material application. For example, if a material will be used for a product that must withstand weight being placed on it, compressive tests are relevant, whereas, if the product requires the product to bend or undergo lots of torsion, a flexural test may be in order.

Similarly, tensile tests give an indication of a material's response to being pulled in tension. These tests are common in materials science because they give ample information about a material's properties, such as stiffness, ductility, impact strength, toughness, tensile strength, elasticity, and more.

Any combination of the techniques presented here can be used to map out the characteristics of a novel material, and this project intends to use them to better understand the design space available to Interwoven materials at their current developmental stage.

# Literature Review Takeaways

Interwoven structures have the potential to disrupt multiple industries as sustainable alternatives to existing materials. Among engineering materials, there are four categories that the characteristics of Interwoven structures can be classified as: (1) Bio-fabricated materials - specifically under Growing Design, (2) Textiles (Non-woven), Composites (NFRCs), and FDM-printed samples. The four categories listed are analogs to Interwoven structures and can serve a template to understanding the properties and potential applications of Interwoven materials.

## Knowledge Gaps

There are no precedents for characterizing a material with the same complexity as Interwoven, but there four analogous materials each provide information to define a starting point. The following research questions, are based on relevant findings regarding each material class.

### 1. Bio-Design (Growing Design)

*Complex structures like the Silk Pavilion underwent complex simulations and mechanical testing, what are similar tests to perform on Interwoven structures?*

### 2. Textiles (Non-woven)

*Interwoven root structures resemble non-woven materials. Can standardized testing methods for textiles be applied to Interwoven structures?*

### 3. Composites (NFRCs)

*Natural fiber composites are prevailing as sustainable alternatives to synthetic fibers. What potential does Interwoven present for this field? Can it be characterized similarly to other natural fiber reinforcements?*

### 4. 3D-Printed Specimens

*Digital fabrication methods like FDM printing allow form freedom when making hollow structures. Does the form freedom in Interwoven's patterned structures give rise to anisotropy?*

### 5. Characterization

*Consistency is key for a thorough characterization of Interwoven structures. What are the most relevant techniques to achieve this? What is the correlation between the (micro)structural elements of Interwoven and the observed mechanical properties?*

## Conclusions

Fulfilling the purpose of this project has two components that are equally important. First, the resulting characterization of technical properties must be reproducible to some extent, connecting as many of the elements of the characterization pentahedron as possible. Second, the results of said characterization must be presented in a way that is accessible and easy to understand by other designers without them having to reproduce all of the tests performed here.

*How can the mechanical properties of Interwoven be characterized in a **reproducible** manner and presented in a way that is **accessible**?*



# **3 - Tinkering with Parameters**

# Material Parameters

Recall from the first chapter that there are many parameters that go into designing Interwoven structures. Now that there is a bit of a precedent set from analogous materials in literature, these parameters can be explored more thoroughly. This section explores the material parameters, which are related to the plant used its growth.

In her work with Interwoven, Zhou explored various plants from both fibrous and taproot root systems, but she decided to work with oats after her experimentations. Oats are a type of grass plant, so they have a fibrous root system. The dense and uniform formation of roots in fibrous root systems is better suited for creating an Interwoven structure with uniform root dispersion.

For the purposes of limiting the number of parameters that were being modified

throughout the project in the interest of time, most of the material parameters chosen were based on information from personal interviews with both Ford and Zhou, as well as their reported work. **Fig 3.1** gives an overview of the parameters chosen.

## Parameter Overview

### Plants used - oats.

Oats have a relatively quick cycle (about 2 weeks).

### Seed Density - $0.27\text{g}/\text{cm}^2$

Previous works used enough seeds to create a 2cm layer above the soil. For the sake of consistency, the mass of seeds taken up per surface area was calculated at 0.27 g of seeds per every  $1\text{cm}^2$ .

## Growing Conditions

The oats were grown on **universal soil**. The room they were grown in kept a **stable temperature** with the use of heaters in the winter months. Seeds were watered heavily at the beginning of the two weeks. More water was only added if the soil was too dry (mainly seen when the environment warmed up). A purple growing light set up with red and blue LEDs was kept on the plants for **14 hours per day** (as set by a timer). The plant station setup is seen in **Fig. 3.2**.

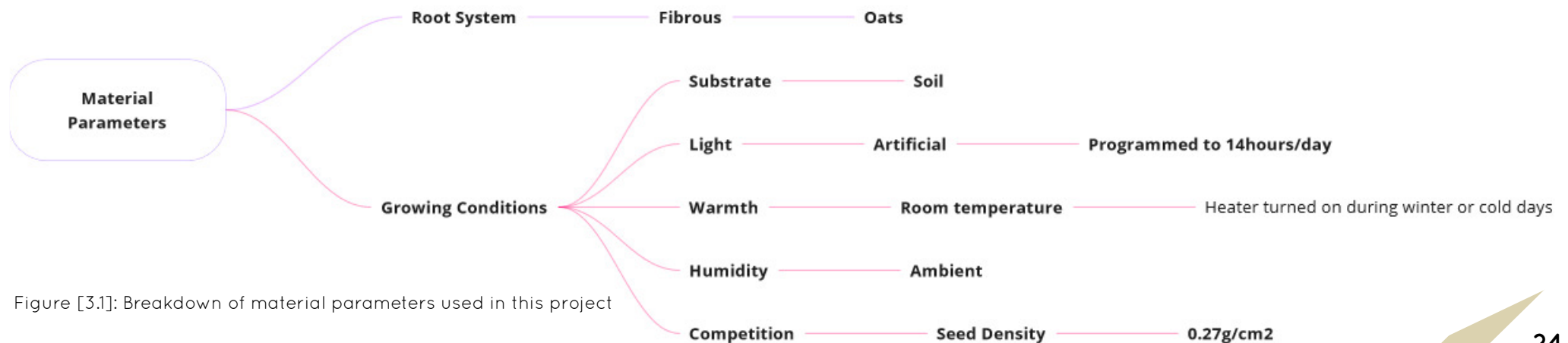


Figure [3.1]: Breakdown of material parameters used in this project

## Planting Station Setup

Despite having the growing lights, the plants were placed on a window sill to maximize exposure to natural light. The bottom image in the figure shows the removable shelf that was designed to make caring for the plants easy while the top one shows the setup a few days into the growing process.

Note that the distance of the growing light was placed relatively close to the plants. The window was also sealed off with a plastic film that had aluminum foil on the inside (the side facing the plants) so as to reflect some of the purple light back at the oats.

Material parameters relate to plant growth and health. Things such as light, type of soil or growing substrate, and plant nutrients or hormones can have an effect on the efficiency and speed of plant growth. An extended breakdown of the parameters seen in the previous section can be found in Appendix: Interwoven Parameters - Material Parameters.

Most of the decisions made here were based on previous works iterations for this group of parameters requires waiting for the plant to fully grow for comparison. The next section, design parameters, is where most of the tinkering and iterations took place because those parameters can be more readily influenced and changed by the designer. The influence of material parameters is where the collaboration with nature is most prevalent. The designer has little predictable impact on the effect of these parameters.



Figure [3.2]: Plant station. Placement in the window (top) and shelf built to hold the plants (bottom).

# Design Parameters

Design parameters are the subsection that the designer has the most control over. They encompass everything ranging from the obstacles used in plants growth to the composition of the matrix components in the composites. **Figure 3.3** is an overview of the parameters explored in this section. The details of some explorations are excluded to abide with the non-disclosure agreement. They will be kept only in the Confidential Appendix.

## Parameter Overview

The parameters that were tinkered with in this section can be divided into three categories: template pattern, template design (mostly redacted), and composite design. A short discussion of these results follows.

### Template Pattern

Interwoven structures are built upon the design of a template that molds the pattern that the roots grow into. Pattern possibilities are endless. Ford explored the experiential properties of various patterns in his work with Interwoven, but this work only focuses on **square grids**. The simplicity of this pattern makes a correlation between material structure and performance clearer than complex patterns, yet the results can be extrapolated of this study can be applied and extrapolated to more complex template patterns.

### Template Design

This section contains the most confidential parts of the report. The complete details will only appear in the Confidential appendix. The results of tinkering in this category led to the design of a template with a 3mm thickness that was 3D printed with draft angles for easy de-molding.

### Composite Design

A thorough exploration of composite designs is beyond the scope of this work. It would require the mechanical testing of various polymeric matrices to test the compatibility with oat roots, a thorough analysis of root percentages in the matrix, and characterization of interfacial adhesion. This work limits itself to identifying the composition and processing methods relevant for an agar-agar as a bio-polymer matrix as proof that composites could potentially increase Interwoven mechanical properties.

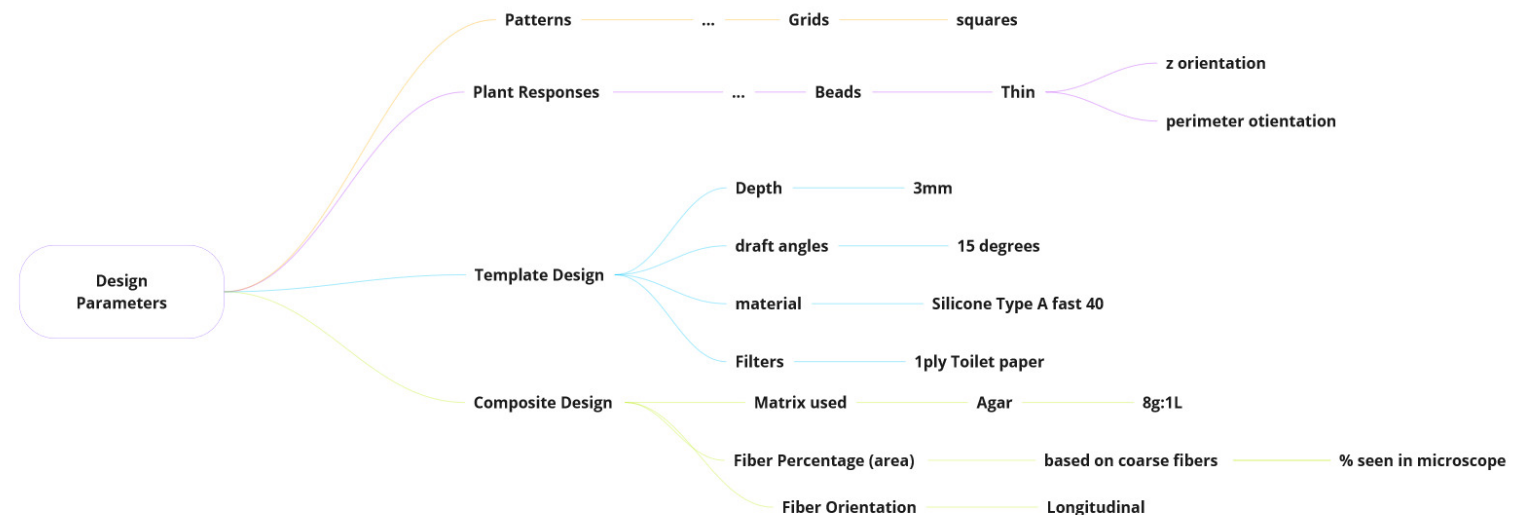


Figure [3.3]: Summary of design parameters explored in this work.

## Template Pattern

Ford's work with Interwoven revealed that part the appeal of these structures is the combination of natural materials with unexpected patterning. Different patterns clearly elicit varying responses to the senses that, but the impact on mechanical properties is unclear. Since this work is the first to characterize the structure and properties of Interwoven, simpler patterns are needed. Simpler patterns make the effects of load orientation with respect to root alignment more clear. **Figure 3.4** shows a variety of patterns. note that the alignment of the root with any particular orientation is seen most clearly in the gridded pattern at the top.

Chapter 4 will cover the effects of root alignment orientation in detail, but it is clear that anisotropy can be largely detrimental to mechanical properties. As such, an alignment between roots orientation and the load direction is imperative.

### Takeaways

Of the patterns presented here, the square grids provides both of the necessary elements for effective characterization - simplicity and reduced anisotropy. Furthermore, the tests performed on simple patterns make it easier to correlate root structure with certain responses, which cannot be deduced from more complex patterns.

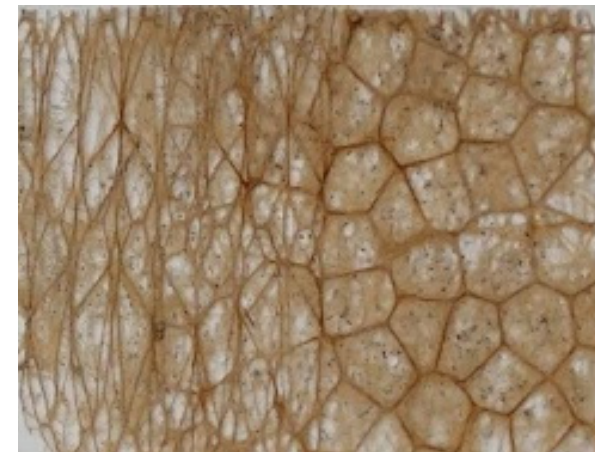


Figure [3.4]: Examples of patterned with varying degrees of complexity

## Template Design (abridged)

The design of the template contains the most confidential information in the report, so the complete details will only appear in the Confidential Appendix. Nevertheless, the results of tinkering with these parameters are summarized here.

Two fabrication methods for the template were tested to find whichever one resulted in the most desirable samples. The resulting samples of these fabrication methods are seen in **Fig. 3.5**. The fabrication method with the image on the left provided less control over the result. The thickness was predetermined at 1cm, which complicated the process of removing the samples from the template. The second fabrication method allowed for much more precise and intentional decision to be made about the mold. This resulted in a thinner sample (right) that was 3mm in thickness with no complications in separating the roots from the plant.

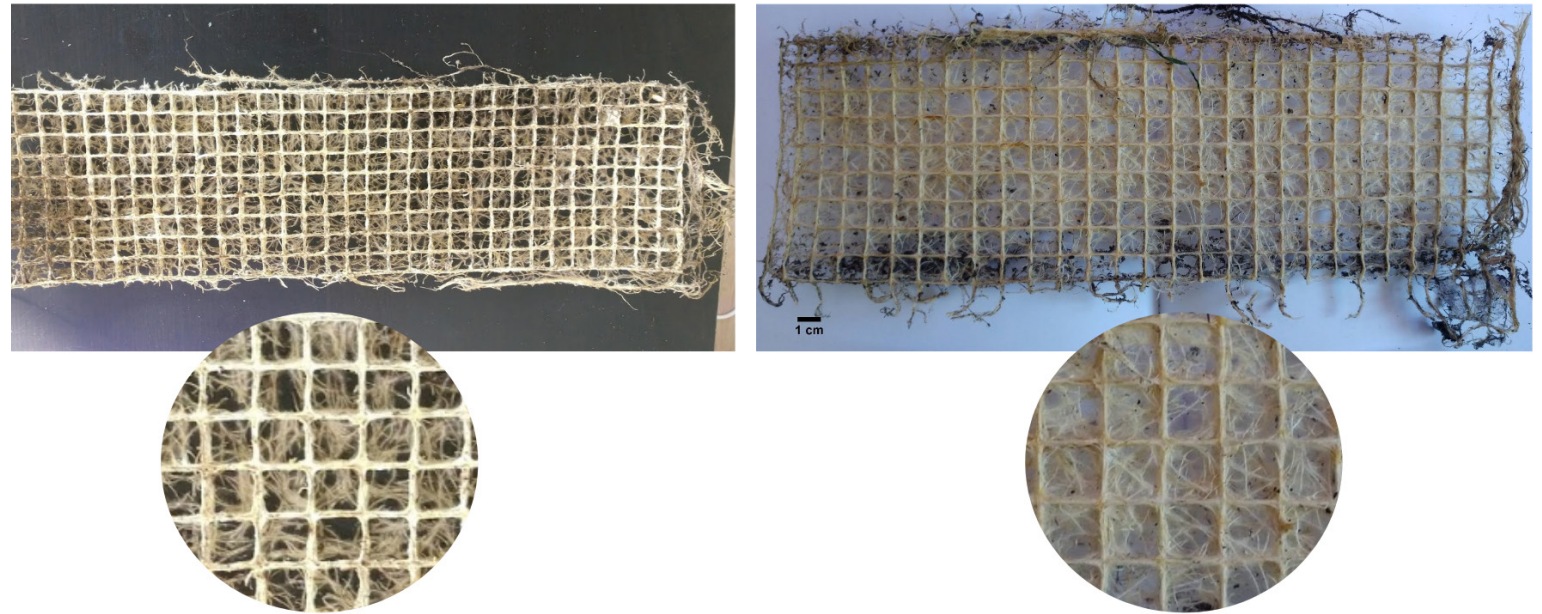


Figure [3.5]; Comparison between a 1cm template and a 3mm template

Sample thickness and ease of fabrication were not the only differences between the two samples. The structure was notably different as well. Though both templates had the same square grid mold, the thickness resulted in different samples. The thicker samples had more of a three dimensional feel, and the fine roots seen within the squares of the grid were not on the same plane as the squares.

The thinner sample resulted in a more homogeneous, planar structure. Instead of a three dimensional structure, these samples resembled a textured sheet 3mm thick. The fine roots that grew for these samples was also more dense. More importantly, the fine roots were in the same plane as the coarse roots, which resulted in different mechanical properties. Tensile test results (covered in the next chapter) prove this correlation.

### Takeaways

Template design tinkering resulted in the fabrication of thinner samples (3mm thick) fabricated with the second method (described in detail in the confidential appendix).

## Composite Design

A thorough characterization of a composite should, in theory, include all three phases - reinforcement, matrix, and composite. However, the scope of this project is not to find the optimal composite design and composition, but rather to identify Interwoven structures' potential as a reinforcement phase. As such, the characterization is limited to the effects of composite manufacturing and choosing a matrix composition that is suitable for the purposes of a comparative study.

In their exploration of Interwoven composites, both Ford and Zhou mentioned using agar-agar gelling agent as a matrix. Zhou used it as a substrate instead of soil to grow clean roots, while Ford used it as a more traditional composite. Since their method of preparing agar was already identified, agar-agar was chosen as a matrix for this study, but the fabrication method and agar composition were tinkered with to find a suitable matrix.

As a gelling agent, agar is cooked in water, and cooling down the solution results in a stiff gel. The ratio of agar powder to water in this solution greatly affects the stiffness of the gel. The three parameters tested for composite design were the agar matrix composition, root infusion method, and post processing (though the latter falls under fabrication parameters in the next section).

The matrix composition was tested by through observational experiments performed on samples infused with different agar:water ratios. The procedure for this is as follows:

### Agar Preparation:

1. Measure out the desired amount of water and agar. Three ratios were used here (1) 4g agar/1L water (**0.4%**), (2) 8g agar/1L water (**0.8%**), (3) 16g agar/ 1L water (**1.6%**).

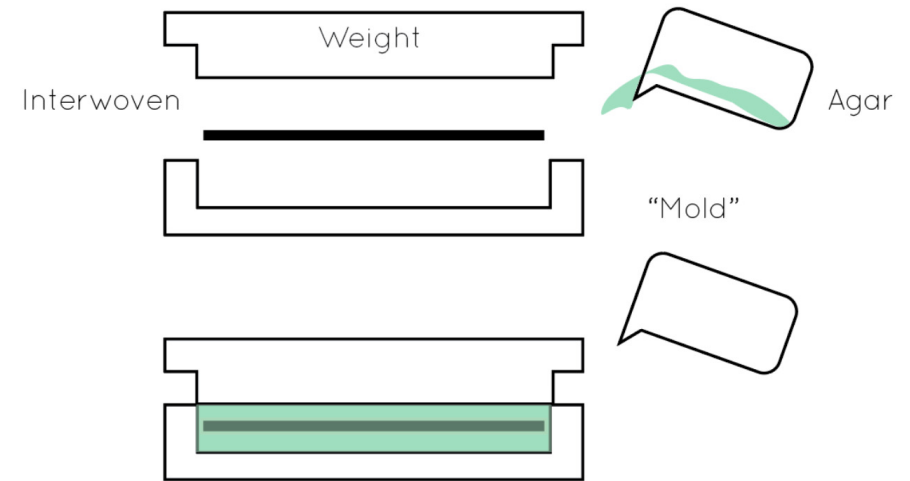


Figure [3.6]; Schematic of agar composite preparation

2. Place the measured water in a pan and bring it to a soft boil.
3. Add the desired amount of agar powder to the boiling water and mix until completely dissolved.
4. Allow the solution to cool down and thicken.
5. Place Interwoven sample on a surface with the desired shape, which can support liquid.
6. Once the solution is more viscous, pour it over the Interwoven roots.

7. Cover the roots and gel with aluminum foil and place a weight on top (see **Fig. 3.6** and **3.7**)

8. Allow the solution to dry completely (may take up to a week).

Note: If the sample is small enough, a humidity chamber with controlled temperature speeds up the process. Placing it at 30°C and 50% humidity dries the composite in as little as six hours.



## Matrix Composition

Despite the water agar-to-water ratio being very low, the differences between the three matrix compositions were evident. There was a clear correlation with the perceived hardness and malleability of the matrix and the amount of agar in the solution. Though no rigorous tests were performed on these samples, they were each folded and bent to test malleability qualitatively. A plywood medallion was used to test elasticity as well.

Figure 3.8 shows the composites' responses to the medallion being dropped on them. The bottom left image (0.4% agar) is seen drooping. The matrix in this sample was much easier to bend, but the stiffness it added to the Interwoven structure was minimal. The top sample (0.8% agar) had some of the malleability of the first sample, but it also resisted deformation better than the first sample. Lastly, the bottom right sample (1.6% agar) led to the stiffest sample. Bending it was harder and it did not respond well to



Figure [3.8]; Agar-root composite samples with a plywood medallion on them

reshaping like the first two samples did.

## Takeaways

Increasing the amount of agar powder in the gel solution can change the observed matrix drastically. Of the

three samples tested, the middle composition (0.8%) was deemed most suitable for further testing because it was versatile enough to add both ductility and stiffness to Interwoven samples.

# Fabrication Parameters

The fabrication parameters for Interwoven are closely tied to the material parameters covered earlier and the design of the template, so some of them have already been covered. However, the fabrication of composites have are more suitable for this category. There are two agar-related fabrication parameters that were explored here: the pre-processing methods, and the post-processing methods, as seen in **Fig. 3.9**.

## *Pre-Processing*

Agar was chosen as the polymer matrix for the composites based on previous works. The method explained in the previous section infused the Interwoven roots in a gel, but Zhou's work had grown the roots in agar instead, which left behind a thin agar-film. If growing the roots in agar could make a composite while nourishing the roots as well, it could optimize composite production, so a comparison between both processes was conducted as well.

## *Post-Processing*

During the drying process, agar experiences extensive shrinkage and promotes warping. As a measure to counteract warping, two clamping systems were developed to keep the roots taut throughout. The first system clamps the entirety of the Interwoven sample/grid in a process of bulk clamping, then the specifically sized samples are cut into the desired dimensions after drying. The second method uses clamps that have the predetermined size of the end-product to clamp down on.

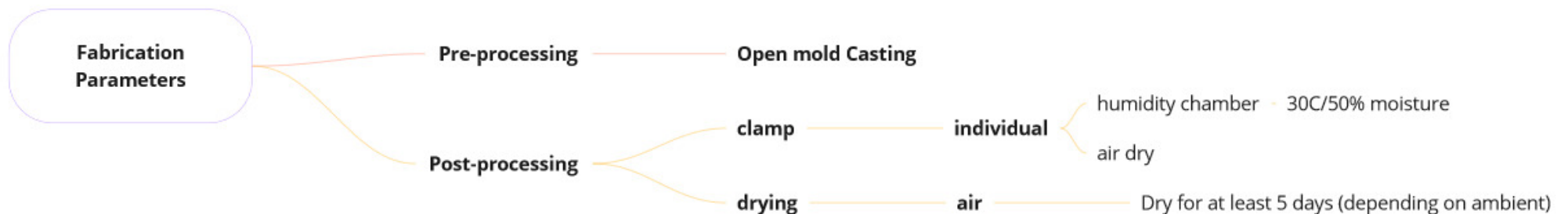


Figure [3.9]; Agar-root composite samples with a plywood medallion on them

## Pre-Processing

There are two methods to make an agar-root NFRC with Interwoven structures: (1) Using agar as a growth substrate and (2) Infusing the roots with agar gel. Composite samples were made with both methods. The results are shown in **Fig. 3.10**.

Growing the roots in agar does not leave behind a film of agar, but it is not uniform enough to be called a matrix. The film was also so thin that some parts resembled flakes rather than a continuous polymer.

Following the method detailed in the fabrication parameters page to infuse the Interwoven grids after they have been dried results in a more uniform matrix. The resulting composite is notably much more easy to handle than both the roots on their own and the samples grown in agar, which felt fragile.

### Takeaways

It is possible to grow oat plants in agar, which results in roots that are much cleaner than some of the soil-based samples because of the absence of soil. However, these samples are not successful composites because the agar matrix is not homogeneous and does not connect all the root structures to each other like a matrix should.

The best pre-processing method is to infuse the roots with agar gel to make a composite that feels much stronger than the other samples. However, warping must be eliminated with post-processing methods.



Figure [3.10]; Agar-root composite grown in agar (top) and infused with agar (bottom)

## Post-Processing

The shrinkage that occurs when the agar gel dries causes notable warping on the composite sample, which is unfavorable for a designed part. To reduce this warping, it was decided that the interwoven grids should be clamped in place by a mechanism such as the one shown in **Fig. 3.11**.

Interwoven samples are produced in a large piece that is cut to the desired dimensions when preparing testing samples, so there are two methods for clamping the composites - a bulk method and an individual method.

The bulk clamping method was produced with laser cut plywood and a series of screws, as shown in the top two images of **Fig. 3.12**. The clamping only occurs at the edges of the samples to keep the roots taut, but another piece is added to allow even distribution of weight (and agar gel). The individual samples (shown in the bottom image) are designed to fit the size of tensile tests samples. The details of this are explained in Chapter 4.

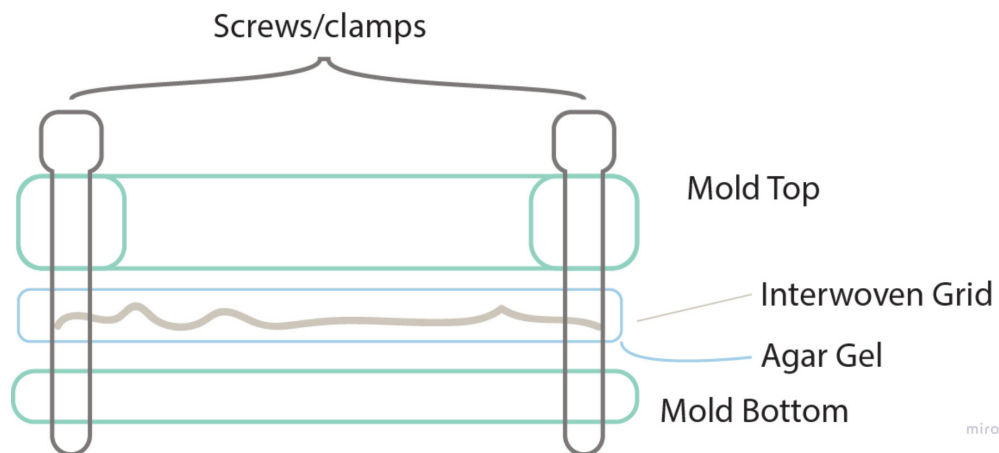


Figure [3.11]; Basic components of a clamping mechanism

## Takeaways

Mechanical testing proved that the individually clamped samples have a much more efficient distribution of load. This is possibly due to the disruption of the matrix that occurs when the bulk samples were cut down to the dimension of the desired testing samples. The clamping mechanism should reflect the application for which the composite will be used. In this case, the individual samples were superior.

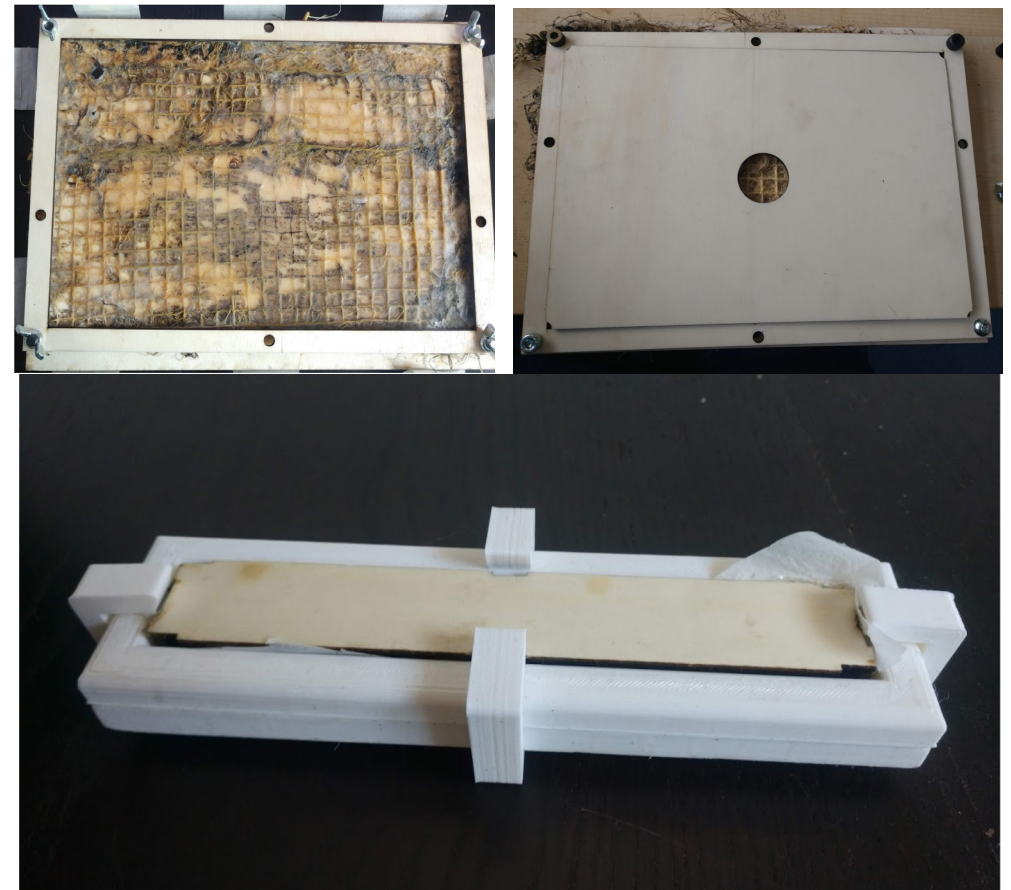
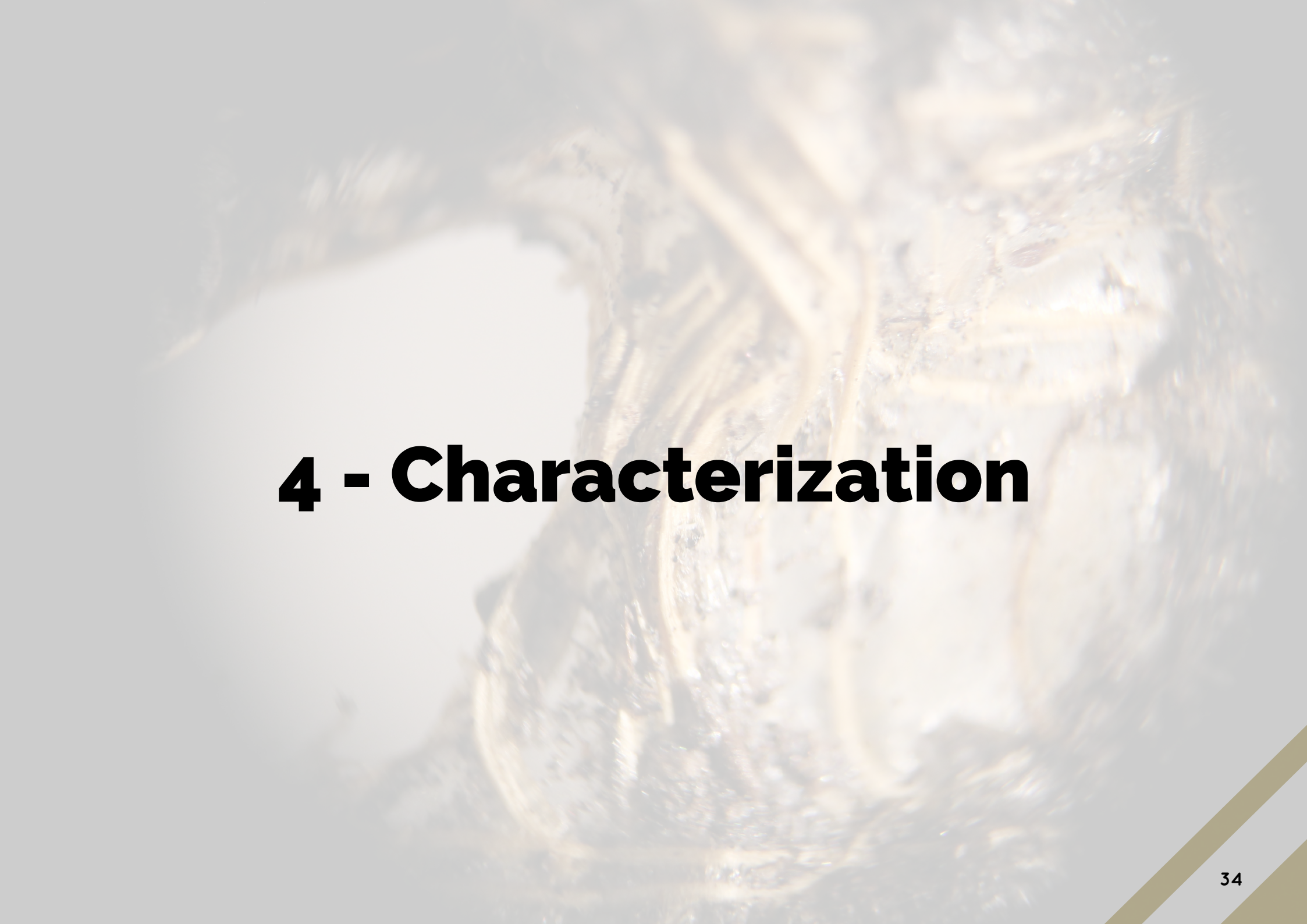


Figure [3.12]; Bulk (top) and individual (bottom) clamping mechanisms



# **4 - Characterization**



# Understanding Mechanical Properties

## Mechanical Properties in Tension

The purpose of this project is to expand the technical characterization of Interwoven structures and understand the design space and opportunities offered by them.

Interwoven members are novel, textile-like structures composed of oat plant roots. The roots grow into designed patterns by intertwining and weaving. A detailed explanation of the parameters is seen in Chapter 2. The mechanical properties of Interwoven structures are not yet fully understood. In materials science, mechanical properties are used to determine which material is most suitable to perform a desired function. Examples of such properties are seen on the right.

The four properties on the right tell a lot about a material, and can all be empirically determined through tensile testing.

Tensile tests provide an overview of a material's response to uniaxial loading conditions (being pulled in one direction) until the sample fails (breaks or rips).

The material's tensile response is used to derive a stress-strain curve. The four defined properties can be derived from

these curves, as well as the ultimate tensile strength - the maximum stress that can be sustained before failure.

**Figure 4.3** summarizes some of the key points to be derived from stress-strain curves.

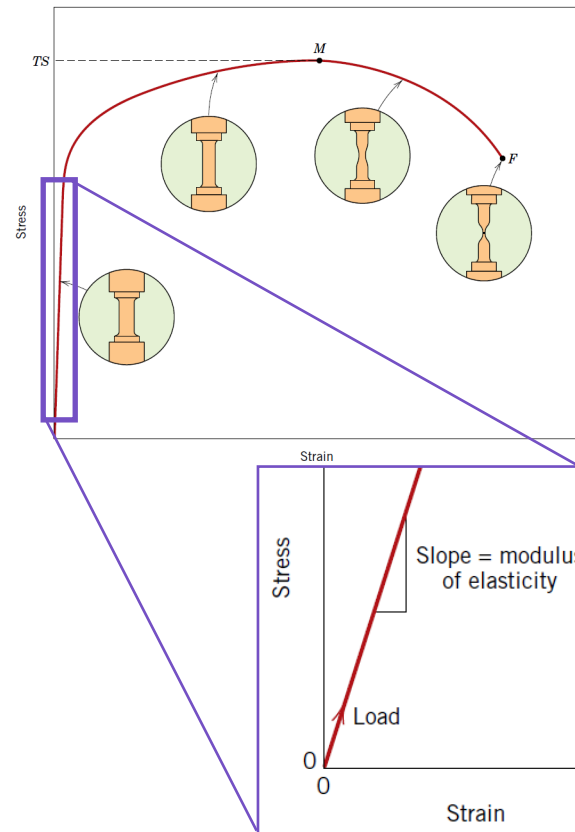


Figure [4.3]: Typical Stress-Strain Behavior (Callister and Rethwisch 2013, figure 6.5 and 6.11)



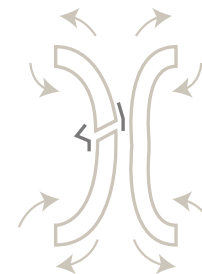
### Elasticity

A material's ability to return to its original shape after a deforming force is applied.



### (Yield) Strength

Maximum stress that can be applied to a material before permanent deformation.



### Ductility

Measure of how much plastic (permanent) deformation can be sustained before failure.



### Stiffness

Measurement of a material's resistance to deformation when a load is applied.

## Considerations for Interwoven Structures

The slope of the stress-strain curve's linear portion is known as the modulus of elasticity, a material property that can be related to stiffness. Within this linear-elastic region, the material deforms temporarily, but does so permanently beyond this (delineated by the yield stress).

The properties above are defined with **stress-strain** curves, but tensile data is collected in **force-displacement** curves. The main difference between the two is that stress-strain curves take into consideration geometric factors, given that stress is defined as the force acting on a cross-sectional area. Strain is a measure of displacement as a fraction of the original sample's length (**Fig. 4.4**).

The tensile properties of Interwoven structures will be tested in this study, but the concept of stress needs more attention for these samples. Interwoven samples do not have a uniform cross-section. They are made up of a bundle of fibers. The planar nature of these structures resembles that of non-woven fabrics, whose tensile properties are tested differently.

The tensile properties of fabrics can be tested with either of two methods - the strip tests (based on ASTM D5035) and the grab tests (based on ASTM D5034). In the strip test, the jaws of the tensile tester grabs the full width of the sample (including any frayed edges of the fabric), while the grab test only grabs the center section of the sample to avoid defects caused by frayed edges. Non-woven fabrics are tested with strip tests (Yalcin, n.d.).

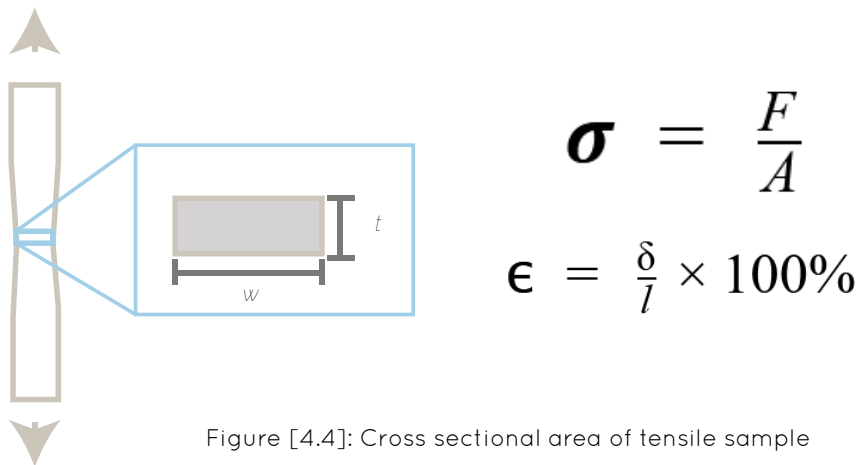


Figure [4.4]: Cross sectional area of tensile sample

# Root Orientation Tests

*How does the orientation of roots in the pattern affect the tensile properties?*

## Purpose

At the beginning of the project, the samples in **Fig. 4.5** were provided by Diana Scherer. A brief interaction with the samples (holding them, tugging at the ends, etc) gives the impression that they behave differently when pulled from different directions - a phenomenon known as anisotropy.

To test the effects of root orientation with respect to the applied load, tensile samples were made cut from the sections of the pattern with linearly aligned roots. The orientations tested are shown in **Fig.4.6**. Previous works with Interwoven used dimensions based on a modified ASTM D5034 sample, which had the dimensions of 25mm x 110 mm (Ford, 2019; Zhou, 2019).

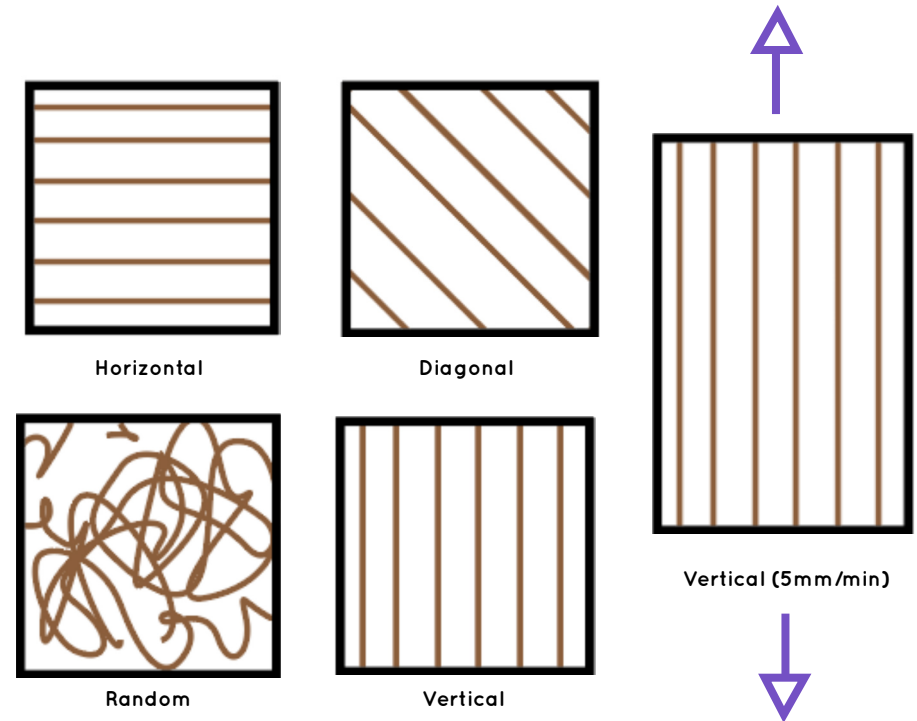


Figure [4.6]: Root Orientations Tested (purple arrows show the pulling direction for all tests)

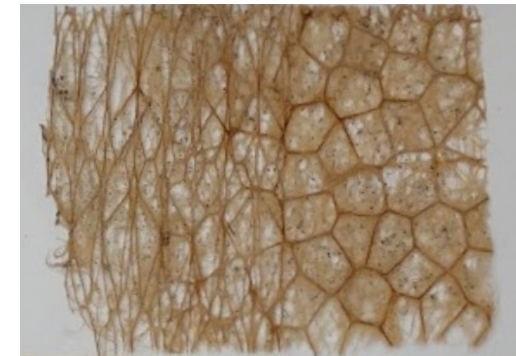


Figure [4.5]: Interwoven Samples provided by Diana Scherer

## Testing Procedure

For the sake of comparison with previous works, the effects of root orientation were tested using the dimensions mentioned above. A total of five samples were taken for each of the four different testing orientations. These samples were tested using a Zwick/Roell Z010 tensile tester with 10 kN grips (**Fig. 4.7**). The strain rate (rate of pulling) was arbitrarily chosen as 2mm/min. After testing these, five additional samples from the group that saw the highest breaking force (vertical orientation) were tested at a higher strain rate of 5mm/min to the effects of this parameter. A picture of the setup with a randomly oriented sample is seen in **Fig. 4.8**.



Figure[4.7]: Zwick/Roell Z010 Tensile Tester Figure [4.8]: Test setup with a randomly oriented sample

Sand paper was used between each sample and the tester grips to improve friction and prevent failures caused by the gripping force.

Before pulling the samples, one final consideration for sample preparation was the moisture content in the samples. Plant roots have an affinity for water and easily absorb moisture from the environment. This could affect the mechanical performance, so the samples were left in the same environment that the procedure would be performed for at least 6 hours. This was all in accordance with standard conditioning procedures for textiles (ASTM International, 2020a). Finally, the conditions to stop recording data were arbitrarily set to the point at which the load response dropped 40% from its highest peak.

## Results

Recall that the test samples did not have a uniform cross-sectional area, so the test results are expressed in Force-Displacement curves. The values of interest from these curves are the breaking force, defined as the maximum load in the graph, and its corresponding elongation values (ASTM International, 2019). **Figure 4.9** plots a representative curve from each orientation and the average values for the breaking force and elongation are reported in **Table 4.1**.

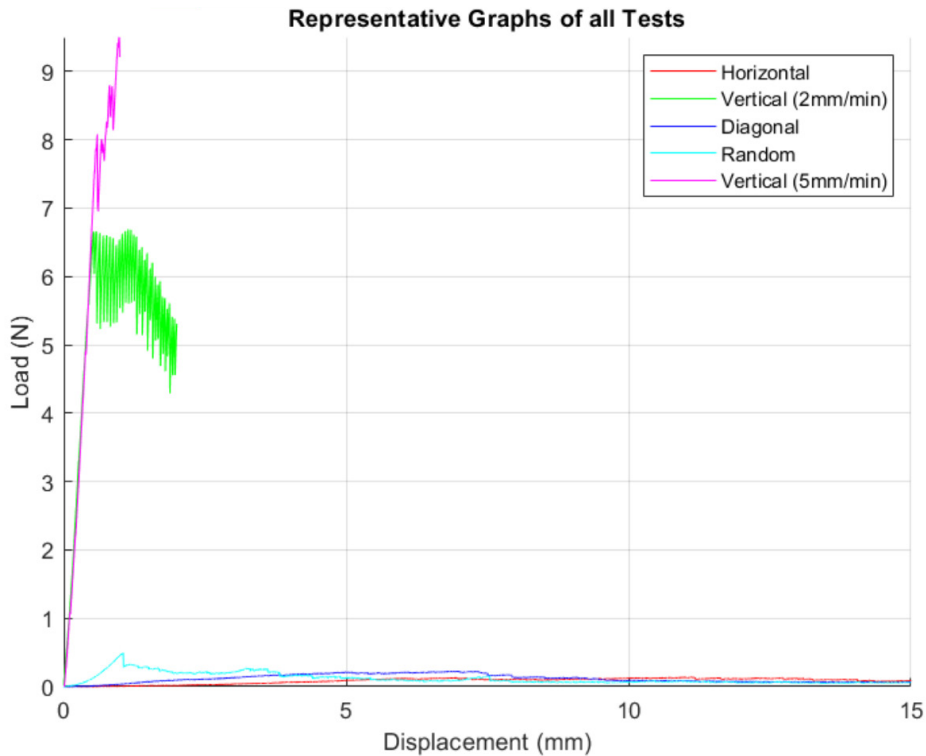


Figure [4.9]: Representative Force-Displacement Curves

## Overview

The figure above shows one representative curve from each root orientation. Note that both vertical groups had a much higher breaking force than the others groups (**7.80 N** and **10.13 N**). The linear region for these samples is the same, suggesting that this root orientation yields a similar response across different samples. The samples pulled at a slower rate saw a drop in their response at an earlier point than the one with a faster strain rate (5mm/min).

## Root Orientation Results

Averages	Breaking Force (N)	Displacement (mm)	Standard Deviation	Variance (%)
Horizontal	<b>1.397*10<sup>(-1)</sup></b>	11.10	± 0.046	32.61
Diagonal	<b>2.216*10<sup>(-1)</sup></b>	6.93	± 0.198	89.28
Vertical	<b>7.803*10<sup>0</sup></b>	1.14	± 3.751	48.07
Vertical (5mm/min)	<b>1.013*10<sup>(1)</sup></b>	0.98	± 2.990	29.50
Random	<b>1.514*10<sup>0</sup></b>	1.05	± 1.297	85.67

Table 4.1 Average Results per Root Orientation

The random orientation has the next-highest breaking force (**1.51 N**), but it was an order of magnitude lower than the vertical samples. The linear region has a much smaller slope, but continues elongation even after yielding, the behavior is very different.

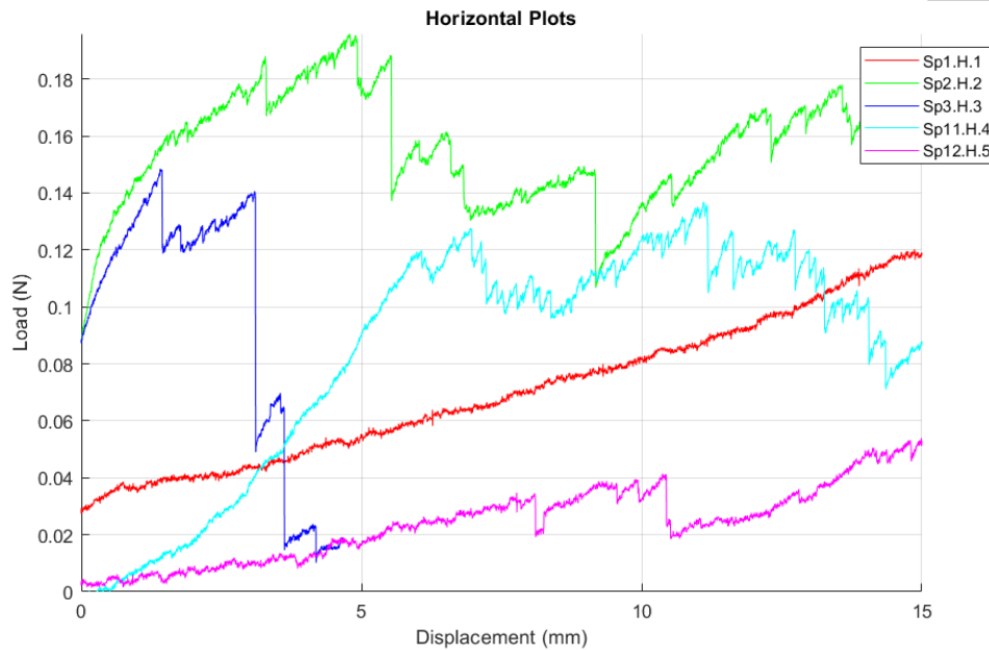
The response of both horizontal and diagonal samples was very similar and virtually negligible next to the other samples (**0.14 N** and **0.22 N**, respectively). The diagonal sample has a slightly higher slope in the linear region and reaches a higher maximum than the horizontal sample. Both of these groups surpassed a 15mm displacement. The following sections will show the data spread from within each of the five categories.

## Horizontal Orientation

As mentioned above, samples with a horizontal (transverse) orientation exhibited the weakest response. The results for each of the five samples also varied a lot (**Figure 4.10**). Samples Sp2.H.2, Sp3.H.3, and Sp11.H.4 had a similar response where a somewhat linear response is first seen. The load and displacement both increase proportionally until a sudden drop in the load. The behavior becomes erratic after that with some increase in load, but without surpassing the maximum point seen in the first peak.

Samples Sp1.H.1 and Sp12.H.5 were different in that their response continued to increase almost linearly within the specified range. The first sample saw no significant drops, while the latter had one at around 10mm but then continued to rise beyond the first peak.

Horizontal tests showed the highest propensity for error while testing because the clamp from Zwick placed stress directly along the weakest part of the sample and acted as a stress concentrator. There is little consistency within this root orientation, but the average breaking force value (calculated as the maximum load of the curve) is  $0.14 \pm 0.046$  N with a corresponding displacement value of **11.10 mm**. The samples tested are shown below.



Figure[4.10]: Results for Horizontal Orientation



Figure [4.11]: Horizontal samples

## Diagonal Orientation

The response of diagonal samples (**Fig. 4.12**) is varied, but the magnitude is comparable to horizontal samples. Samples Sp13.D.1 and Sp17.D.4 had similar slopes for the semi-linear section, but the first sample dropped sooner and saw a quick decline in the load it could take. The latter saw a continued increase before plateauing and elongating past the 15mm limit.

Plots Sp15.D.2 and Sp16.D.3 had a similar shape in that they both elongated proportionally to the load applied before reaching a maximum and rapidly declining after that. The former of these two failed at around 11 mm (seen as a sharp drop in the load). The blue curve shows how the sample had a more steady decline in the load after an initial drop beyond the maximum value.

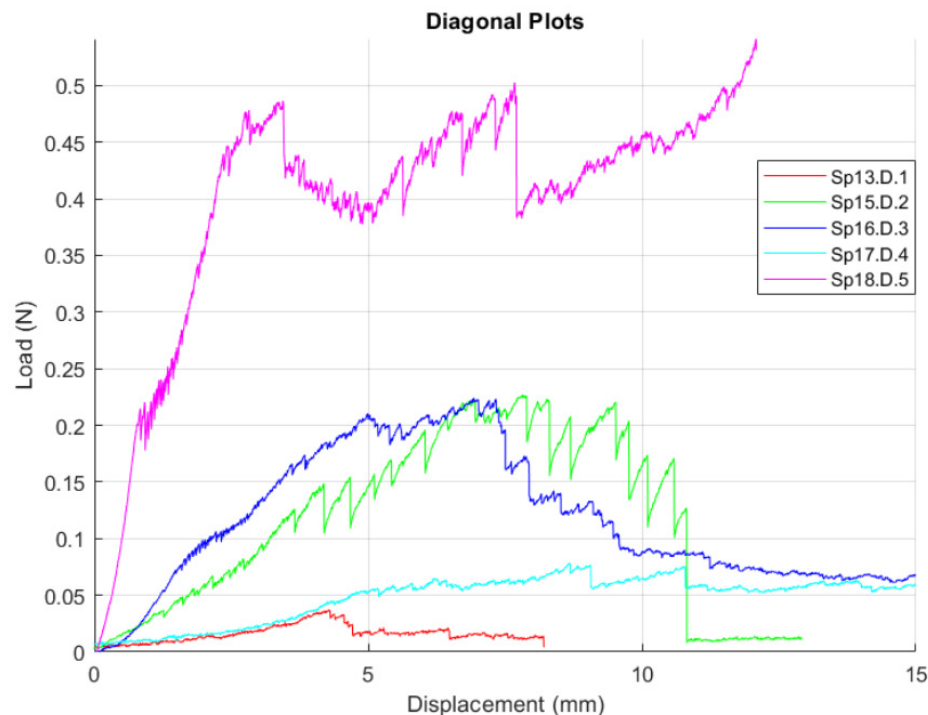


Figure [4.12]: Results for Diagonal Orientation

Finally, Sp18.D.5 had an atypical response. The slope of the linear section was much higher here, and even after yielding and dropping, it saw two more increases in the load it could take before the test ended. Unlike the other samples, the maximum was not achieved until the very end. Despite a dip occurring at around 8mm, a steady increase followed until the test ended. The low average breaking force ( $0.22 \pm 0.198\text{N}$ ) and relatively high elongation ( $6.93\text{ mm}$ ) largely resemble the horizontal samples.

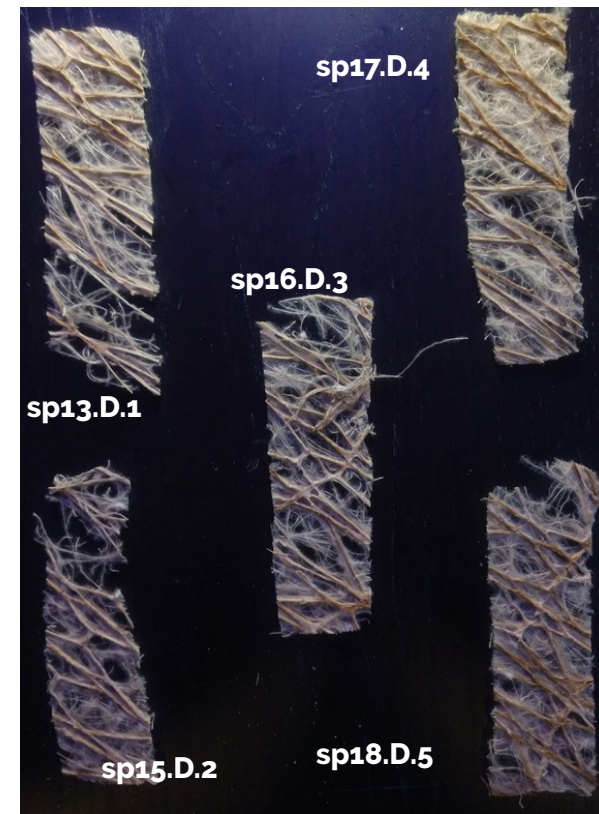


Figure [4.13] Diagonal samples

## Vertical Orientation - 2mm/min

The vertical root orientation showed the highest breaking force. (Fig 4.14) For this group, the clamps completely held onto the roots and the load was transferred completely. Three of the samples (Sp5.V.1, Sp6.V.2, and Sp8.V.3) had a similar slope linear response. Although the slope of the curve was lower for Sp9.V.4, its behavior mirrors Sp5.V.1 with a continuous increase even beyond the linear region until a maximum value is formed and the load drops significantly. Beyond the elastic region, Sp6.V.2 had a response that remained between 5-6N without dropping below that. Sp10.V.5 had the lowest slope in the linear region, but it also exhibited the same plateaued response, albeit a zigzagged plateau. Sp6.V.2 also saw this fluctuation that is likely due to various fine roots fracturing at different times (all roots do not fail at once). This was evidenced by audible crackling.

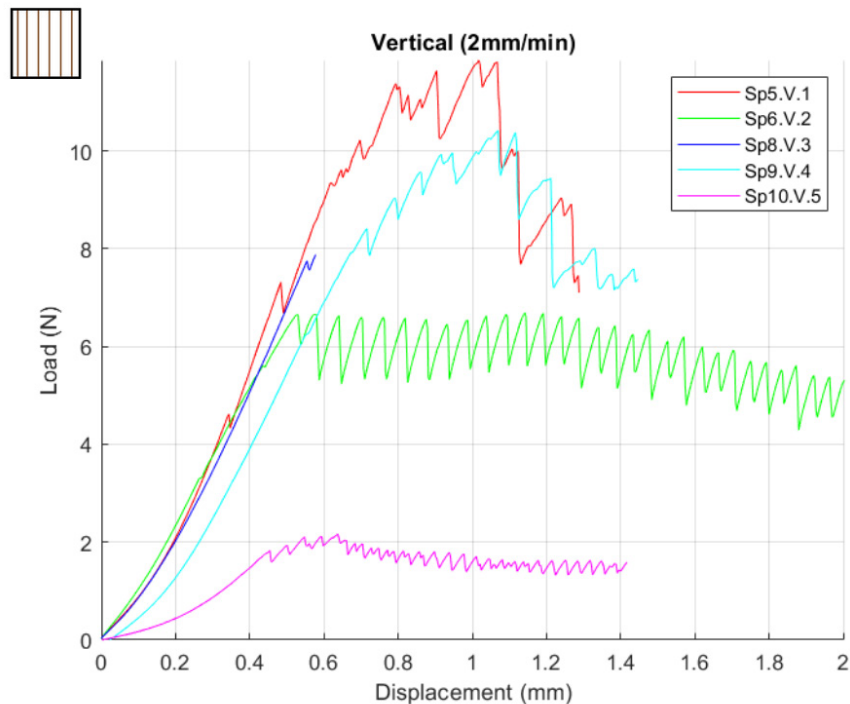


Figure [4.14]: Results for Vertical Orientation

The average breaking force of these samples was an order of magnitude higher than the horizontal and diagonal samples at  $7.80 \pm 3.751$  N, but the average elongation was much lower at 1.14mm. The apparent trade-off between breaking force and elongation is indicative of higher stiffness in these samples.

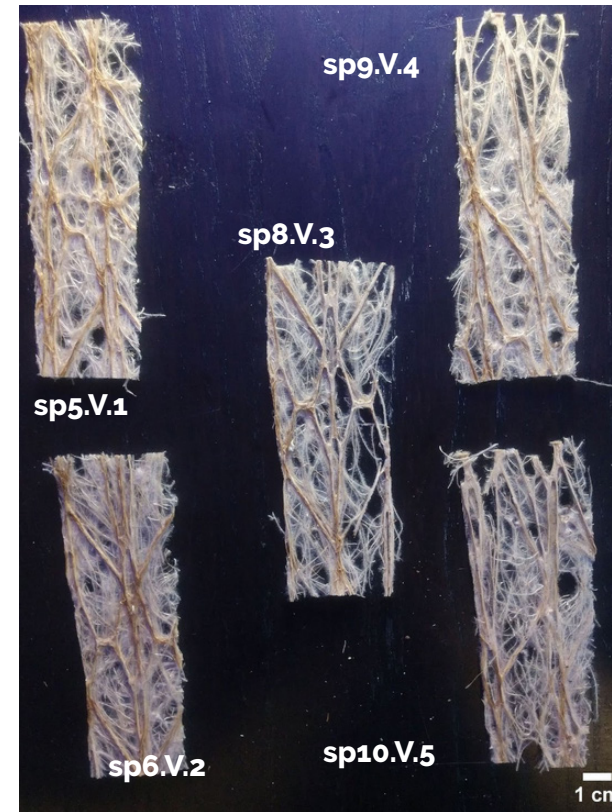


Figure [4.15]: Vertical Orientation Samples

## Vertical Orientation - 5mm/min

In order to evaluate the effects of strain rate on the samples, vertical samples were tested once more, but with an increased strain rate (pulling rate) from 2mm/min to 5mm/min. The curves seen for these tests resemble those of the 2mm/min group, but these samples reached higher maximum values (**Fig. 4.16**). Sample Sp25.T.2 had the highest peak above **15N** before dipping down to around 11N and steadily decreasing until the test ended. The linear portion of all the curves had similar slopes with a maximum value corresponding to the initial slope. The two samples with the smallest slope experienced the most elongation (Sp24.T.1 and Sp 26.T.3). The first sample had the highest elongation, bypassing the 2.5mm mark, while the latter only passed 2mm.

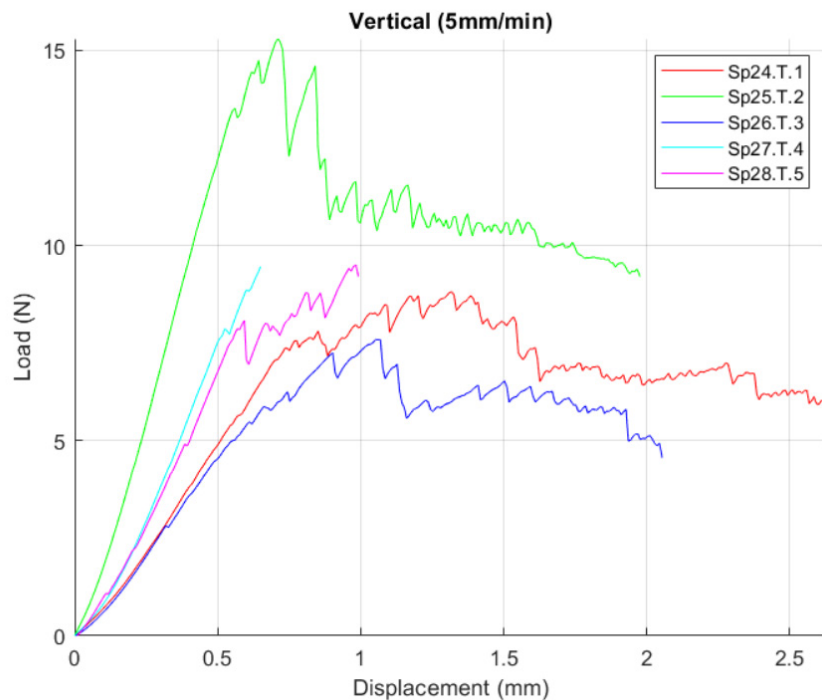


Figure [4.16]: Results for Vertical Orientation (5mm/min)

The same breaking force-elongation trade-off evident in the previous group is seen here. The average breaking force is **10.13 ± 2.99 N**, but the elongation is **0.98mm**.



Figure [4.17]: Vertical (5mm/min) Samples

## Random Orientation

While the orientation of the roots tested in the previous sections were biased according to the template they were grown in, there was also a set of samples tested that was grown without a directional bias - the random orientation. These samples act as a control variable to show the influence of the directional bias. The results of these samples were predictably inconsistent (**Fig. 4.18**).

Samples Sp19.R.1, Sp21.E3, and Sp23.R.5 all had a linear region with a similar slope. Despite the ability to withstand a higher load than the other samples, neither of these three extended more than 3mm. On the other hand, samples Sp20.R.2 and Sp22.R.4 had results that were much more elastic, but weaker. The

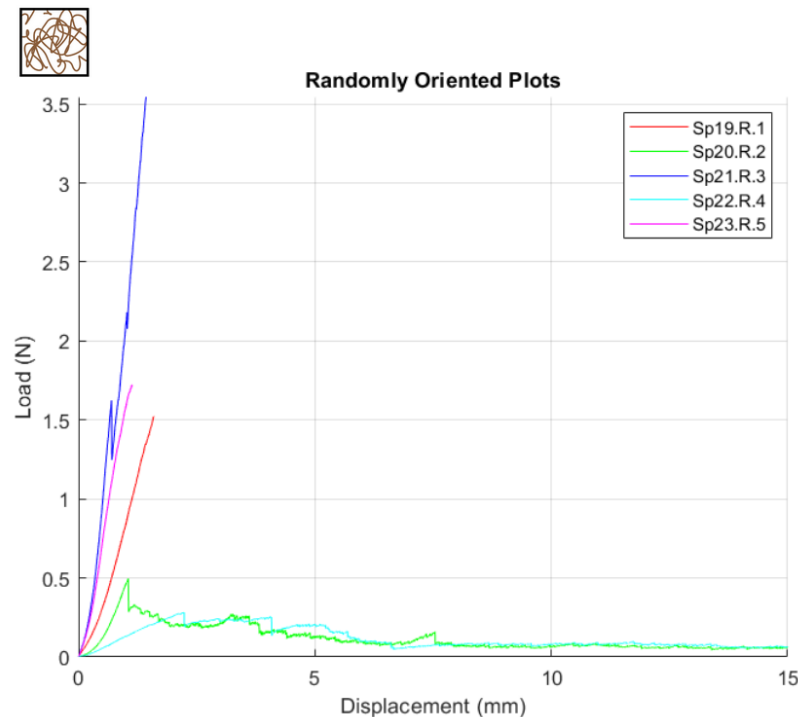


Figure [4.18]: Results for Random Orientation

slope of the linear part of Sp20.R.2 was similar to that of Sp19.R.1, albeit slightly less steep. After reaching a maximum load around 0.5N, the curve then plateaus and sees two more dips before flattening out around 7mm. Sp22.R.4 had a similar trend with two peaks, but the slope of the linear portion was much less steep than any other sample. The lowest maximum value of the dataset was also recorded for this sample.

While the response for these samples was higher than that of the horizontal and diagonal samples, it was still much lower than the vertical samples with an average breaking force of  $1.51 \pm 0.1297\text{N}$  and a corresponding elongation of **1.05mm**.



Figure [4.19]: Random Orientation Samples

### 3.3.4 Discussion

The test results are largely scattered, with a variance ranging from 29% for vertical samples pulled at 5mm/min to 89% for diagonal samples. Both vertical orientations were the strongest by more than an order of magnitude, so looking at these samples closely might explain the underlying strength mechanisms for Interwoven samples.

The vertical orientations were the only ones where the coarse roots were pulled along their longitudinal axis. Individual root structure provides insight into why this is relevant.

Roots are composed of various cell tissues and vessels that transport nutrients from the soil to the rest of the plant. Individual roots also have lateral root hairs that increase surface area and help anchor the plant (**Fig. 4.20**). The branched off root hairs interact and get tangled with nearby roots.

Though the complexity of the interaction between roots and root hairs is not visible to the naked eye, the vertical samples do show some of these elements. **Fig.4.21** shows areas with the darker, stiff roots, henceforth known as *coarse roots*, surrounded by a network of thinner *fine roots* and the white *root hairs* that bind them all together. Large porous sections are evident throughout, which also affects the response to loading conditions. It is important to note here that coarse roots are an amalgamation of fine roots that are aligned in such a way that they appear to be a thicker root. The alignment of these allows them transfer load better and act like a different phase to the individual fine roots.

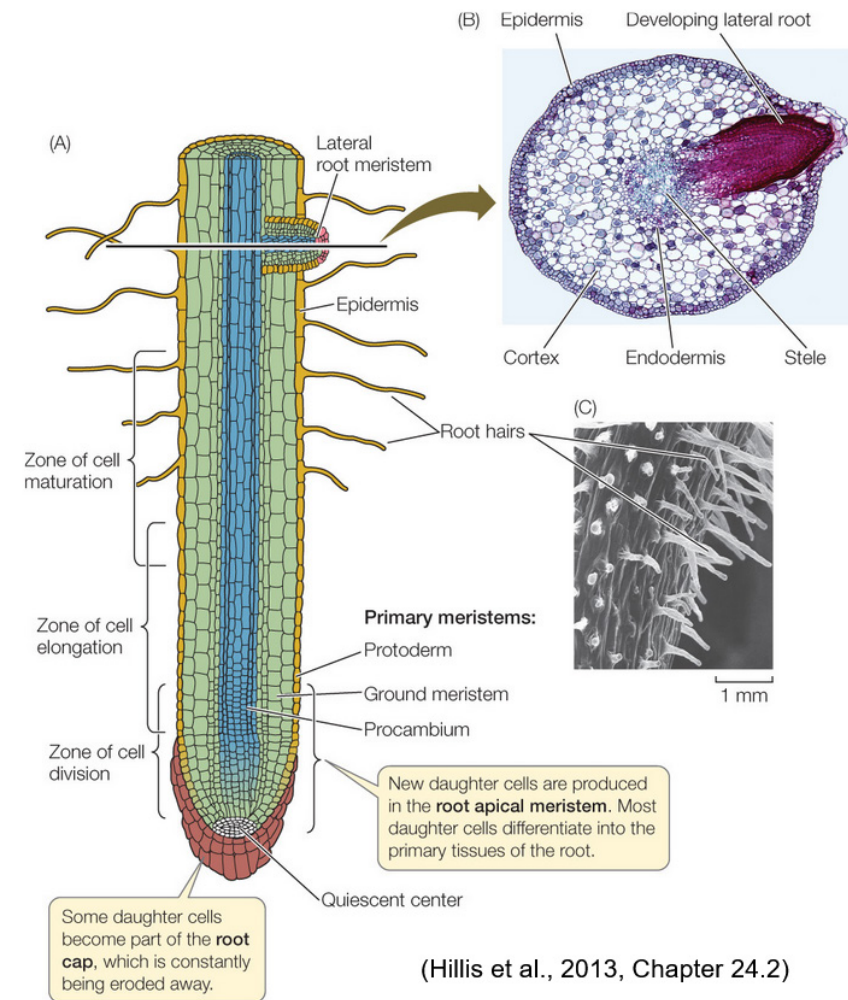


Figure [4.20] Schematic of the root structure (Hillis, et al., 2013, Chapter 24.2)



Figure [4.21]:  
Vertical Interwoven sample showing the three structural “phases”.

The root orientations that were not aligned with the grips had much lower performance because the coarse roots were not bearing the majority of the load. Horizontal samples had the coarse roots perpendicular to the applied force, so the load was mainly placed on the fine roots between the coarse roots. The same can be said about diagonal samples, coarse roots were partially aligned with the loading direction, but only one side of the coarse root was pulled at a time. In both of these case, the tensile response was determined by the fine roots, rather than the coarse roots, so these samples are not testing the same phase as the other groups.

Randomly oriented roots had a much larger heterogeneity within them, which made it harder to distinguish coarse roots from fine roots. This homogeneous mixture of phases is the reason these samples were also stronger. It is difficult to trace the response of each phase, but the response serves as evidence that the load was transferred better in these samples than the horizontal and diagonal ones.

## Conclusion

These tests proved Interwoven samples experience large amounts of anisotropy. The orientation of coarse roots with respect to a loading have a large impact on the tensile properties. Samples aligned with the loading direction exhibit the most strength, while those perpendicular to the loading direction were weakest. Despite trends being visible across all root orientations, the spread of the data was shows incredible variability in samples. To increase the reproducibility of these test results, a standardized testing method is necessary. The load-displacement curves shown here do not take into consideration geometrical factors. Characterizing mechanical behavior that is indicative of all Interwoven structures requires the use of stress-strain curves and standardized testing methods.

# Experiential Characterization

With a better understanding of Interwoven mechanical properties, a brief study about its experiential properties is in order. Recall the fifth element of the materials science (and design) pentahedron - elicitation (**Figure 4.2**). An experiential study is necessary to understand potential users' reactions and concerns when interacting with Interwoven structures.

Other than samples, Diana Scherer provided the four templates to grow the samples shown in **Fig. 4.22**. These samples, along with some of the ones that shown in a previous chapter, were used to perform an exploratory experiential characterization.

## Ma2E4 Toolkit

There are many ways to probe users with the hope of understanding the experiences with a material, but Camere and Karana developed a systematic toolkit that compiles some of these methods into one interview (Camere and Karana 2018). The toolkit serves as an interview guide, where participants interact with a material as the interviewer probes their thought processes. The interview is composed of four activities - Performative, Sensorial, Interpretative, and Affective.

Since the focus of this study is placed on the technical characterization of Interwoven structures, this dive into experiential characterization was meant to gather potential users' opinions on the structures. More specifically, their interest in a more "earthy" version of Interwoven samples (ones that have more visible soil) was probed. This last part was in response to one of the interests that Scherer expressed in a personal interview at the start of the project.



Figure [4.22]: Interwoven templates provided by Diana and the samples that were grown with them.

## Experiential Characterization Setup

The experiential characterization process was tested with six individuals. Given that this was done in the exploratory phase of the project, the demographics of the users were not very diverse. All six are students at the faculty of Industrial Design Engineering with some background in engineering. The nationalities of all these students varied, however, with people from Greece, Africa, Europe, and North Americas tested.

### Performative Level

Each activity in the Ma2E4 toolkit requires preparation prior to testing users. The performative level relates to the actions that the material elicits from participants. For this, the seven Interwoven samples in **Figure 4.23** were prepared. The toolkit

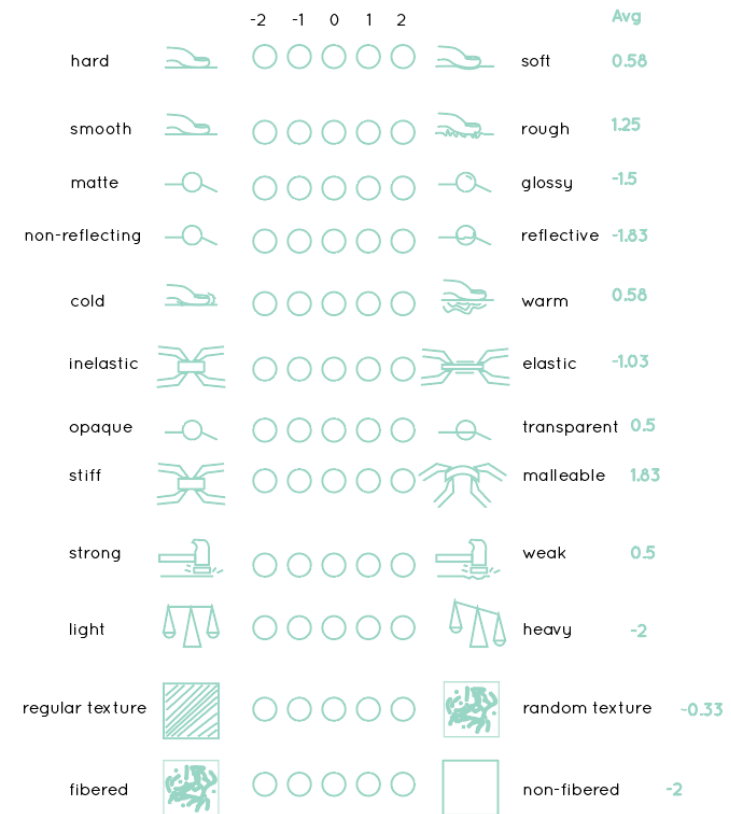


Figure [4.23]: Experiential characterization interview setup

also provides a series of images and actions to look out for at this stage.

### Sensorial Level

The sensorial level is focuses on how the senses are stimulated by the material. For this section, the booklet is handed to participants, where their activity includes rating their sensorial experience on a Likert scale. A total of 24 key words (**Fig. 4.24**) are used in the scale to provoke the participant's thoughts. They are also asked to explain their thought process.



Figure[4.24]: Sensorial Level

## Affective Level

Affective responses are the emotions that are evoked from interacting with the material. For this, a list of 24 emotions is given to the users and they choose (at least three) emotions from the list that they felt during the interaction. Then, they are asked to map out the intensity of the emotion on a graph like the one in **Fig. 4.25**.

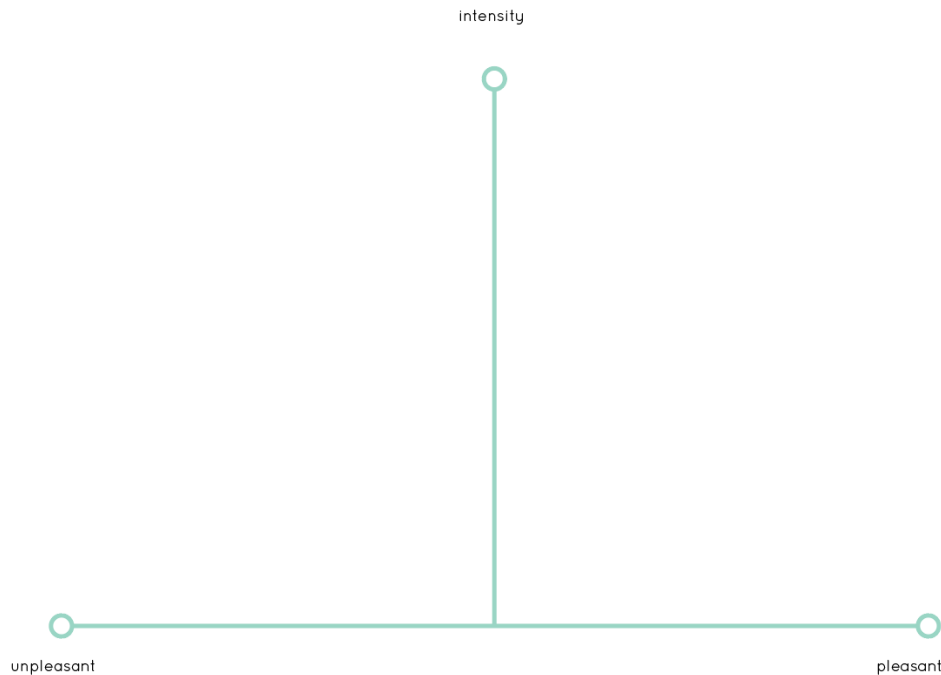


Figure [4.25]: Affective Level

## Interpretative Level

The final level is the most abstract since it involves the interpretations or meanings that users give to their interaction. To keep the responses somewhat consistent, a list of 23 possible interpretations are handed to the participants. Prior to the test, the interviewer produces a card for each word, where three images associated with the word are picked to elaborate on the interpretation. The cards prepared for this session are seen in **Figure 4.26**.

Once a participant has picked an image, they are asked to further elaborate on why they chose that image out of the three and write it down in the booklet.

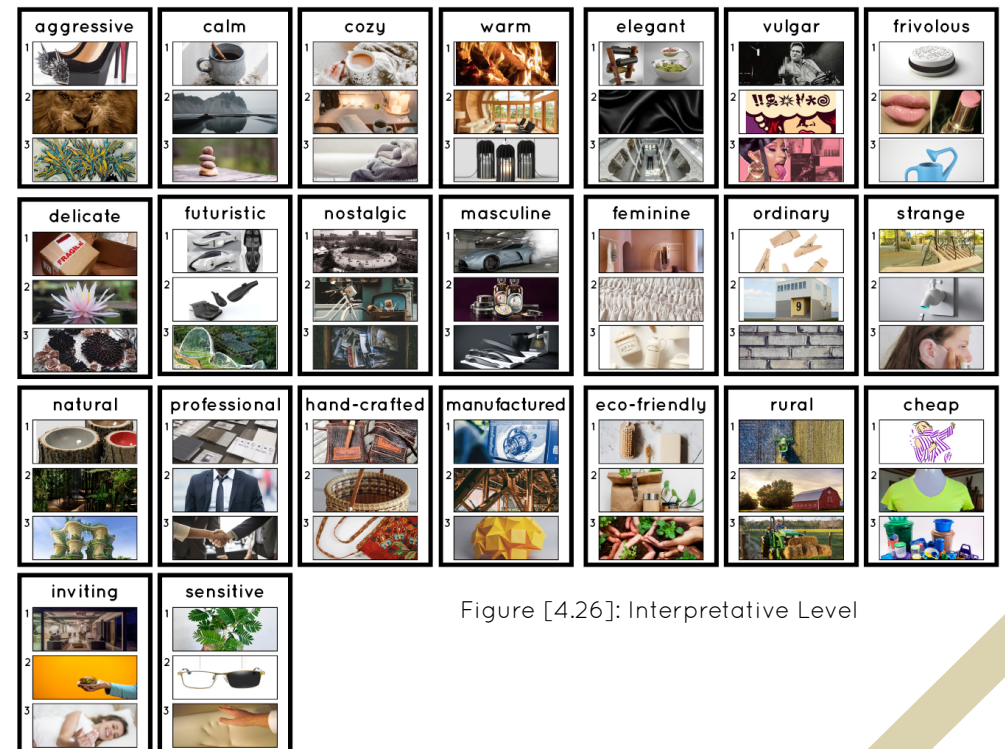


Figure [4.26]: Interpretative Level

## Experiential Characterization Results

An overview of the compiled results of the experiential characterization is presented in this section.

### Performative Level

When told to “play with the samples to [their] liking”, most users were hesitant and very gentle with the material at first. Little by little they gained confidence and exploring more (**Fig. 4.27**). The most common and uncommon interactions are listed here:

### *Common Interactions*

- Pulling
- Grabbing
- Pressing
- Rubbing
- Pinching
- Looking Through

### *Uncommon Interactions*

- Tearing
- Flapping
- Folding



Figure [4.27]: Common user interactions

## Sensorial Level

All of the Leikert scale responses for the sensorial level are laid over each other in **Figure 4.28**. Based on the most common responses, the group of tested individuals would describe the Interwoven structures as “light”, “fibered”, “malleable”, “rough”, and “weak”. Responses were consistent, but some uncertainty arose when participants distinguished the coarse and fine fibers. In these cases, they “averaged out” their thoughts and went for a middle score rather than either extreme.

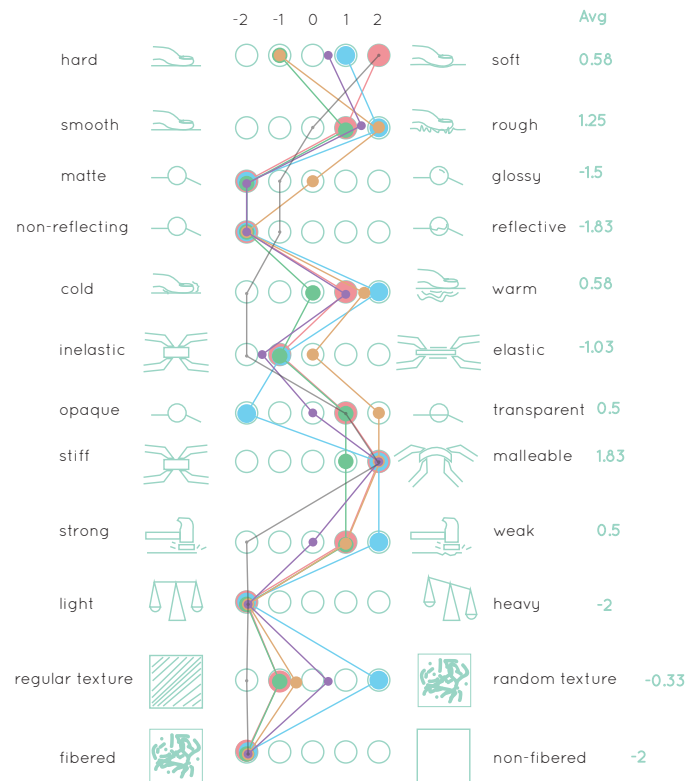


Figure [4.28] Sensorial Level

## Affective Level

Though varied, a majority of the responses for the affective level were concentrated toward the pleasant and intense emotions. The most commonly used words were “**curiosity**” (6/6 respondents), “**doubt**” (4/6), “**amusement**” (3/6), and “**reluctance**” (2/3). The frequency of use for these words explain the behavior seen in the performative level. Most participants showed hesitation at first, but a sense of fascination with the samples. However, the perceived weakness of the samples made them doubt the possibilities they could explore in their interactions.

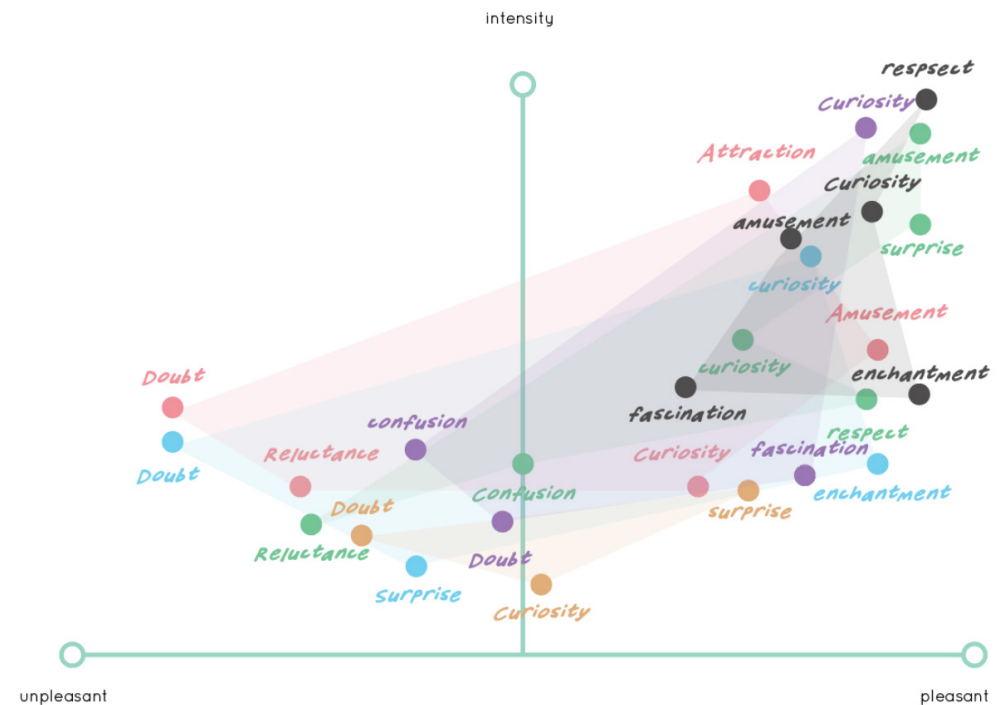


Figure [4.29]: Affective Level (each color is a different participant)

## Interpretative Level

Due to the wide range of interpretations available in the list of words and the images used, the interpretative level had the least obvious overlap. Words like “delicate”, “natural”, and “eco-friendly” had the most frequency, but the most interesting interpretations came from the ones that were not common.

One user described the samples as “feminine” because the samples represent something that is delicate on the outside, but it has a “hidden potential”. The associations with nature evoke a connection with the environment that is not present in manufactured materials. These sentiments are also echoed in the experiential tests performed in previous tests by Zhou and Ford, whose tests were more robust than the ones performed here.



Figure [4.30]: “Delicate” association with Interwoven samples

## Conclusion

Interwoven structures provoked a wide variety of responses from the participants tested, but the common thread in all of these responses is that the patterns inspire fascination. This was especially true for samples that had patterns that were obviously not natural because the origin of the samples (being grown in nature) brings a sense of dissonance that inspires curiosity. However, the weakness and fragility of these samples made participants hesitant at first. It also makes them doubt the structural integrity of the samples. The main takeaway from these tests is Interwoven samples must be strengthened to become more appealing to users. The following section explores a strengthening mechanism by making composites out of the Interwoven structures.

# Interwoven Composites

The root orientation tests and experiential characterization both made it clear that, despite Interwoven structures inspiring curiosity due to its unique production method, their fragility is off-putting. For a commercial success to be feasible, the structures need to be strengthened somehow. The extensive tinkering with the design and fabrication parameters of Interwoven structures, as well as the work laid out by Zhou and Ford led to the decision that the root layout of Interwoven is optimal to for designing natural fiber-reinforced composites (NFRPCs) with a polymer matrix. (Refer to Chapter 2 for more details)

In his 2019 work with Interwoven, Ford tested various bio-polymer matrices from pectin, to agar, and more (Ford, 2019). His work found that pectin gave the most desirable results for his purposes, despite its discoloration. Zhou, on the other hand, found that agar was able to nourish roots and create a thin film as a consequence (Zhou, 2019). Though Ford's results had more potential as pure NFRCs, these made it difficult to identify the roots as such, which takes away from one of the central wishes stated by Diana Scherer to emphasize that Interwoven structures come from the Earth.

Because of these reasons, and to limit the parameters being tested, this study explores and characterizes production methods using agar-agar as the polymer matrix for NFRPCs. Other relevant parameters include sample thickness and Interwoven pattern, as summarized below:

## Chosen Parameters

- **Pattern:** Square Grid (as in **Fig. 4.31**)
- **Template Thickness:** 3mm
- **Polymer Matrix:** Agar-agar
- **Matrix Composition:** 0.8%wt Agar-water Solution

Chapter 1 explored some of the composites that use textiles as fiber reinforcement of a polymer matrix (Cicala et al., 2010; Ramadan et al., 2015). The potential of agar matrices as a strengthening mechanism for Interwoven structures is identified in this study through a series of tensile tests. These tests standardize the procedures for testing the tensile properties of Interwoven structures; correlate properties to structural elements; and compare root properties to those of root-agar composites.

The full study is composed of the following tests: (1) Dimensional calibration tests for tensile properties (10mm), (2) Control Group - 1 cm grid cell tests (3mm), (3) Cell Size Tests, (4) Root-Agar Composites (Bulk), (5) Root-Agar Composites (Individual), and (6) Single Root Tensile Tests (DMA). The complete details of each individual test are found in **Appendix B: Technical Characterization Tests**. The following pages focus only on the comparative study and the results relevant to understanding the structure of Interwoven and its correlation mechanical properties and performance.



Figure [4.31] 1 cm grid used for NFRPMC

# Grid Cell Size Tests

*What are the effects of coarse root density?  
Does the density of root tips at vertexes impact  
tensile properties?*

The grid cell size tests revealed the most about the correlation between the structure and performance of Interwoven. The dimensions for ASTM D5035 samples were used, which had three coarse roots running along the width (25cm) (Appendix B-1; B-2). It was postulated that the strength of the structure is dictated by the number coarse roots along the width of the sample.

## Purpose

This correlation between strength and coarse roots is evaluated by changing the size of the cells in each sample, effectively changing the number of longitudinal coarse roots. **Figure 4.32** explains the differences between cell size (the length of a square in the grid), vertices (intersection of cells), and grid (sample made up of multiple cells).

## Procedure

To test the effects of cell size on mechanical properties, ASTM D5035 samples (25 x 150mm) were cut from templates with three different cell sizes: 1cm, 2cm, and 0.5cm (**Fig. 4.33**). Before preparing the samples, the grids were taken to a DHX Keyence® microscope, where the average root tip density within each cell was quantified using differences in brightness. The root density measurements give insights about differences in fine root formation caused by the templates. **Figure 4.34** shows an example of this with a 2cm cell, and the figures on the next page are the sections of the 2cm and 0.5 cm grid cells that were measured, respectively.

**Figure 4.36** is an example of a root tip density analysis being performed on a 1cm cell.

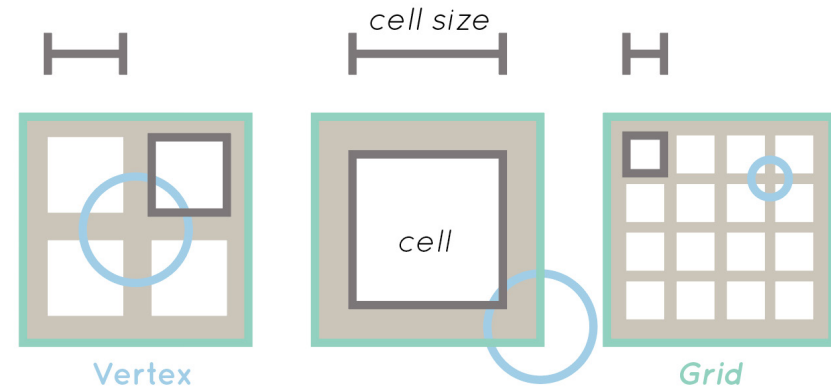


Figure [4.32]: Cell Terminology used here

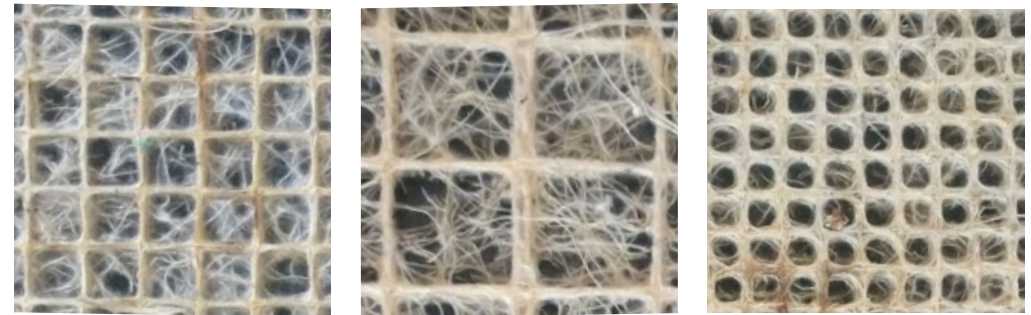


Figure [4.33]: Three cell sizes tested: (1) 1cm cell, (2) 2cm cell, (3) 0.5cm cell



Figure [4.34]: Fiber root density measured on a 1cm cell



Figure [4.35]: Fiber root density measured on a 2cm (left) and 0.5cm cell (right). Note the rounded edges of the 0.5cm cell.

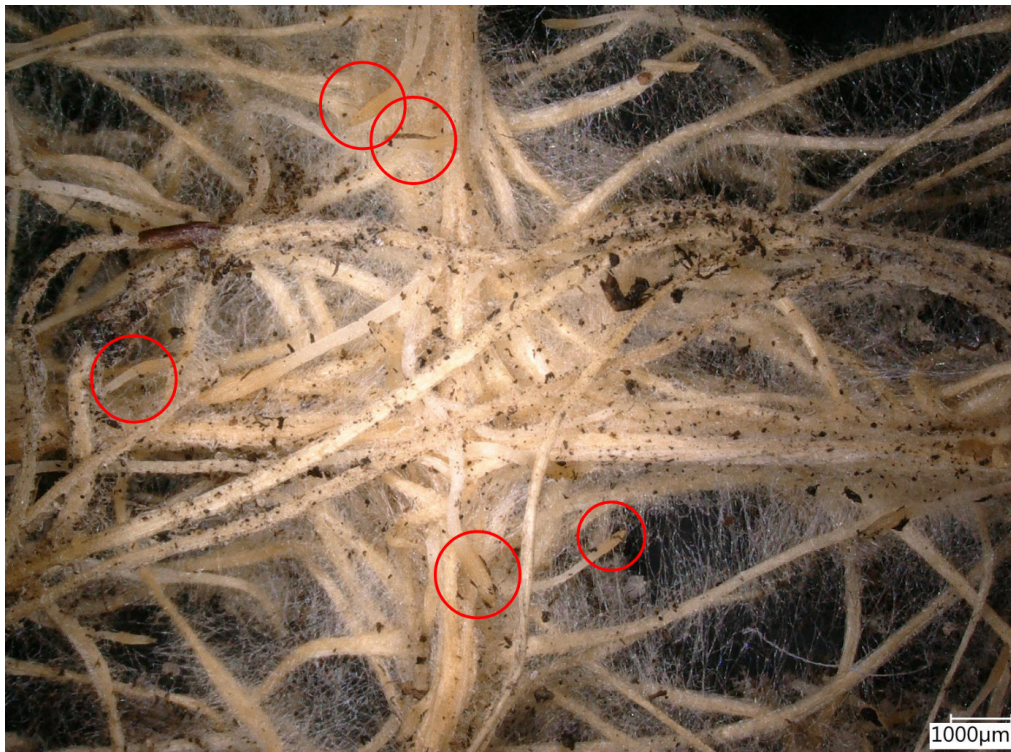


Figure [4.36]: Root tip density on a 1cm cell vertex.

This analysis is performed to further evaluate the correlation between the interwoven structure and the measured tensile properties first seen in the control group's tests (Appendix B-2).

Since the tensile test procedure is the same version of the ASTM D5035 standard used in the calibration tests and control group, (Appendix B-1; B-2), the details of the process will not be explained again. However, a summary of the parameters used for testing is provided here, The resultant tensile test coupons are shown in **Fig. 4.37**.

Due to time constraints and the size of the templates used for growing the samples, only 3 samples of each size were tested.

#### Summary of Test Parameters

- *Sample Dimensions:*  
25 x 150mm
- *Template Thickness*  
3 mm
- *Number of specimens:*  
3 x 1cm cell size  
3 x 2cm cell size  
3 x 0.5cm cell size
- Gauge Length:*  
75mm
- *Strain rate*  
15mm/min



Figure [4.37]: ASTM D5035 samples for (top) 1cm cell, (mid) 2cm cell, and (bottom) 0.5cm cell-sized grids.

## Results

At first glance, it is clear that the fine root density within each cell differs with size. However, the 2cm cells had the most visible fine root hairs, but the lowest overall root density within the cell with  $72.25 \pm 7.41\%$ . As expected, the smallest grid size had the highest root density with  $79.75 \pm 5.5\%$ . The 1cm cells had  $78.75 \pm 7.14\%$ . The differences between these values was not large, but the root density was considered representative of the cross sectional area of the samples (as was done in the control group tests of Appendix B-2), so these percentages were used to calculate cross-sectional area and derive stress-strain curves. The average modulus and tensile strength of each cell size were computed. The sample with the modulus closest to the average of each size was plotted against that of the other sizes to compare results (Fig. 4.38).

### Stress-Strain Curves

The stress-strain plots in figure Fig. 4.38 include a representative curve from each sample group based on proximity to the average values of the modulus, which are summarized by the bar graph in Fig. 4.39. The group with 2cm cells had the steepest modulus with  $0.324 \pm 0.051$  MPa, followed by 0.5cm samples at  $0.196 \pm 0.086$  MPa, which is only slightly higher than the 1cm group's average,  $0.182 \pm 0.046$  MPa.

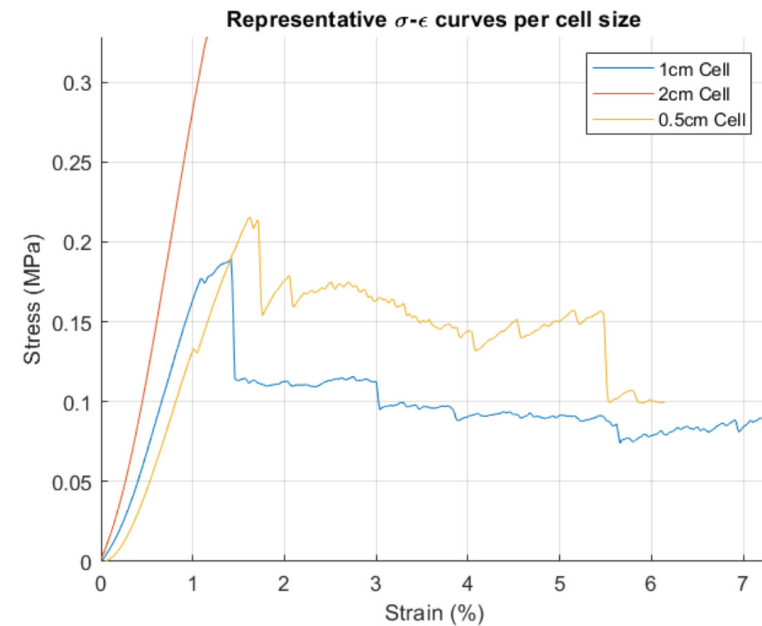


Figure [4.38]: Representative Stress-Strain Curves for each cell size

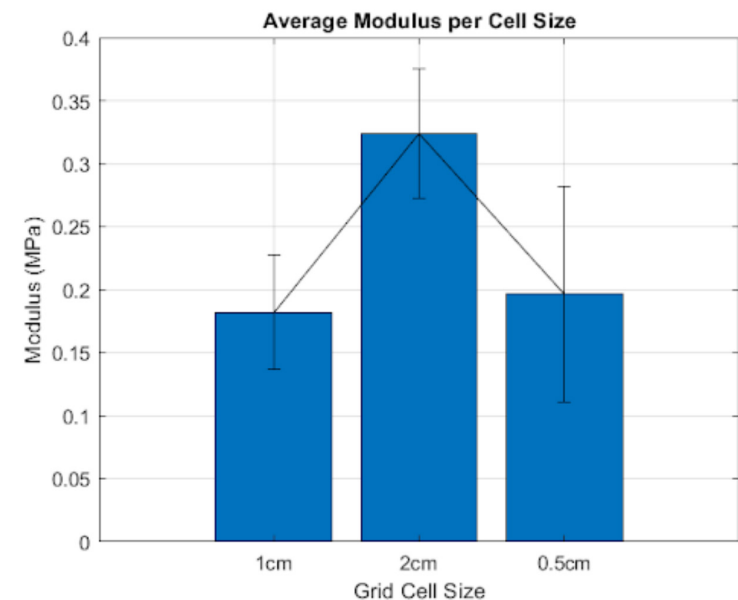


Figure [4.39]: Average modulus per cell size

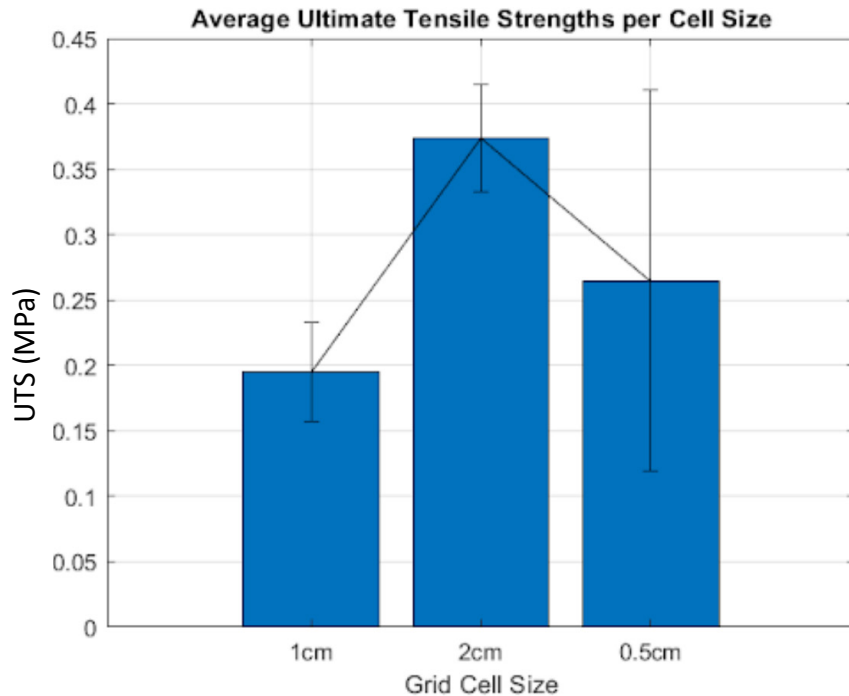


Figure [4.40]: Average tensile strength per cell size

### Average Tensile Strength

The ultimate tensile strength averages per group followed the same trend as the moduli (Fig. 4.40). 2cm grid cells yielded the strongest samples with an average UTS of **0.374 ± 0.041 MPa**, 0.5cm cells were next (**0.265 ± 0.146 MPa**), and 1cm cells had the lowest UTS (**0.195 ± 0.038 MPa**).

### Vertex Root Tip Density

One final correlation found with the samples was the number of root tips present at the vertexes. The root tip density reflected the same trend presented by the two previous bar graphs. Below is a visual summary. On average, 2cm cells had **16.13 ± 5.13** root tips at each vertex. The next densest vertexes were found in 0.5cm cells, which had **3.88 ± 1.97**, and 1cm cells had an average of **3.84 ± 1.92**. The difference in root tip density was hardly

evident in the last two groups, but one key difference between them was also how the roots looked in the cell. The smaller cells had roots turning corners around a small diameter, which gave the small squares a more circular look, whereas the 1cm samples only had slightly rounded edges. This effect is even less evident in the 2cm cells.

### Conclusion

The tensile properties of ASTM D5035 coupons with varying grid cell sizes (1cm, 2cm, and 0.5cm) were tested. The largest cell size exhibited the highest elastic modulus and UTS. A direct correlation between root tip density and mechanical properties was identified through digital microscopy. The strongest samples also had the highest number of roots per vertex, suggesting root tip density is a better indicator of tensile properties than the number of coarse roots along the sample's width.

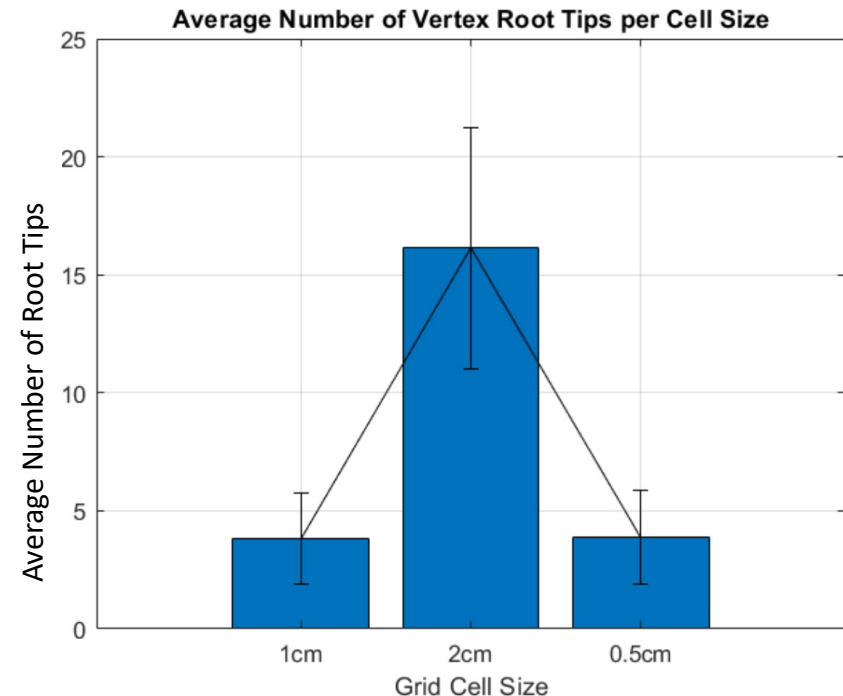


Figure [4.41]: Average number of root tips per cell size

# Root-Agar Composites

The study up to this point has slowly been mapping the properties of Interwoven structures to polymer-matrix composites as a way of strengthening its properties. As mentioned in Chapter 3: Tinkering, Ford already performed extensive tests on various composite matrices compatible with Interwoven, and Zhou paired this with their own tests, choosing agar to be the best choice for practical applications (Ford, 2019; Zhou, 2019).

## Purpose

Tensile tests performed on the Interwoven samples, as well as individual roots (Appendix B-4), suggest that the interwoven configuration of roots alone is inefficient at transferring loads. Polymer matrices are better at uniformly transferring loads to fibers in composites. This study follows Zhou's work and tests the properties of agar-matrix composites through tensile testing.

## Procedure

A 0.8%wt agar-water matrix is used to prepare ASTM D3039M samples to execute the standard test methods for Tensile Properties of Polymer Matrix Composite Materials. Due to the many possibilities of polymer matrix composites (PMCs), the standard provides guidelines for deciding on sample dimensions rather than precise dimensions (D30 Committee, 2017).

The guidelines in the standard were mainly fulfilled by the sample dimensions for testing textiles (ASTM D5035 samples), so the parameters were left the same to facilitate comparison within this study. The only parameter in the standard that could not be fulfilled was that of using a 1cm thickness because agar shrinks into a film that was thinner than this. Finally, ASTM D3039M samples are meant to be manufactured flat, and that was tested here in two different methods described below.

## Sample Preparation

The composition of agar was determined during the tinkering phase of the project. Chapter 3 describes the reasoning behind choosing a matrix composition of 0.8wt% agar (8g agar:1L water), as well as its preparation method.

Recall from the fabrication parameters that the shrinkage that occurs when agar dries induces warping, which is not desirable for tensile testing. The Interwoven grids used to produce ASTM D3039M samples were clamped down throughout the drying process (which takes about 5 days in ambient temperature, and 6 hours in a humidity chamber at 30°C and 50% humidity).

## Clamping Mechanisms

The two clamping methods can be described as bulk clamping and individual clamping. Bulk clamping used a large clamp to hold down the edges of the entire Interwoven grid (Fig. 4.42), whereas individual clamps were 3D printed to produce samples with the exact dimensions for tensile testing (Fig. 4.43).

## Bulk-Clamped Samples

Using the clamping mechanism seen in the upper images, the agar gel was poured on top of an Interwoven grid with 1cm cells. This cell size was used to compare directly with the “control” group (Appendix B-2). Once poured, the top of the mold (seen in the second image) was added and weights were added on top of the

samples to evenly distribute the agar-agar and keep the inner sections of the grid flat as they dried.

The resulting bulk clamp and individual tensile coupons are seen in Fig. 4.44 and 4.45, respectively. Note from the bulk composite that the fibers of the grid are not distributed evenly

throughout. The samples taken from this bulk grid were chosen from areas that were most consistent, but some sections had holes in the agar matrix. Another notable observation is that the bulk grid was smooth and slightly curved (likely due to internal stress caused by the shrinkage), but the individual coupons are less smooth. This



Figure [4.42]: Bulk Clamping Mechanism



Figure [4.43]: Individual Clamping Mechanism



Figure [4.44]: Agar-Root composite sheet (bulk clamped)

## Individually Clamped Samples

could be a result of internal stresses being relieved when the composite sheet was cut into individual coupons. The internal stresses were no longer evenly distributed throughout the root fibers after this, which led to some deformation.

The 3D printed clamp/mold for individual samples is seen in **Fig.4.43**. Each mold had 4 clamps to hold the edges of the roots in place and prevent shrinkage. A laser-cut top was added to provide even pressure throughout the sample. Sample preparation here was similar to that of the bulk samples, except that most of the cutting took place before pouring the agar.

Samples were cut from a large grid, but in this case, they were left slightly oversized on each side so that the clamps could hold down the roots. The opening at the top has the sample dimensions, of the ASTM D5035 samples used thus far. Once the roots are clamped into place, the agar is poured on top (just enough to cover the roots) and the top is pressed lightly on it so that any excess agar is pushed up and out. The samples are then left to dry at room temperature (about 5 days). The resulting samples are seen in **Fig. 4.47**.



Figure [4.46] Individual Clamps



Figure [4.45] :ASTM D3039M samples (bulk)



Figure [4.47] ASTM D3039M Samples (Individual)

## Results

The samples in the last image are the resulting composites before being cut down to the exact dimensions. Note the rugged edges of some of the samples. These are the roots that were clamped down and were not covered in agar-agar, and they are removed prior to testing. Though there was some deformation in the left-most sample, that was caused by improper clamping of that sample and not internal stresses like what was seen with the bulk samples. Below are the testing parameters.

### Summary of Test Parameters

- *Sample Dimensions:*  
25 x 150mm
- *Template Thickness*  
3 mm
- *Number of specimens:*  
Seven (7)
- *Sample Thickness*  
Varied - (standard suggests 1mm)
- Gauge Length:*  
75mm
- *Strain rate*  
15mm/min

Once the agar matrix was fully dried, it flattened the cross section of the sample, so it was assumed that the porosity seen in the pure root samples was filled. As such, the cross sectional area of the composite samples was calculated by multiplying the average measurements of thickness and width based on three separate measurements for each dimension.. These values were then used to convert force-displacement curves the stress-strain curves seen below. Though 7 samples were tested, two of them were discarded because the modulus was less than half of the average of the rest of the samples.

### Bulk-Clamped

The bulk composite samples' response to load gave a different curve than what has been seen thus far (**Fig. 4.48**). All samples exhibited the same behavior. The initial slope is very low for all samples, which exhibit a similar positive curvature to the one seen in the DMA samples (Appendix

B-4). At 0.5% strain, all samples enter a very short linear region before reaching an inflection point, at which the curvature becomes negative, but the slope continues to increase slowly. This continues until the fracture point, which occurs abruptly on all samples except Sample 5, which shows peaks at about 1.7% strain. During the testing, slight cracking sounds were heard at the time when the peaks occurred.

The linear region for these samples was very small, so the slope was determined from the region between 10-30% of the UTS. The process for this is explained in more detail in Appendix B-2. **Fig. 4.49** summarizes the elastic moduli that were calculated with these slopes.

The average elastic modulus of the set was **1.313 ± 0.544 MPa**. As expected of Interwoven

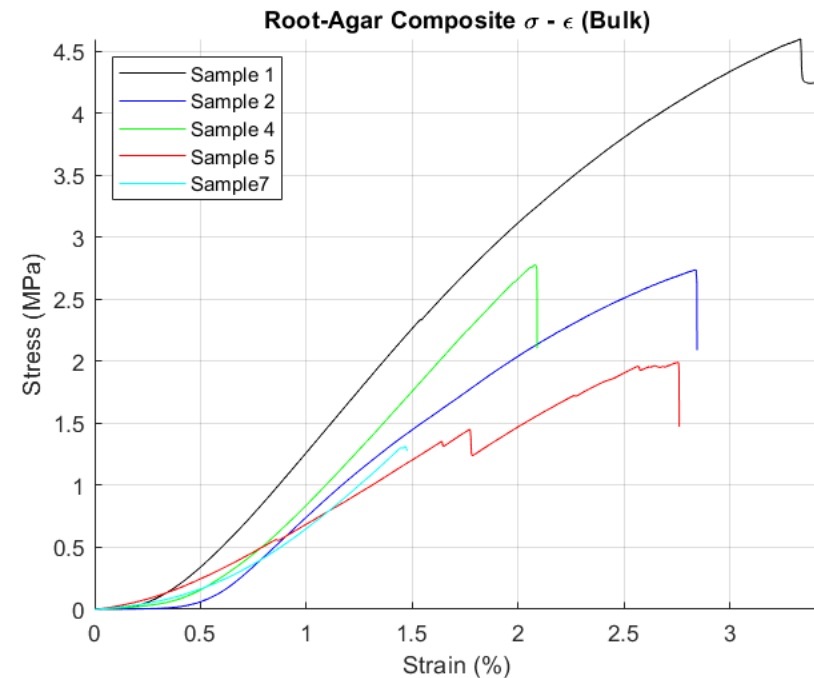


Figure [4.48] Stress-Strain curves of Bulk samples

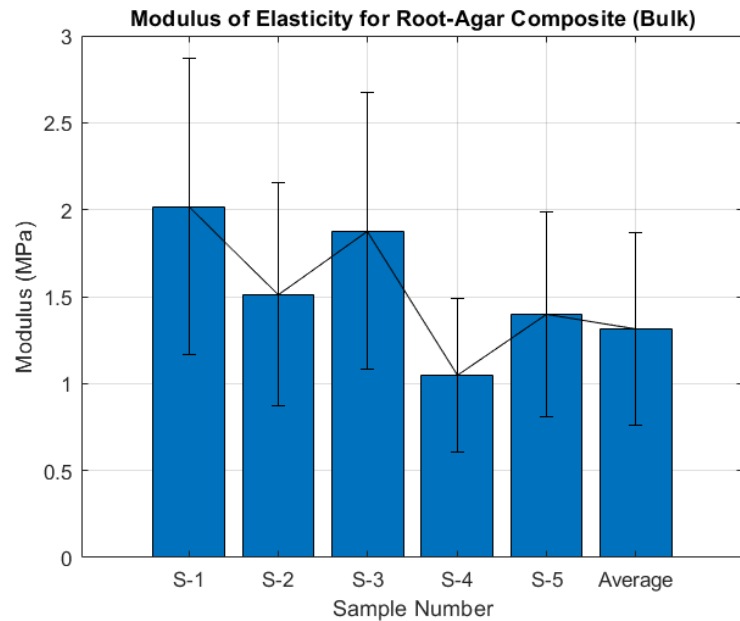


Figure [4.49]: Modulus of Elasticity for Composites (bulk)

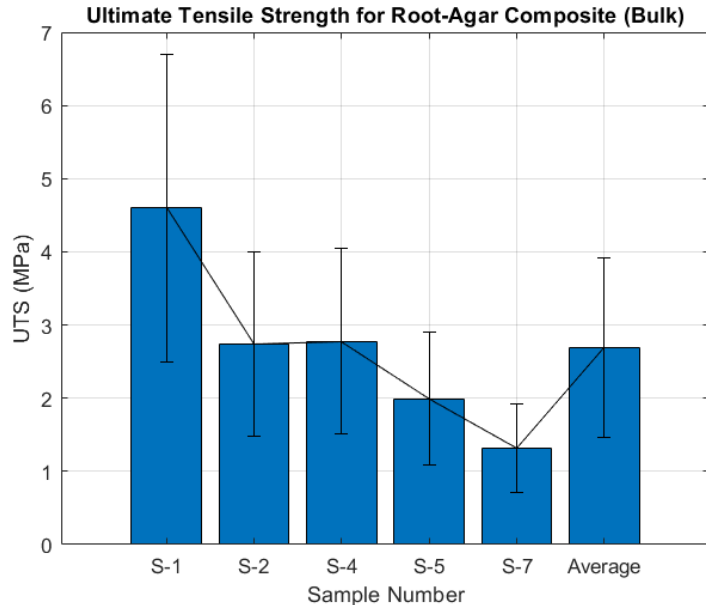


Figure [4.50]: UTS for Composites (bulk)

structures, the modulus was not the same throughout the different samples. The UTS of the samples was considerably higher than that of any non-composite Interwoven structures. The average UTS was **2.69 ± 1.228 MPa**, which is one order of magnitude higher than the next strongest structure (2cm cell grids). A summary of all tensile properties across the samples can be found in **Table 4.1**.

## Individually-Clamped

The clamping process played a significant role on the mechanical properties of the composite samples. Clamping down individual tensile coupons resulted in stiffer samples, as evidenced by the steeper stress-strain curves in **Fig. 4.51**. The general shape of the curves was the same as the bulk samples - an initial upward curvature followed by a short linear region, after which the curvature becomes negative (while still increasing).

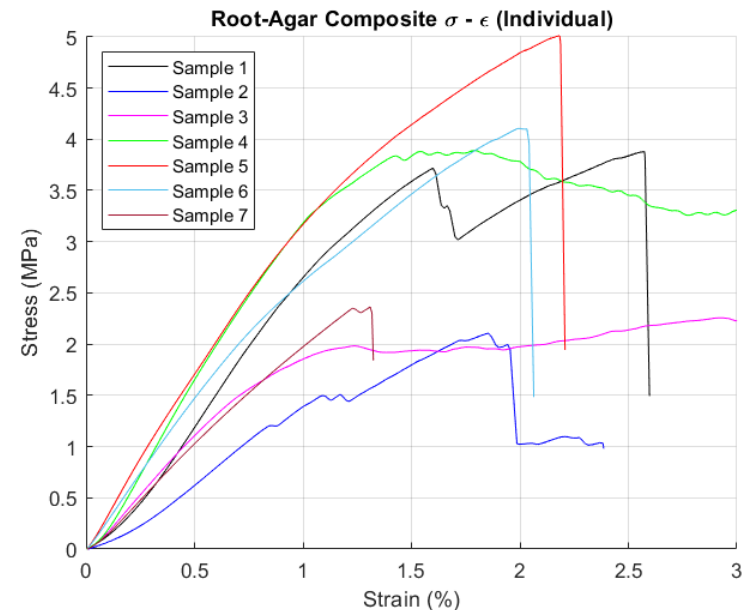


Figure [4.51]: Stress-strain curves of individually clamped composites

Failure was less abrupt for these samples, as multiple samples exhibited multiple peaks related to individual coarse roots breaking. Sample 3 and 4 showed more plastic deformation rather than a brittle failure.

These samples were stiffer than bulk samples and the modulus was higher, with an average value of **2.705 ± 0.5711 MPa**. Individual clamping molds for the samples consistently doubled the modulus of elasticity and halved the variance (only 21.11%). While the average tensile strength was not doubled, it was still considerably higher than that of the bulk samples, with a value of **3.479 ± 1.057 MPa**. Figures **4.53** and **4.54** show the spread of both of these values, and **Tables 4.1 and 4.2** show the elastic moduli and UTS of all data sets in the study in descending order.

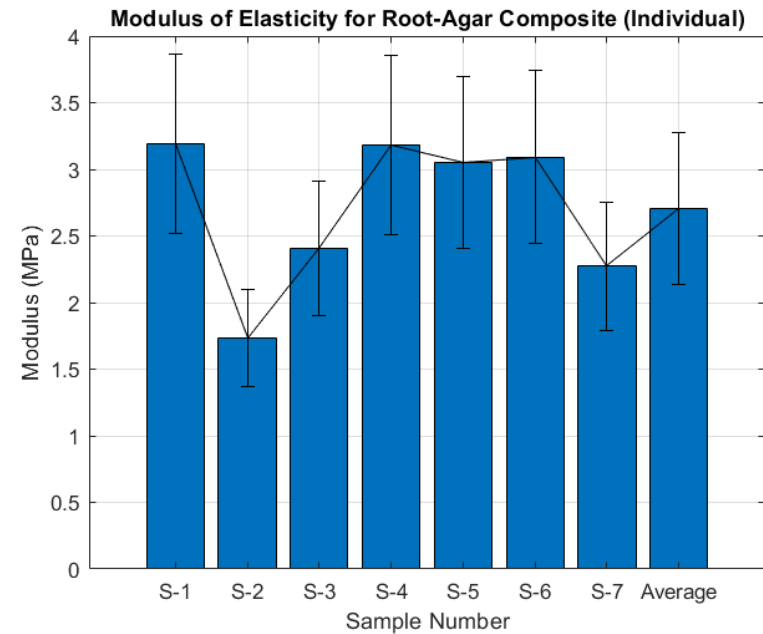


Figure [4.53]: Modulus of Elasticity for Composites (individual)

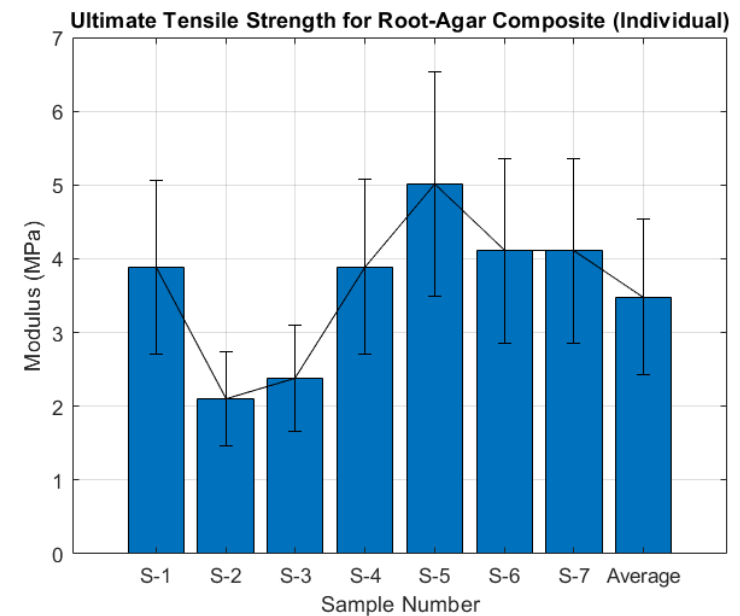


Figure [4.54]: UTS for Composites (individual)

Modulus Values per Test Group			
Group	Average Modulus (MPa)	Standard Deviation	Variance (%)
Root	<b>4.610*10<sup>1</sup></b>	± 24.01	52.07
Agar(Ind.)	<b>2.705*10<sup>0</sup></b>	± 0.571	21.11
Agar (Bulk)	<b>1.3125*10<sup>0</sup></b>	± 0.554	42.22
2 cm Cell	<b>3.235*10<sup>(-1)</sup></b>	± 0.051	15.89
Control	<b>2.931*10<sup>(-1)</sup></b>	± 0.125	42.68
0.5 cm Cell	<b>1.964*10<sup>(-1)</sup></b>	± 0.0859	43.74
1 cm Cell	<b>1.822*10<sup>(-1)</sup></b>	± 0.046	24.97

Table [4.1]: Comparison of all moduli tested in descending order

UTS Values per Test Group			
Group	Average Modulus (MPa)	Standard Deviation	Variance (%)
Root	<b>1.018*10<sup>2</sup></b>	± 61.98	60.86
Agar (Ind.)	<b>3.479*10<sup>0</sup></b>	± 1.057	30.37
Agar (Bulk)	<b>2.685*10<sup>0</sup></b>	± 1.229	45.76
2 cm Cell	<b>3.74*10<sup>(-1)</sup></b>	± 0.041	10.94
0.5 cm Cell	<b>2.65*10<sup>(-1)</sup></b>	± 0.146	55.04
Control	<b>2.63*10<sup>(-1)</sup></b>	± 0.074	28.04
1 cm Cell	<b>1.95*10<sup>(-1)</sup></b>	± 0.038	19.51

Table [4.1]: Comparison of all moduli tested in descending order

## Discussion

Agar is very compatible with Interwoven structures as a polymer matrix. The fracture surfaces of these samples were mainly catastrophic, where both the matrix and reinforcement were fractured. This is a sign of proper matrix-fiber adhesion and means that the agar matrix is effectively distributing the load to the Interwoven roots. The tensile properties of the composite samples are still small compared to a single root, but they are much larger than that of the Interwoven structure on its own. The more curved response to loading on these samples suggests that, although the agar makes the samples stronger and stiffer, they

are less brittle than roots on their own. The negative curvature of the samples' responses indicate that plastic deformation is happening without immediate failure, which makes sense considering the composite samples feel more malleable when held.

Bulk clamping helped distribute the load quite well, but it did have much weaker samples than the individually processed ones. This is likely due to the relaxation of fibers that occurs when the roots were cut down to the dimensions for testing.

Throughout the process of agar drying out, the taut roots held together by the clamp build up internal stresses. However, by trimming the bulk sample down to the testing dimensions, the roots are also cut, so the internal stresses are relieved. The tensile coupons even deformed a bit as a result of this.

The relaxation of the reinforcement phase was not evident in the individually processed samples because the roots that are cut off for sample preparation were not cast in agar, so trimming the edges off did not remove any internal stresses in the sample.

### Comparing Composites to pure Interwoven

As this study has shown with all of its different tests, there are many parameters and microstructural elements that make up the tensile properties of Interwoven structures, but using agar to form natural fiber-reinforced polymer matrix composites (NFR-PMCs) is an effective strengthening mechanism. The matrix properties could also

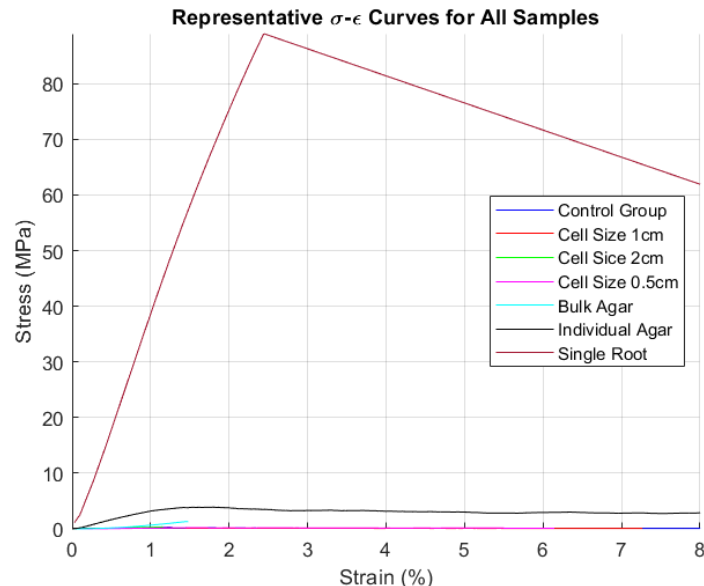


Figure [4.55]: Representative stress-strain curves of all samples

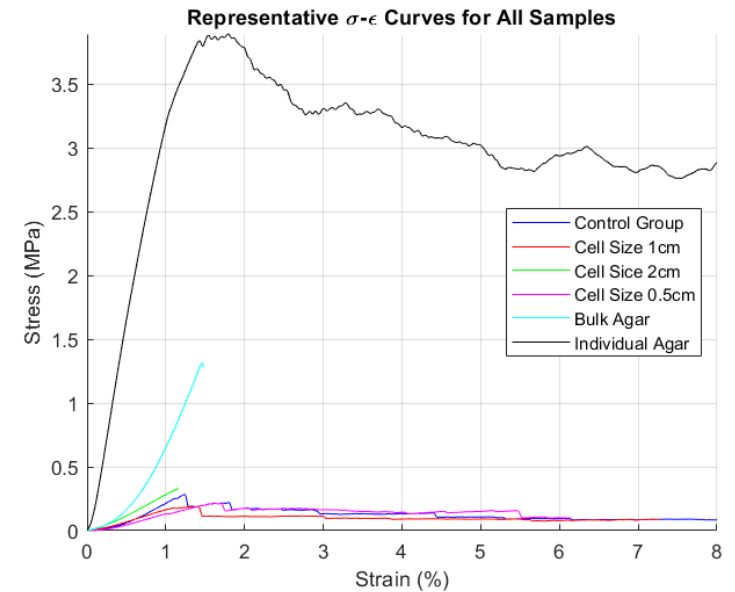


Figure [4.56]: Representative curves of all data sets, excluding single roots

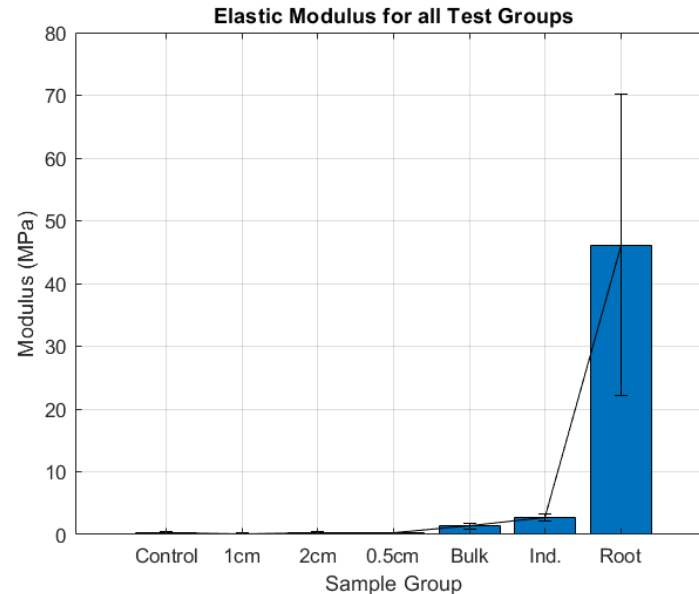


Figure [4.57]: Comparison of all moduli

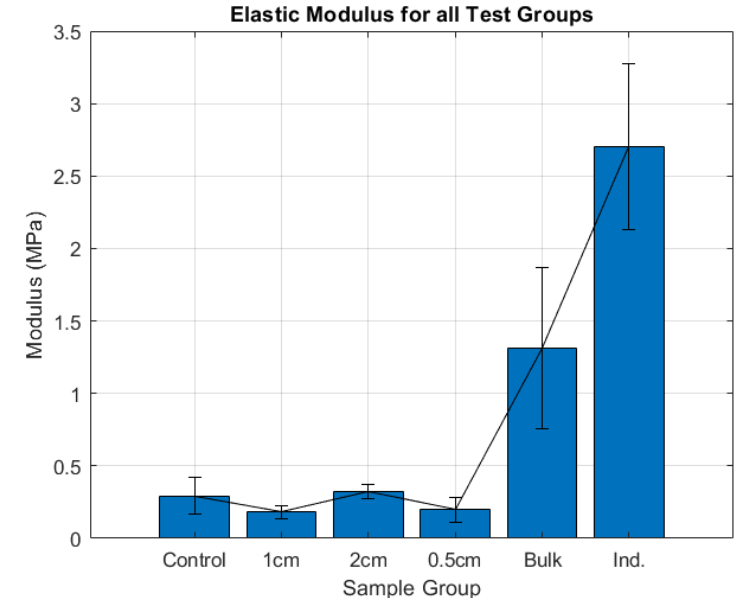


Figure [4.58]: Comparison of all moduli, excluding single roots

be optimized to ensure that all of the applied load is properly distributed throughout the structure, and a stiffer matrix might even better represent the strength of individual roots. The graphs below show how agar-root composites more closely behave like the single root than the other variations of Interwoven structures tested here.

## Conclusions

Interwoven structures are complex structural members composed of many roots that intertwine and get tangled in such a way that, when pulled from one end, the load is distributed throughout. The mechanism of transfer is still unknown, but it is clear from this study that load transfer is largely improved by adding a compatible matrix. Root-agar composites were developed using two different processing mechanisms. One in which the composites were processed in bulk and the other where they were individually processed. Composite properties can be further customized if the parameters explored in this study are implemented. The volume fraction of the reinforcing phase (the Interwoven structures) can be altered by varying grid cell sizes, and this also changes the properties of the root grids. Changes in the matrix (both in composition and in the polymer used) will also greatly influence the mechanical properties of the structure in a way that has yet to be studied in depth. Interwoven offers a promising manufacturing technique to design structures in collaboration with nature that also have customizable mechanical properties, something that will become more evident as the material properties of the structures are further developed. This study has only scratched the surface of understanding the complexities of Interwoven structures, but it lays the foundation from which more extensive explorations may be conducted. The following section aims to demonstrate and communicate these characterization results in a more accessible manner.

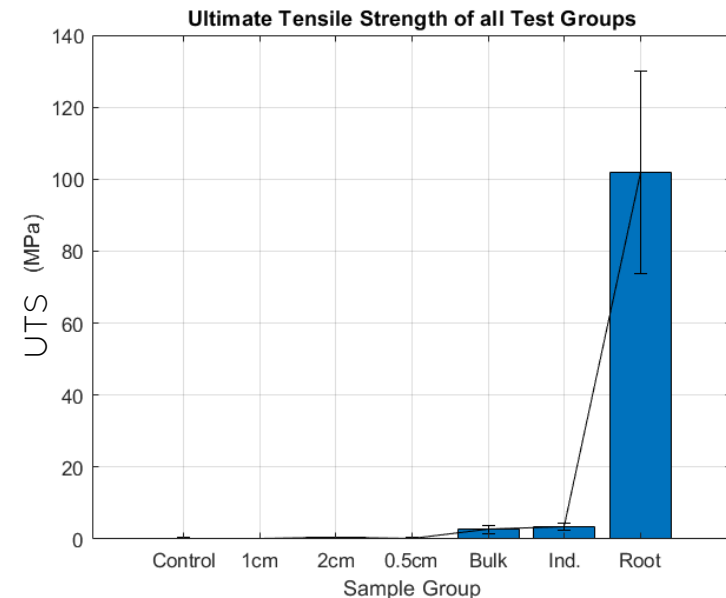


Figure [4.59]: Comparison of all UTS values

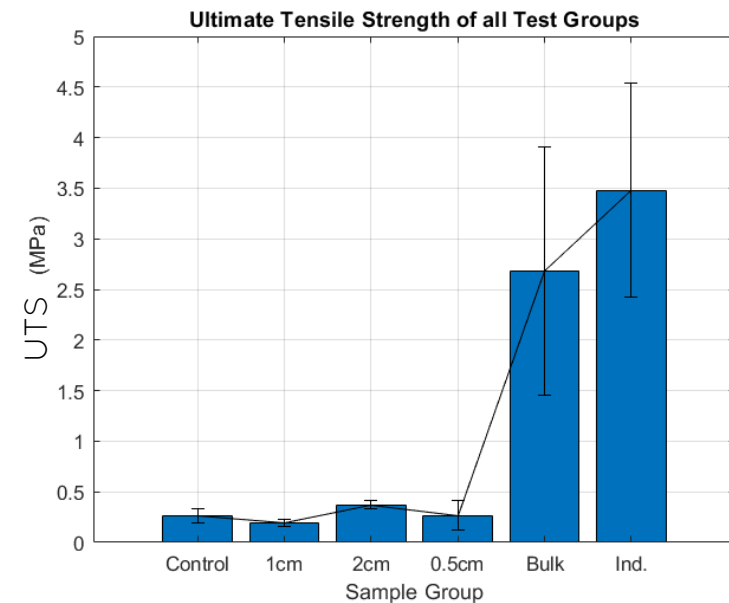


Figure [4.60]: Comparison of all UTS, excluding single roots

# **5 - Material Demonstrator**

# Parameter Overview

Recall that the purpose of this project is to extend the technical characterization and present it in such a way that it is **accessible** to designers. This way, they do not have to perform the same tests to understand and design Interwoven structures. This includes correlating the mechanical properties to the parameters identified in the opening chapters. Parallel processes of tinkering and technical characterization led to the correlations seen below.

Of the three types of parameters identified (materials, design, and fabrication-related), the design parameters and fabrication parameters are the ones that the designer has the most control of. These include the shape and size of a pattern, the templates used to make the structure, and the uses that are given to the Interwoven structure (i.e. as a reinforcement for NFRCs).

Material parameters, such as the type of plant used and the factors that influence plant growth also have an impact, but those were not studied extensively and are thus excluded. This chapter now focuses on presenting the results obtained from the tinkering and experiments conducted in a clear and concise manner through a material demonstrator.

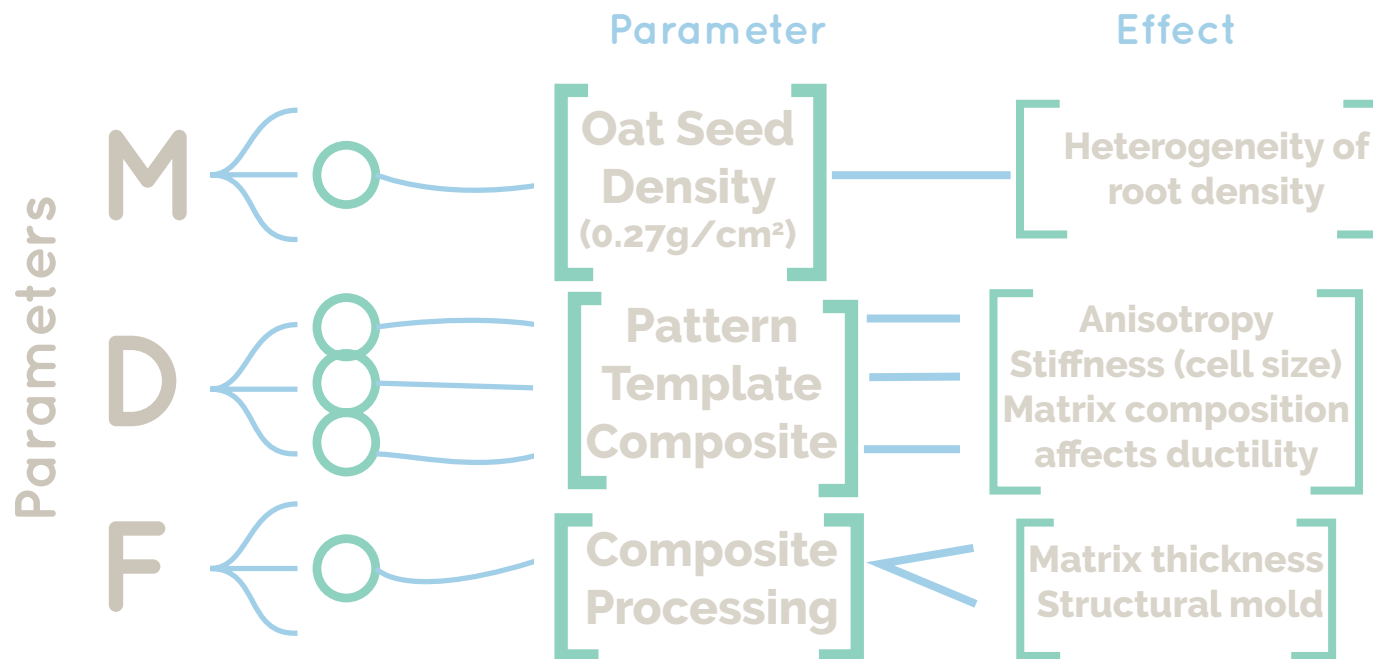


Figure [5.1]: Correlation between parameters and their effect on the Interwoven Structure

## Material Demonstrator

The material demonstrator focuses on the main findings of the technical characterization:

- (1) cell sizes affect tensile properties like the amount of elongation and stiffness of a sample,
- (2) the use of agar as a polymer matrix for Interwoven composites effectively makes the material much stronger
- (3) The fabrication method of Interwoven lends itself to designing structures with localized properties.

The three points above became the starting point of a brainstorm session for designing the demonstrator. The demonstrator should be able to visually summarize the information obtained from the stress-strain curves and microscopic analysis in Chapter 4. The best way to make that happen is by maintaining a simple approach that showcases the material's response to tensile stress. With this in mind, the following vision was used to brainstorm the embodiment of the material demonstrator.

*How can an Interwoven structure in tension effectively exhibit the properties identified through technical characterization?*

## Brainstorming: Objects in Tension

Every day, objects in tension can be easily encountered: whether this includes an umbrella's fabric pulled taut by wires, a hammock hanging from tree branches, or a plastic bag loaded with groceries. A brainstorming session revolving around products in tension resulted in the collection of images seen below. Interwoven materials are not yet developed enough to make a full product, nor do they have the strength to withstand critical failure. It was determined that a large Interwoven sheet that is deformed at various points with attached weights was one way to take advantage of the localized properties available to Interwoven designs.

*A large sheet with weights hanging from it will showcase the localized properties available through Interwoven designs.*

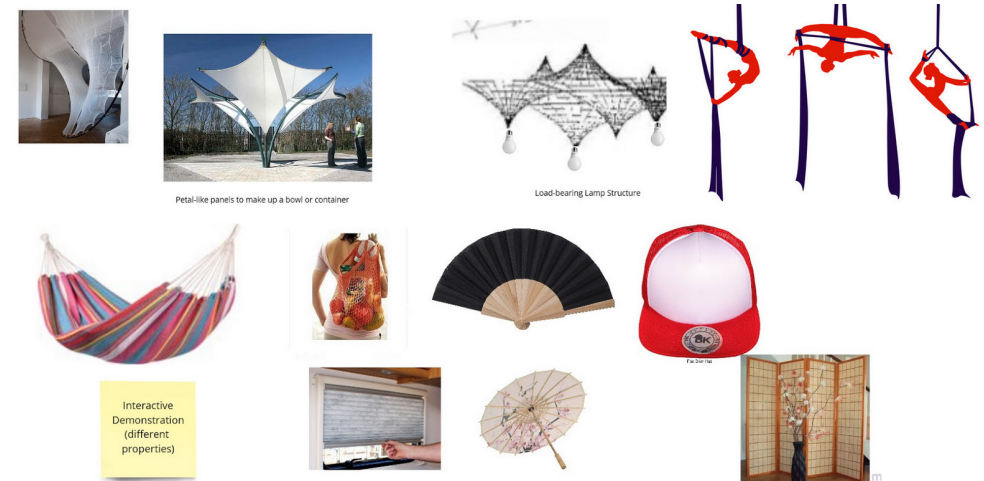


Figure [5.2]: Examples of objects and architecture in tension

## Tensile Structures

Tensile architecture has many examples of large pieces of fabrics being pulled in tension to create interesting structures. In some of these cases, the structural elements that pull the textiles are hanging from something, as seen Fruto Vivas' Venezuelan Pavilion below.

A more common example of a hanging structure that exhibits tension is seen in the Wooden Music Mobile in the right. Though the tensions is kept mainly in the strings and wooden supports of the

structure, mobiles for babies are interesting because there is tension acting on the main structure from both above and below. The pulley holding the two wooden beams pull it up, while the weight of the plush fish pull it down in balance. In the interest of showcasing different types of deformations available to Interwoven materials, this same principle will be replicated.



Figure [5.4]: Wooden Music Mobile - Ocean Mint



Figure [5.3] Venezuelan Pavilion - Fruto Vivas

*The material demonstrator will be a hanging plane that itself has objects hanging from it, deforming the sheet from two directions like the beams in a children's mobile.*

## Designing the Demonstrator

The tensile tests from Chapter 4 had four different structures that will be included in the demonstrator. An example of each is shown in the images on the right.

### 4 types of structures used

- (1) 1cm cell grid
- (2) 2cm cell grid
- (3) 3cm cell grid
- (4) Agar-Interwoven NFRC

Each of the four structures had different mechanical properties. Group (1) has moderate elongation, but weak tensile strength, (2) had the highest stiffness out of the pure-root structures, while (3) had the most elongation and is easiest to bend. Lastly, (4) had the highest strength of the four and is least likely to deform under the same amount out weight as the other structures.

A successful material demonstrator will showcase the individual strengths of each group without reaching a critical point (or failure).

For the sake of bringing attention directly to the structures, the planar sheet will not have a complex shape. It will remain a flat rectangle only to be deformed while hanging. An interesting addition to these

four structures that has not yet been explored is the addition of multiple shapes to the same plan. All four structures will remain as parts of the same structure to showcase the ability to customize the properties of Interwoven structures for different responses located in specific areas.

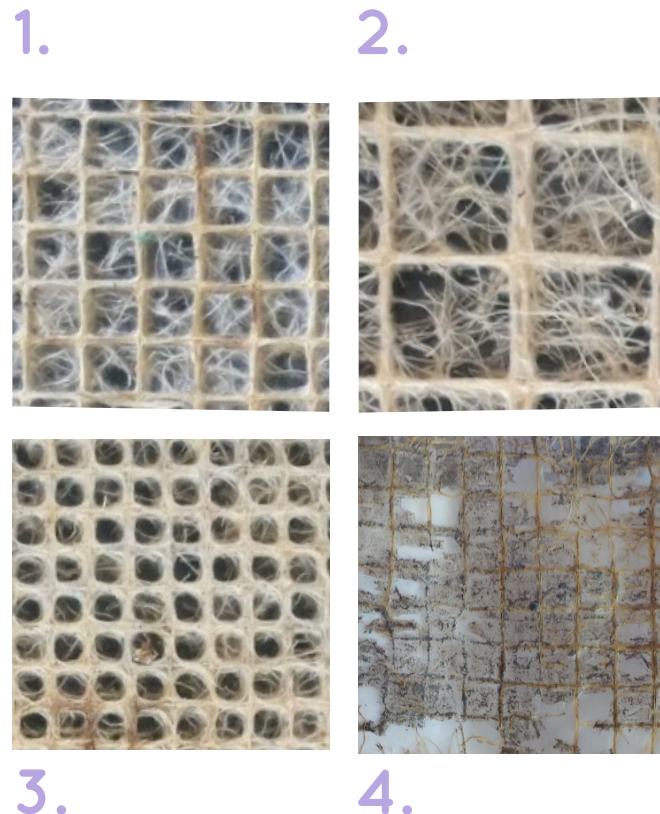


Figure [5.5]: Four structural phases tested

## Demonstrator Design Requirements

The demonstrator had to meet the following requirements to be considered a success.

- (1) Showcase all four structural phases
- (2) Exhibit tensile deformation
- (3) Demonstrate differences in ductility through bending
- (4) Deform in two directions
- (5) Pair different structures next to each other
- (6) Make it as large as possible

Though the list is not extensive, these requirements helped ideate different forms of deformation. Requirement (6) was limited to 72 cm x 35 cm by the available space for growing the plants. This list helped ideate on the combinations of structures that could produce interesting deformations. **Fig. 5.6** became the guiding source for the final design seen in the following page.

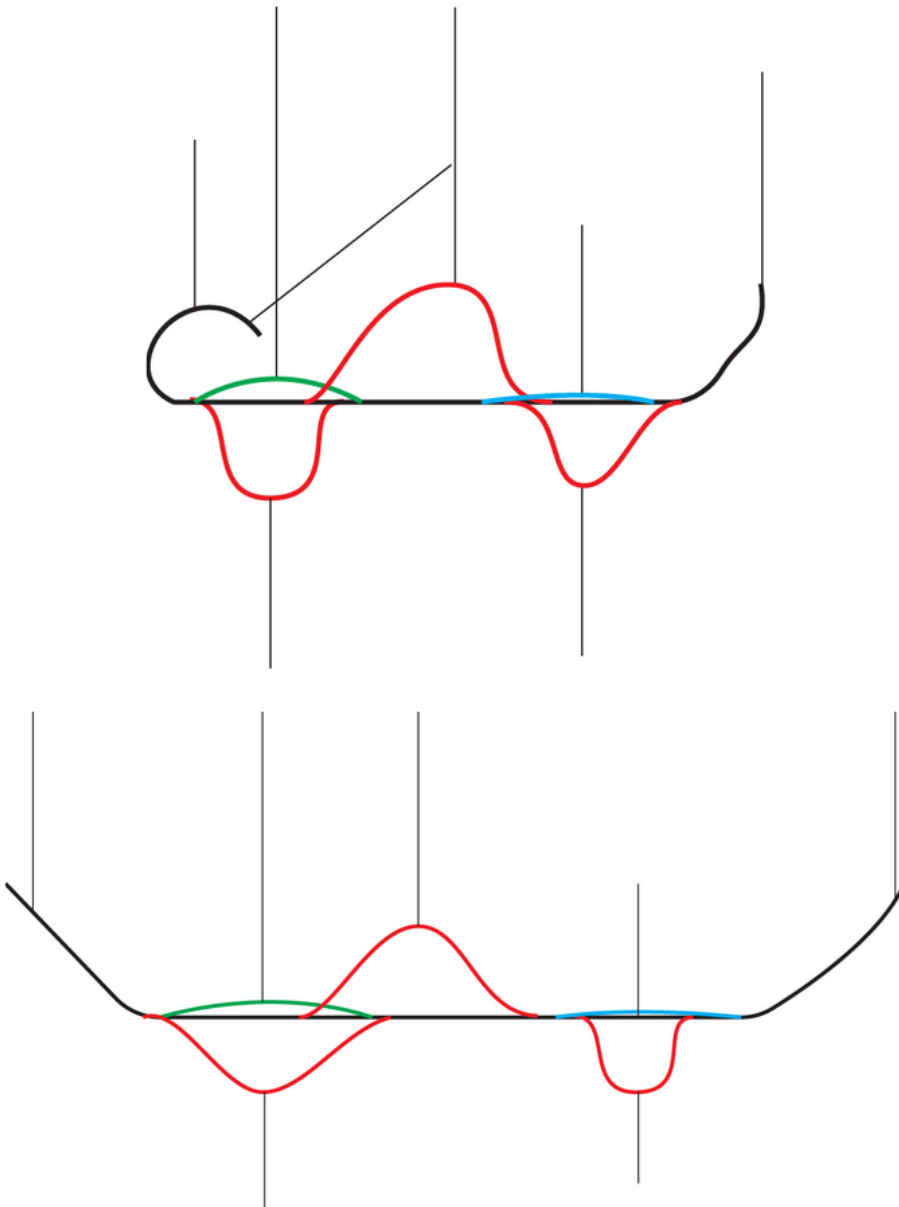
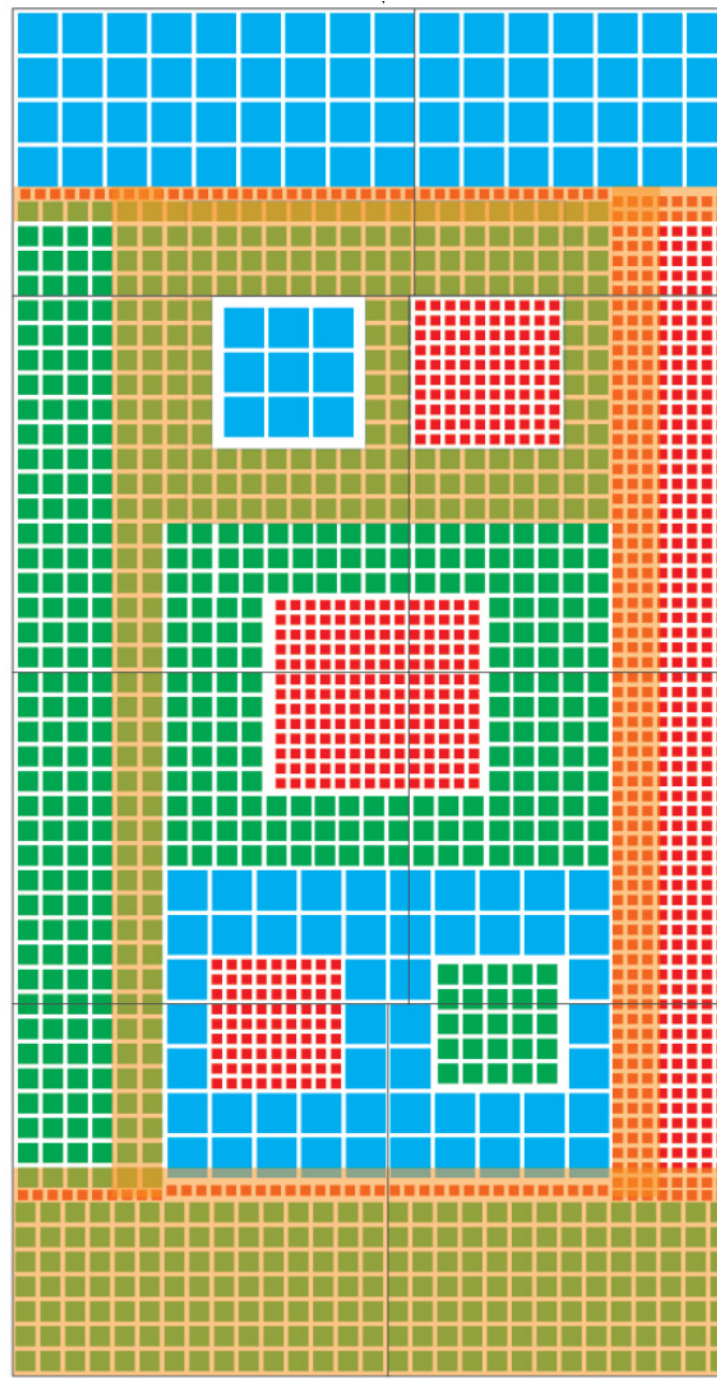
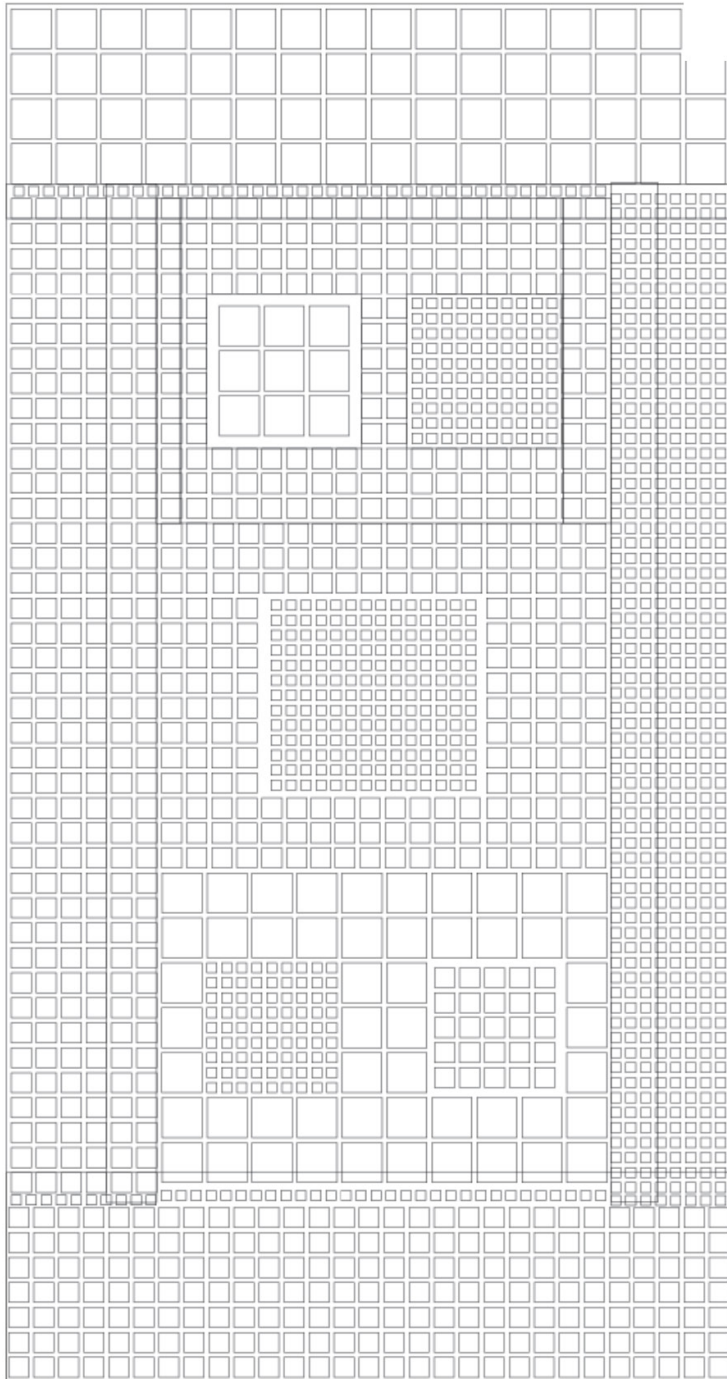


Figure [5.6]: Side views of the hanging plane as it is deformed in two directions.



The final demonstrator design is seen in **Fig. 5.7 and 5.8**. Both images show the same information, but one is color coded to facilitate the differentiation of phases. The final dimensions are (72 cm x 35 cm).

Each one of the edges has a section with a different structural phase. The shortest edges have the strongest sections (2cm grids and agar NFRC). The long edges have the more malleable structural phases. Agar was added to the “hinges” of each phase - the sections where one ends and the next begins. This is to prevent unwanted ripping. Five squares ~100cm<sup>2</sup> each are in the central plane. Each one has one of the three cell sizes and is surrounded by the next stiffest phase.

The 0.5cm squares deform the most, so it is surrounded by three matrices to result in a different deformation, each. A simulation of this is seen in the next page.

■ Sections with Agar    ■ 2 cm  
■ 1 cm                    ■ 0.5 cm

Figure [5.7]: Outline of planar sheet (to scale) full dimensions 35 cm x 72 cm

Figure [5.8]: Color coded demonstrator with different structural phases

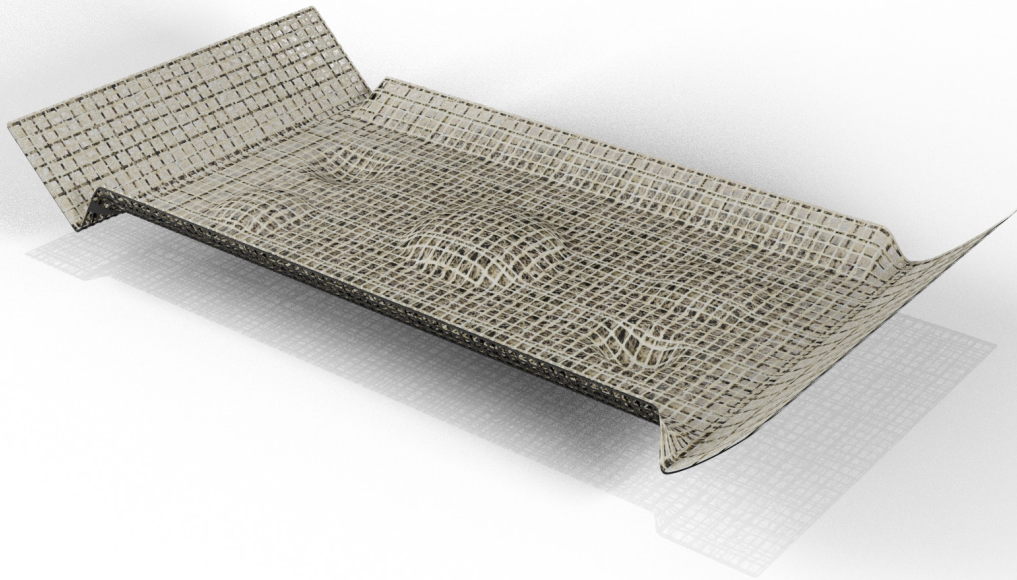


Figure [5.9]: Isometric view of a simulated demonstrator under tension



Figure [5.10]: Side view along the length of a simulated demonstrator under tension

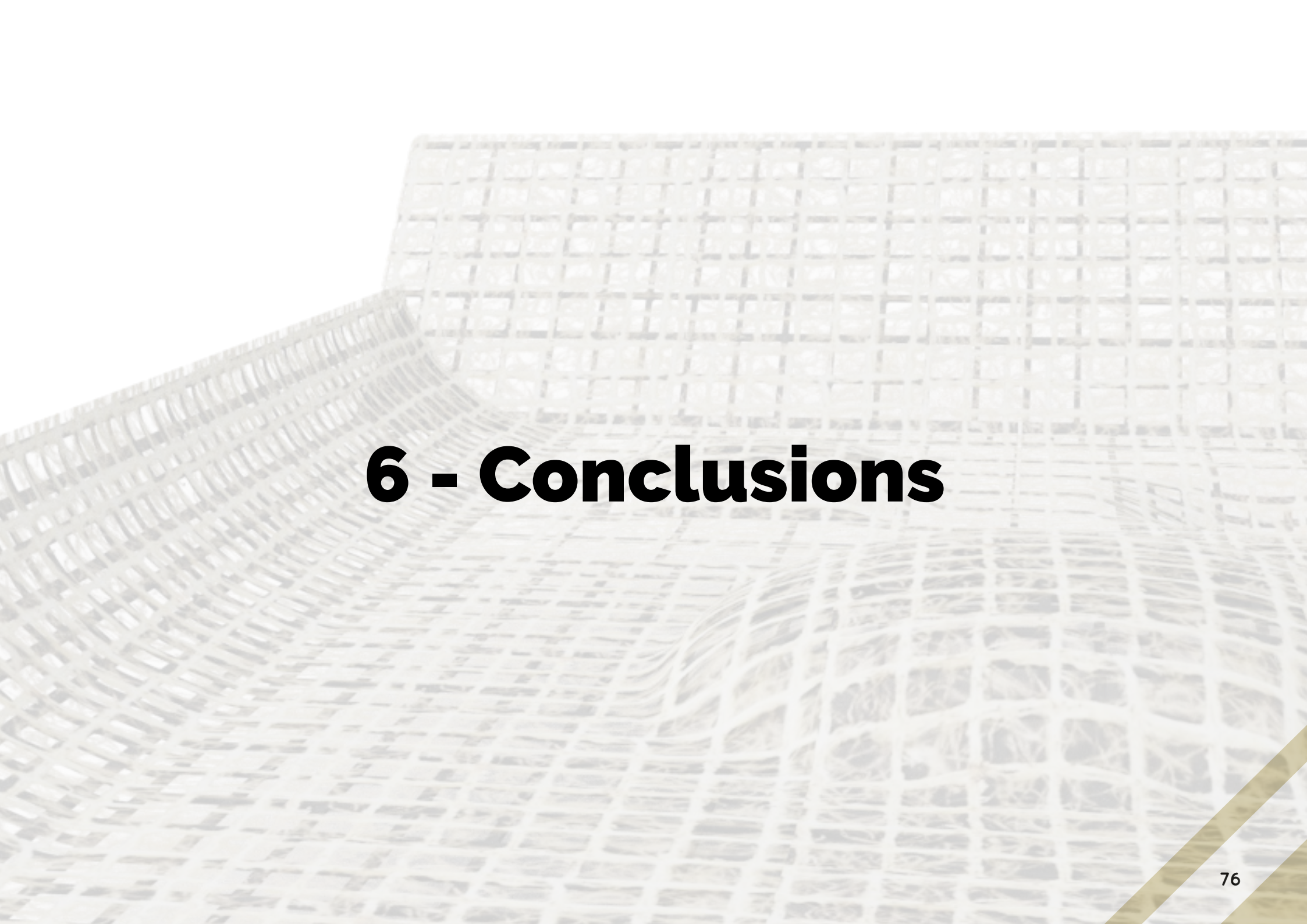


Figure [5.11]: Side view along the width of a simulated demonstrator under tension

**Figures 5.9-5.11** are a digital reconstruction the plane depicted in the previous page. Due to the long production time of Interwoven structures with composite samples (about 3 weeks) and last minute changes, the physical demonstrator could not be harvested from the oat plants at the time of submitting this report. The Confidential Appendix contains the process of creating the template for these as it is growing now (at the time of writing this report) to be showcased at the public presentation of this study.

The digital recreation uses the original line sketches from **Fig. 5.6** to extrapolate the expected behavior of deforming the entire structure under tension. This will also serve as a guide once the roots are harvested and the structure is assembled.

**Fig. 5.9** has the clearest example of variable deformation caused by the different structures when a load is applied. Cell size differences are not noticeable in the render, but the physical demonstrator will allow users to immediately relate the structural phase to a certain amount of deformation or bending.



# **6 - Conclusions**

# Conclusions

Interwoven structures are much more complicated than originally thought. The technical characterization presented here has only scratched the surface and is, by no means, complete. The seven sets of tensile tests performed, along with the accompanying microscopic analyses have unearthed important information for designers who wish to design with Interwoven. The main points are summarized here.

(1) The **coarse roots** that make up the designed pattern provide most of the structural support. Any loads that the material will withstand in practice should keep this in mind to minimize **anisotropy**.

(2) The properties of a large structure can be customized by varying the **cell size** of a square grid locally. Larger squares (2cm) are stiffer than the easily bent small ones (0.5cm).

(3) Average **root tip density** at a square vertex (the number of roots that end at a square's intersection) is indicative of the strength of a sample.

(4) **Agar** is a suitable (bio)-polymer matrix from which to create NFRCs with Interwoven, especially when the **gel is cast** over the Interwoven structure, rather than used as a growing substrate.

(5) **Agar powder content** in a matrix is directly related to the **hardness/stiffness** of the matrix.

(6) **NFRC parts should be produced individually** to avoid weakening the material like the bulk.

(7) Interwoven materials are not product-ready. **Safety** must be kept in mind if any **load-bearing functions** are given to these structures.



## Recommendations for Future Works

When designing with a living material, always prepare for the unexpected. The final demonstrator was not to include in the report at the time that it was written, as a consequence of time constraints. Patience is also key. Living materials can be capricious.

A future version of this same work would include a section exploring the physical material demonstrator, and especially the junctions in which the grid changes from one size to another.

### What could be done better different?

If done over from the beginning, this project would have focused immediately on the design parameters that were explored here and left room for more exploration with composites and microscopic analysis.

### Composites

Interwoven NFRCs show a lot of promise that can be exploited and optimized through various means. The polymer matrix was hardly explored in this study, and there is so much more that can be done - testing out different polymer matrices, making 3D molds instead of clamps when processing, changing the composition of agar in matrices, etc. The effects of plasticizers and other additives on composite properties offer another avenue of exploration to customize the properties of the composite to the designer's needs.

The fiber (root) phase can also be explored further. For example, the effects of grid cell size variations on the properties of the composite are not known either.

### Microscopy

The structural characterization of Interwoven is still only minimal. The interaction of roots at a vertex is mostly hidden by entanglement. A more precise characterization focused only on the structure at vertices and the interaction between roots would shed a light on the inner workings of the Interwoven structure.

The meaning of root tips ending at vertices and the reason behind their correlation to strength remain a mystery. Microscopic analysis can continue to shed light into this mystery through, for example, the quantification of roots, or the average length of these. Knowing these parameters would help designers understand the amount of time and care needed before an Interwoven structure is at its prime for harvesting, depending on the desired properties.

## Final (Personal) Reflections

Working with Interwoven posed a unique and very interesting challenge. The process of working with a living material, then trying to characterize it as you would a typical engineering material was very challenging. The novelty of the material made finding a starting point difficult, but once everything started falling into place, the process was very rewarding.

I do wish the physical demonstrator could have been finished on time, but I am confident that the test results presented here are representative of the Interwoven behavior, given that they are based on rigorous empirical data.

# References

- Adolph, S. J. K. (2009). The use of knitted, woven and nonwoven fabrics in interior textiles. In *Interior Textiles* (pp. 47–90). Elsevier.
- Ahn, S., Montero, M., Odell, D., Roundy, S., & Wright, P. K. (2002). Anisotropic material properties of fused deposition modeling ABS. *Rapid Prototyping Journal*, 8(4), 248–257.
- AL-Oqla, F. M., & Sapuan, S. M. (2014). Natural fiber reinforced polymer composites in industrial applications: feasibility of date palm fibers for sustainable automotive industry. *Journal of Cleaner Production*, 66, 347–354.
- Appels, F. V. W., Camere, S., Montalti, M., Karana, E., Jansen, K. M. B., Dijksterhuis, J., Krijgsheld, P., & Wösten, H. A. B. (2019). Fabrication factors influencing mechanical, moisture- and water-related properties of mycelium-based composites. *Materials & Design*, 161, 64–71.
- Ashori, A. (2008). Wood-plastic composites as promising green-composites for automotive industries! *Bioresource Technology*, 99(11), 4661–4667.
- ASTM International. (2019). *Test method for breaking force and elongation of textile fabrics (strip method)*. ASTM International. <https://doi.org/10.1520/d5035-11r19>
- ASTM International. (2020b). *Test method for tensile properties of single textile fibers*. ASTM International. [https://doi.org/10.1520/d3822\\_d3822m-14r20](https://doi.org/10.1520/d3822_d3822m-14r20)
- Baluska, F., Mancuso, S., Volkmann, D., & Barlow, P. W. (2009). The “root-brain” hypothesis of Charles and Francis Darwin: Revival after more than 125 years. *Plant Signaling & Behavior*, 4 (12), 1121–1127.
- Bernava, A., Manins, M., & Strazds, G. (2015). Woven Structures from Natural Fibres for Reinforcing Composites. *Materials Science and Applied Chemistry*, 31(0), 27–32.
- Brandon. (2020, July 5). What is the Materials Science Tetrahedron (Paradigm)? <https://mstudent.com/what-is-materials-science-tetrahedron-paradigm/>
- Callister, W. D., & Rethwisch, D. G. (2013). Mechanical Properties of Metals. In *Materials Science and Engineering: An Introduction, 9th Edition: Ninth Edition* (pp.168–215). Wiley Global Education.
- Camere, S., & Karana, E. (2018). Fabricating materials from living organisms: An emerging design practice. *Journal of Cleaner Production*, 186, 570–584.
- Carrete, I. A., Quiñonez, P. A., Bermudez, D., & Roberson, D. A. (2020). Incorporating Textile-Derived Cellulose Fibers for the Strengthening of Recycled Polyethylene Terephthalate for 3D Printing Feedstock Materials. *Journal of Polymers and the Environment*, 29(2), 662–671.
- Chermoshentseva, A. S., Pokrovskiy, A. M., & Bokhoeva, L. A. (2016). The behavior of delaminations in composite materials - experimental results. In *IOP Conference Series: Materials Science and Engineering (Vol.116, p.012005)*. <https://doi.org/10.1088/1757-899x/116/1/012005>
- Cicala, G., Cristaldi, G., Recca, G., & Latteri, A. (2010). Composites Based on Natural Fibre Fabrics. In *Woven Fabric Engineering*. <https://doi.org/10.5772/10465>
- D30 Committee. (2017). *Test method for tensile properties of polymer matrix composite materials*. ASTM International. [https://doi.org/10.1520/d3039\\_d3039m-17](https://doi.org/10.1520/d3039_d3039m-17)
- Depuydt, D., Balthazar, M., Hendrickx, K., Six, W., Ferraris, E., Desplentere, F., Ivens, J., & Van Vuure, A. W. (2018). Production and characterization of bamboo and flax fiber reinforced polylactic acid filaments for fused deposition modeling (FDM). *Polymer Composites*. <https://doi.org/10.1002/pc.24971>
- Dudescu, C., & Racz, L. (2017). Effects of raster orientation, infill rate and infill pattern on the mechanical properties of 3D printed materials. *ACTA Universitatis Cibiniensis*, 69(1), 23–30.
- Es-Said, O. S., Foyos, J., Noorani, R., Mendelson, M., Marloth, R., & Pregger, B. A. (2000). Effect of layer orientation on mechanical properties of rapid prototyped samples. *Materials and Manufacturing Processes*, 15(1), 107–122.

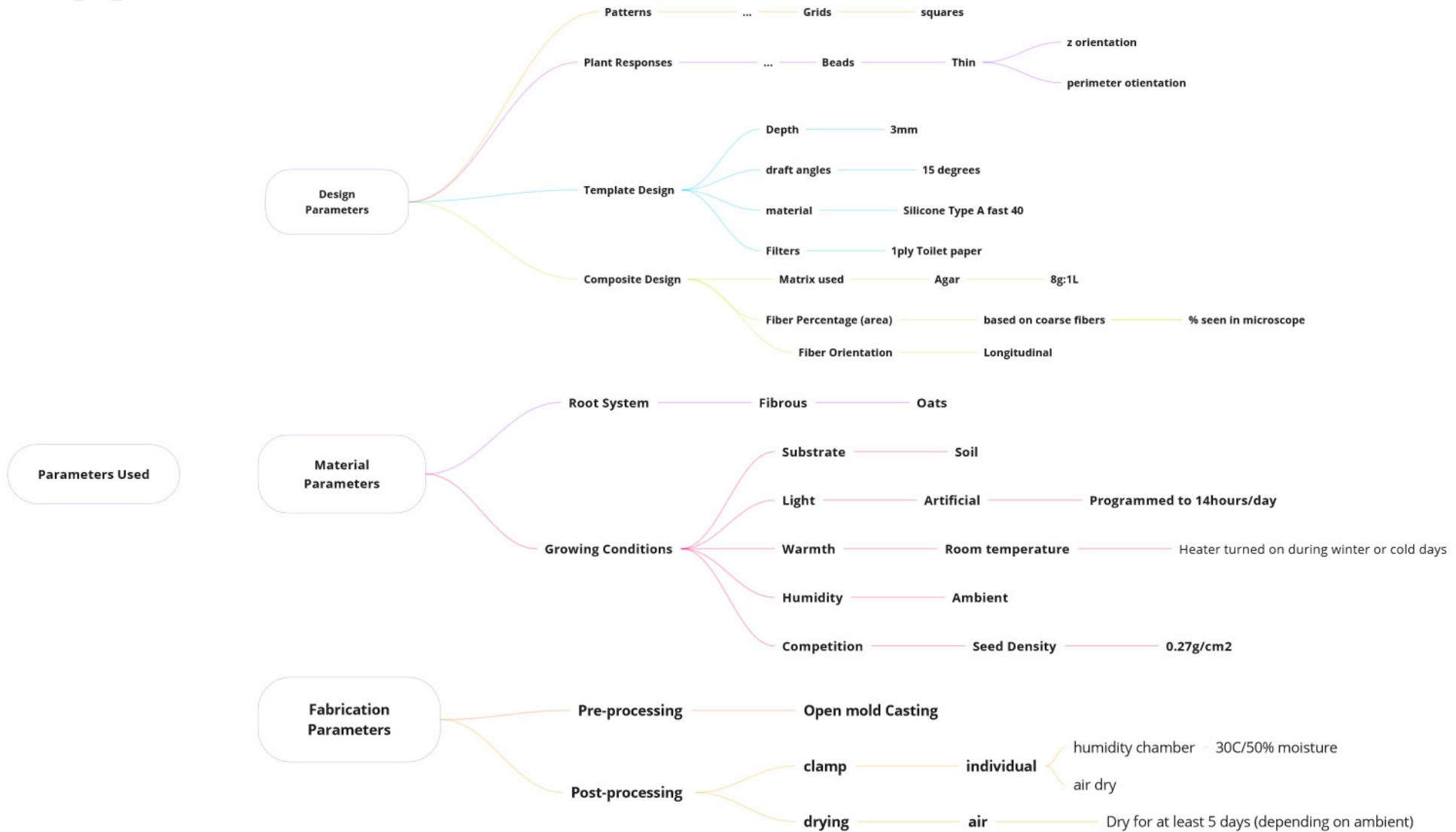
- Ford, D. (2019). *Interwoven: Growing a Durable yet Delicate Composite Textile* (E. Karana & M. Sonnevel (eds.)) [Design for Interaction, TU Delft]. <https://repository.tudelft.nl/islandora/object/uuid%3Af8efc51a-db33-4db9-a74b-10a5d9135b37>
- Front Page - Full Grown. (2014, March 4). <http://fullgrown.co.uk/>
- Gama, M., Gatenholm, P., & Klemm, D. (2016). *Bacterial NanoCellulose: A Sophisticated Multifunctional Material*. CRC Press.
- Haghi, A. K., & Akbari, M. (2007). Trends in electrospinning of natural nanofibers. *Physica Status Solidi*, 204(6), 1830–1834.
- Hillis, D. M., Sadava, D. E., Hill, R. W., & Price, M. V. (2013a). *Loose-leaf Version for Principles of Life*. Macmillan Higher Education.
- Hillis, D. M., Sadava, D. E., Hill, R. W., & Price, M. V. (2013b). Concept 24.2 Apical Meristems Build the Primary Plant Body. In *Loose-leaf Version for Principles of Life*. W. H. Freeman.
- Hodge, A. (2009). Root decisions. *Plant, Cell & Environment*, 32(6), 628–640.
- Jambeck, J. R., Geyer, R., Wilcox, C., Siegler, T. R., Perryman, M., Andrady, A., Narayan, R., & Law, K. L. (2015). Marine pollution. Plastic waste inputs from land into the ocean. *Science*, 347(6223), 768–771.
- Jobbins, M. (2018, August 31). *Fractography*. <https://www.nanoscience.com/applications/materials-science/fractography/>
- John, M., & Thomas, S. (2008). Biofibres and biocomposites. *Carbohydrate Polymers*, 71(3), 343–364.
- Kafle, B. P. (2020). Spectrophotometry and its application in chemical analysis. In *Chemical Analysis and Material Characterization by Spectrophotometry* (pp. 1–16). Elsevier.
- Karana, E., Barati, B., Rognoli, V., & Zeeuw van der Laan, A. (2015). Material Driven Design (MDD): A Method to Design for Material Experiences. *International Journal of Design*, 9(2). <http://www.ijdesign.org/index.php/IJDesign/article/view/1965>
- Khumar, Y.K. and Singh Lohchab, D. (2016). Influence of Aviation Fuel on Mechanical Properties of Glass Fiber-Reinforced Plastic Composite. *International Advanced Research Journal in Science, Engineering and Technology*, 3(4). <https://doi.org/10.17148/IARJSET.2016.341>
- Kirdök, O., Altun, T. D., Dokgöz, D., & Tokuç, A. (2019). Biodesign as an innovative tool to decrease construction induced carbon emissions in the environment. *International Journal of Global Warming*, 19(1/2), 127.
- Kozłowski, R., Kicińska-Jakubowska, A., & Muzyczek, M. (2009). Natural fibres for interior textiles. In *Interior Textiles* (pp. 3–38). <https://doi.org/10.1533/9781845696870.1.3>
- Ku, H., Wang, H., Pattarachaiyakoo, N., & Trada, M. (2011). A review on the tensile properties of natural fiber reinforced polymer composites. *Composites Part B Engineering*, 42(4), 856–873.
- Liboiron, M. (2016). Redefining pollution and action: The matter of plastics. *Journal of Material Culture*, 21(1), 87–110.
- Li, H., & Yang, W. (2016). Electrospinning Technology in Non-Woven Fabric Manufacturing. In *Non-woven Fabrics*. IntechOpen.
- Li, X., Tabil, L. G., Panigrahi, S., & Crerar, W. J. (2006). The Influence of Fiber Content on Properties of Injection Molded Flax Fiber-HDPE Biocomposites. In *2006 CSBE/SCGAB, Edmonton, AB Canada, July 16-19, 2006*. <https://doi.org/10.13031/2013.22101>
- Malkapuram, R., Kumar, V., & Negi, Y. S. (2009). Recent development in natural fiber reinforced polypropylene composites. *Journal of Reinforced Plastics and Composites*, 28(10), 1169–1189.
- Mancuso, S., & Viola, A. (2015). *Brilliant Green: The Surprising History and Science of Plant Intelligence*. Island Press.
- Myers, W. (2012). *Bio Design: Nature, Science, Creativity* (Thames & Hudson (Ed.); UK; p. 288). High Holborn.
- On reducing anisotropy in 3D printed polymers via ionizing radiation. (2014). *Polymer*, 55(23), 5969–5979.
- Oxman, N. (2015). Templating design for biology and biology for design. *Architectural Design*, 85(5), 100–107.
- Oxman, N., Laucks, J., Kayser, M., Duro-Royo, J., & Gonzales Uribe, C. (2017). Silk Pavilion: A Case Study in Fibre-based Digital Fabrication. In F. Gramazio, M. Kohler, & S. and Landenberg (Eds.), *Fabricate 2014: Negotiating Design and Making* (pp. 248–255).

- Peças, P., Carvalho, H., Salman, H., & Leite, M. (2018). Natural Fibre Composites and Their Applications: A Review. *Journal of Composites Science*, 2(4), 66.
- Ramadan, N., Taha, I., Hammouda, R., & Abdellatif, M. H. (2015). Alkali Treatment of jute fabric for Vacuum Assisted Resin Infusion. *2nd International Conference for Industry Academia Collaboration*. <http://dx.doi.org/>
- Root apex transition zone: a signalling–response nexus in the root. (2010). *Trends in Plant Science*, 15(7), 402–408.
- Root - Definition, Types, Morphology, & Functions. (n.d.). Britannica. Retrieved February 18, 2021, from <https://www.britannica.com/science/root-plant>
- Rowe, T. (2009). *Interior Textiles: Design and Developments* (T. Rowe (Ed.)). Woodhead Publishing.
- Saint, A. (2021). The Magic of Mushrooms for Sustainability [sustainability innovation]. *Engineering & Technology*, 16(2), 37–39.
- Shahzad, A. (2013). A study in physical and mechanical properties of hemp fibres. *Advances in Materials Science and Engineering*, 2013, 1–9.
- Scherer, D., Tinga, F., & van Zoetendaal, W. (2012). *Nurture Studies*. Van Zoetendaal.
- Schumacher, E. F. (2014). Microscopy for Materials Characterization: Illuminating Structures With Light and Electrons. In *American Laboratory*. <http://www.americanlaboratory.com/914-Application-Notes/167499-Microscopy-for-Materials-Characterization-Illuminating-Structures-With-Light-and-Electrons/>
- Silvia-DforDesign. (2019, June 14). *Sustainable design: biofabrication is the answer*. <https://dfordesign.style/blog/sustainable-design-biofabrication-is-the-answer>
- Su, I. (2015). *Behavior of a silkworm silk fiber web structure under wind load* [Massachusetts Institute of Technology]. <http://hdl.handle.net/1721.1/99633>
- Tan, T. H., Silverberg, J. L., Floss, D. S., Harrison, M. J., Henley, C. L., & Cohen, I. (2015). How grow-and-switch gravitropism generates root coiling and root waving growth responses in *Medicago truncatula*. *Proceedings of the National Academy of Sciences of the United States of America*, 112(42), 12938–12943.
- Torrado, A. R., & Roberson, D. A. (2016). Failure analysis and anisotropy evaluation of 3D-printed tensile test specimens of different geometries and print raster patterns. *Journal of Failure Analysis and Prevention*, 16(1), 154–164.
- Trewavas, A. (2003). Aspects of plant intelligence. *Annals of Botany*, 92(1), 1–20.
- Trewavas, A. (2017). The foundations of plant intelligence. *Interface Focus*, 7(3), 20160098.
- Trujillo, E., Moesen, M., Osorio, L., Van Vuure, A. W., Ivens, J., & Verpoest, I. (2014). Bamboo fibres for reinforcement in composite materials: Strength Weibull analysis. *Composites. Part A, Applied Science and Manufacturing*, 61, 115–125.
- Vandeurzen, P., Ivens, J., & Verpoest, I. (1996). A three-dimensional micromechanical analysis of woven-fabric composites: I. Geometric analysis. *Composites Science and Technology*, 56(11), 1303–1315.
- van Vuure, A. W., Ivens, J. A., & Verpoest, I. (2000). Mechanical properties of composite panels based on woven sandwich-fabric preforms. *Composites. Part A, Applied Science and Manufacturing*, 31(7), 671–680.
- Vineis, C., & Varesano, A. (2018). Natural polymer-based electrospun fibers for antibacterial uses. In *Electrofluidodynamic Technologies (EFDTs) for Biomaterials and Medical Devices* (pp. 275–294). Elsevier.
- Wambua, P., Ivens, J., & Verpoest, I. (2003). Natural fibres: can they replace glass in fibre reinforced plastics? *Composites Science and Technology*, 63(9), 1259–1264.
- Yalcin, D. (n.d.). *Fabric Strength Testing with a Universal Testing Machine*. Retrieved March 4, 2021, from <https://www.admet.com/fabric-strength-testing-universal-testing-machine/>
- Zhou, J. (2019). *Interwoven: Designing Biodigital Objects with Plant Roots: Exploring Material Structure and Experience* (E. Karana & J. Wu (Eds.)) [Design for Interaction, TU Delft]. <https://repository.tudelft.nl/islandora/object/uuid%3Affdcf947-06df-4941-a587-bdf008f87783>
- Zhou, J., Barati, B., Wu, J., Scherer, D., & Karana, E. (2021). Digital biofabrication to realize the potentials of plant roots for product design. *Bio-Design and Manufacturing*, 4(1), 111–122.

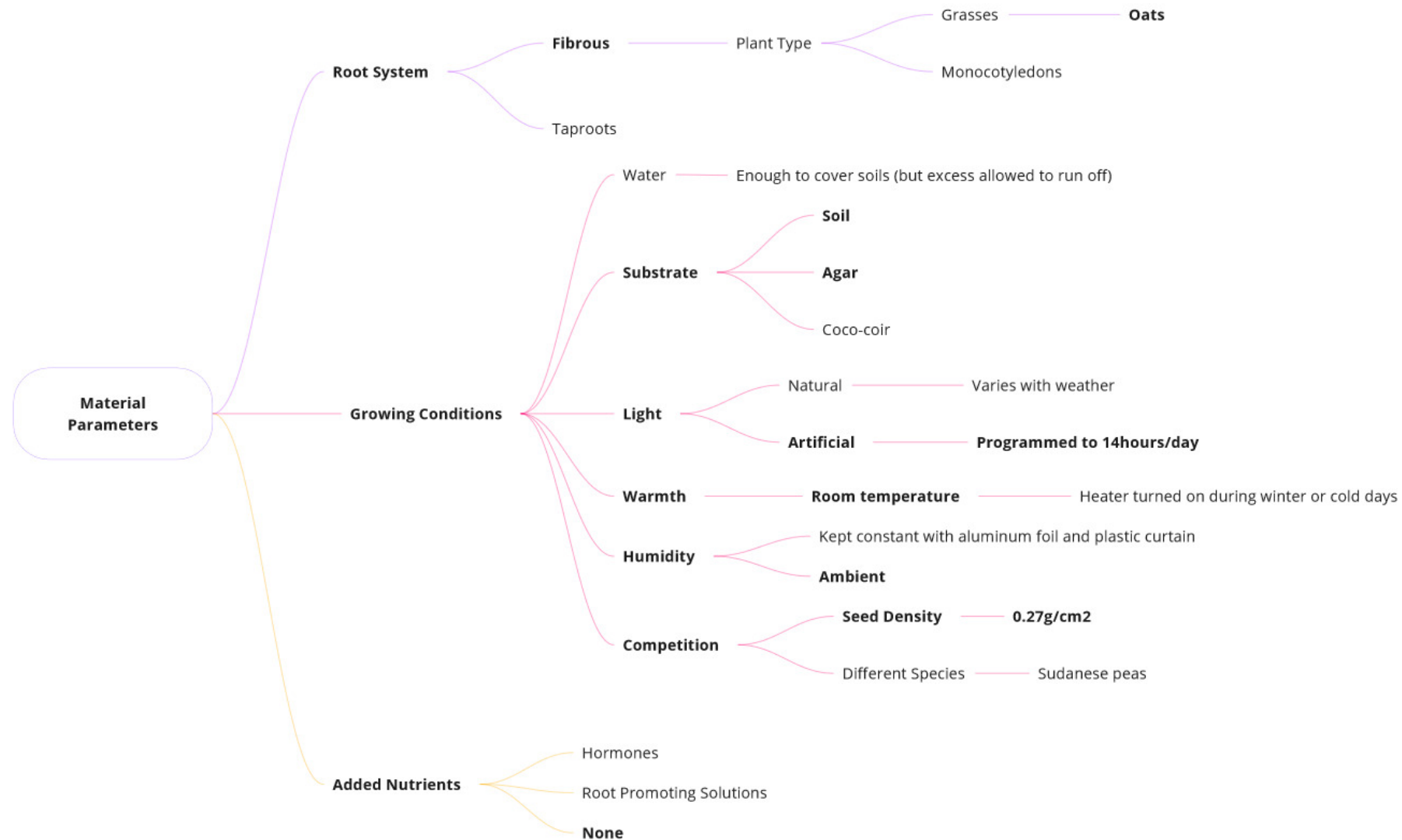
Ziegler, A. R., Bajwa, S. G., Holt, G. A., McIntyre, G., & Bajwa, D. S. (2016). Evaluation of physico-mechanical properties of mycelium reinforced green biocomposites made from cellulosic fibers. *Applied Engineering in Agriculture*, 32(6), 931-938.

# **7 - Appendices**

# Appendix A: Interwoven Parameters (Full)

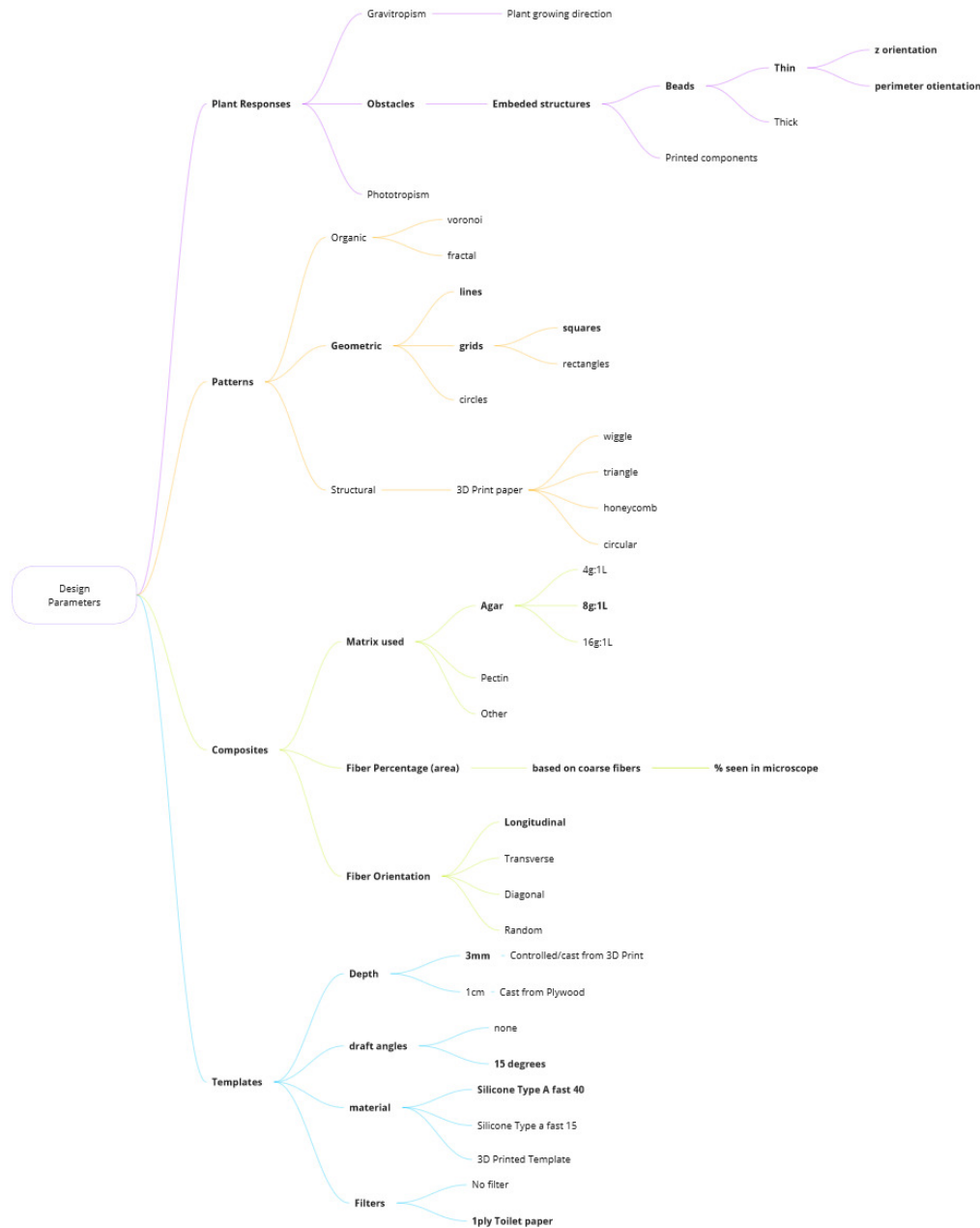


# Interwoven Parameters: Material Parameters



Material parameters relate to the plant growth in Interwoven. The parameters that might affect plant health and growth speed were identified, but most of them were decided based on previous works for the sake of focusing the purpose of the project early on.

# Interwoven Parameters: Design Parameters



Design parameters are the ones that the designer has the most control over. Most of the parameters tested in this study hail from this section. Everything ranging from the obstacles used in plants growth to the composition of the matrix components in the agar-agar composites is listed. The parameters in bold are the ones that were tested at one point or another.

## Interwoven Parameters: Fabrication Parameters



Fabrication parameters are largely focused on the composite creation. more specifically, these were used to figure out the best way to process the composites. Decisions such as agar infusion vs. agar as a growing substrate, or the method of agar infusion being tested in these sections. The parameters in bold are the ones that were tested at one point or another.

# Appendix B: Technical Characterization Tests

## B-1 ASTM D5035 Dimensional Calibration Test

The root orientation tests made the need for standardized tensile testing methods evident. In an attempt to reduce the effects of anisotropy, a square grid pattern was used (Fig. B.1). The linear nature of the coarse roots facilitates the alignment of the coarse roots with the loading direction. Furthermore, the simplicity of this pattern is more suitable to identifying the role of roots in tensile properties. Once a foundational understanding for this is established, the results can be extrapolated to more complex patterns.

### Purpose

The aim of this test is to identify the best sample dimensions, specifically width, for testing tensile properties of Interwoven structures with a gridded pattern.

The structural composition of Interwoven resembles that of non-woven textile. The standard testing procedure for these (ASTM D5035) suggests using samples with a width of either 25mm or 50 mm depending on the number of textile fibers within the width (ASTM International, 2019). The number of fibers does not directly apply to interwoven,

but the number of coarse roots within the grid could be analogous. The squares in the grid had a width of 1cm, so the number of these varies with sample width. Samples 25mm wide only had three coarse roots running through, and it was hypothesized that having another coarse root could benefit the material properties as well.

Samples with two different widths were prepared to evaluate this hypothesis: 25mm (with three coarse roots) and 35mm (with 4 coarse roots) (Fig. B.2). According to the standard, a width of 25cm correlates to a length of 150mm. Using the same proportions, a 35 cm sample should have a length of 210mm.



Figure [B.1]: Square grid pattern used in testing

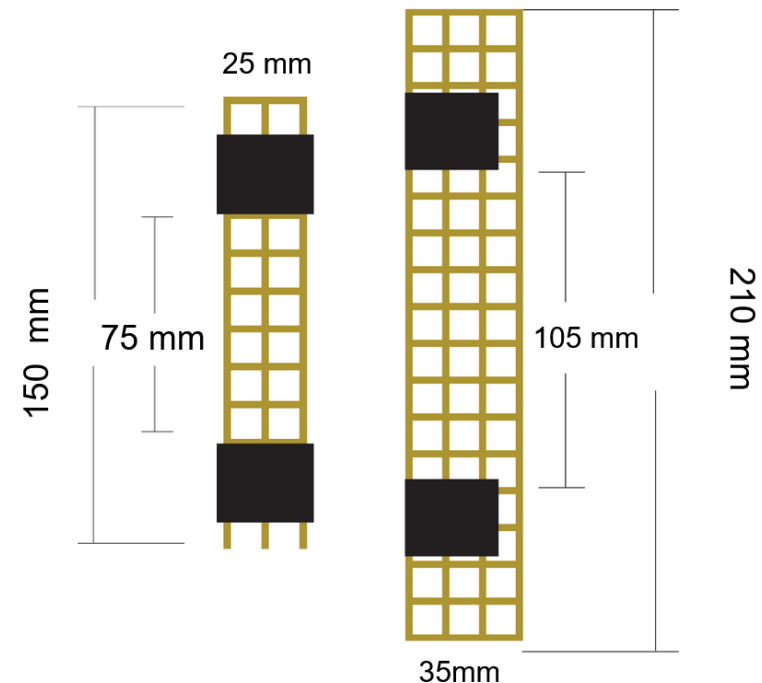


Figure [B.2]: Illustration of sample dimensions in the tensile grips

## Procedure

At the time of testing these samples, the template used for preparing these samples had a thickness of 10cm, unlike those of the root orientation tests, which had a thickness of 3mm. The differences in thickness cause the secondary roots to grow on a different plane from the coarse roots. Compare the grid pattern in the past page to **Fig. B.3** and note the connection between coarse and fine roots.

Ideally, a total of five samples with each of the two dimensions would be tested, but the available templates did not allow for that. The following is a summary of the test parameters used.



Figure [B.3]: Square grid pattern used in testing

## Summary of Test Parameters

- *Sample Dimensions:*
  - 25 x 150mm
  - 35 x 210mm
- *Template Thickness*
  - 10 mm
- *Number of specimens:*
  - 4 x (25 x 150mm)
  - 2 x (35 x 210mm)
- *Gauge Length:*
  - 75mm and 115 mm
- *Strain rate*
  - 15mm/min (based on the standard for testing single fibers, which takes 10% of the length of the specimen). (ASTM International, 2020b)

The number of tested specimens varied due to the size of the template that the samples were cut from. Though unequal, it is believed that these are enough samples to obtain a representative overview of the behavior of each group. Before pulling, each sample was aligned with the center of the clamps. As seen in **Fig. B.4**, the Zwick clamps were not wide enough to clasp the entirety of the 35cm samples, which is why one of the coarse roots was not in the clamps for these samples.

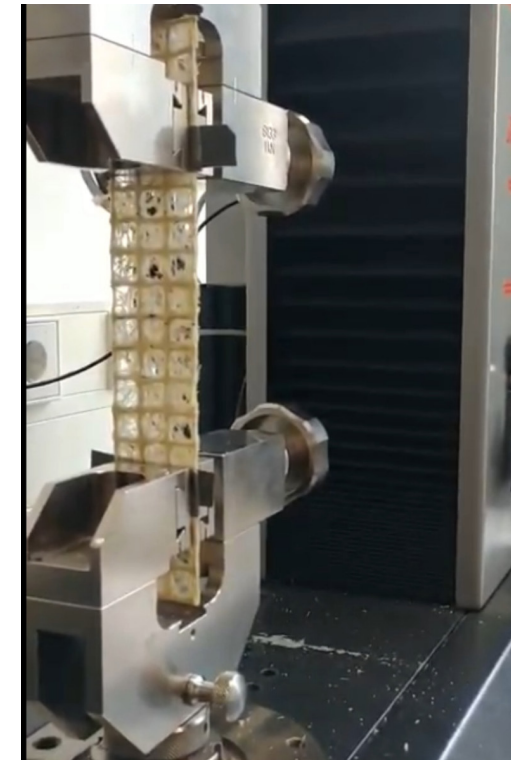


Figure [B.4]: Square grid pattern used in testing

## Results

**Figure B.5** shows the load-displacement curves obtained from pulling all six samples. Note that the samples all had a similar behavior - they curved up into a somewhat linear region and quickly reached a peak, after which elongation occurred differently for each sample. **Table B.1** shows the breaking force and elongation of each of the samples.

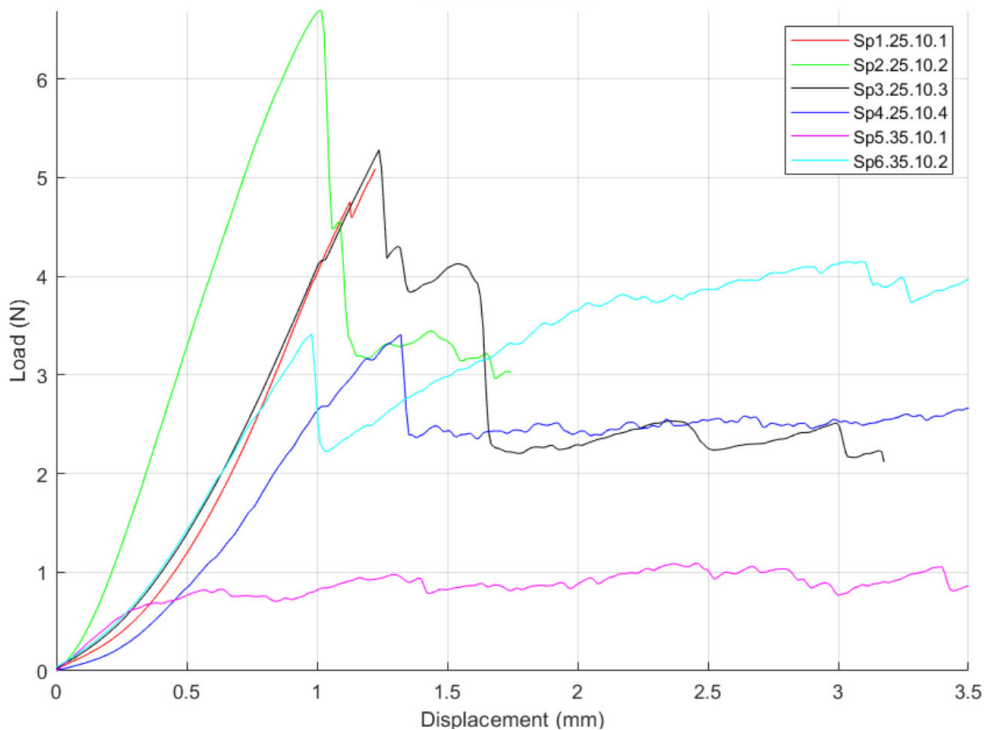


Figure [B.5]: Load-displacement plots for all samples (25 x 150mm)

Sample	Breaking Force (N)	Elongation (mm)
Sp1.25.10.1	5.0830	1.2229
Sp2.25.10.2	6.6904	1.0069
Sp3.25.10.3	5.2791	1.2378
Sp4.25.10.4	3.4069	1.3219
Sp5.35.10.1	3.0515	18.8173
Sp6.35.10.2	4.1457	3.0424

Table [B.1]: Breaking force and elongation for each sample

Figure [B.5]: Load-displacement plots for narrow samples (25 x 150mm)

## Narrow Samples (25 x 150 mm)

The narrow samples exhibited varying degrees of loading capacity. Two samples (Sp1.10.1 and Sp1.10.3) had both similar elongation and breaking forces. The average breaking force for these samples was **5.11 ± 1.345N** with a corresponding elongation of **1.19 mm**.

Sample	Breaking Force (N)	Elongation (mm)
Sp1.25.10.1	5.0830	1.2229
Sp2.25.10.2	6.6904	1.0069
Sp3.25.10.3	5.2791	1.2378
Sp4.25.10.4	3.4069	1.3219

Table [B.1]: Breaking force and elongation of each narrow sample

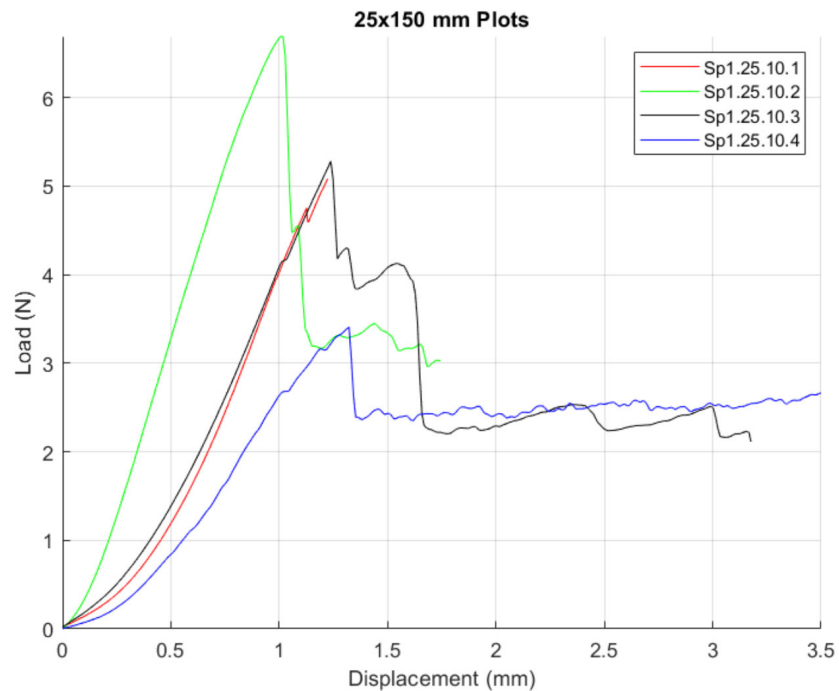


Figure [B.5]: Load-displacement plots for all samples (25 tx 150mm)

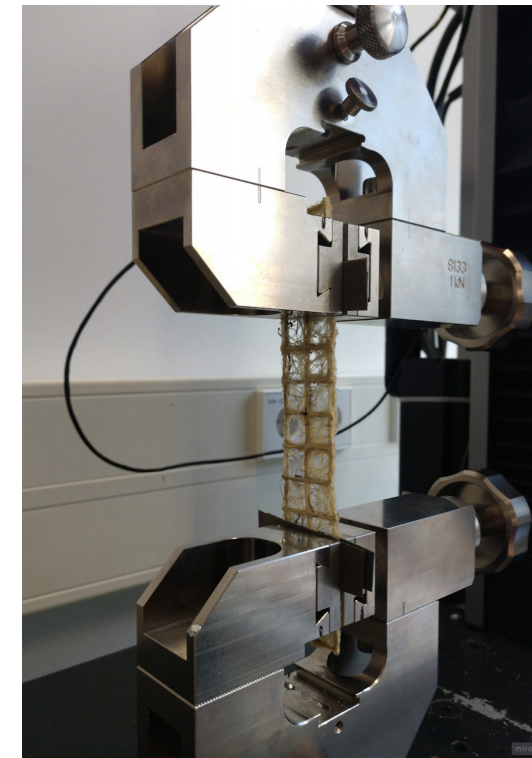


Figure [B.6]: Tensile setup for narrow samples

## Wide Samples (35 x 150 mm)

Figure B.7 shows the load-displacement curves of the wider samples. The difference between the two samples is much larger than the differences seen in the narrow samples. Sample Sp5.35.10.1 elongates before peaking whereas the other sample steadily increases before an initial dip and peak. The zigzagging behavior of Sp6.35.10.1 is likely

due to two factors. One is the alignment of the fine roots and coarse roots with the loading orientation, and the other is due to the breaking of fine roots caused by this alignment, as was evidenced by audible snaps throughout the test. The average breaking force of these samples was  $3.60 \pm 0.77\text{N}$  with an elongation of **10.92 mm**. Individual values for the two samples are seen in Table B.3.

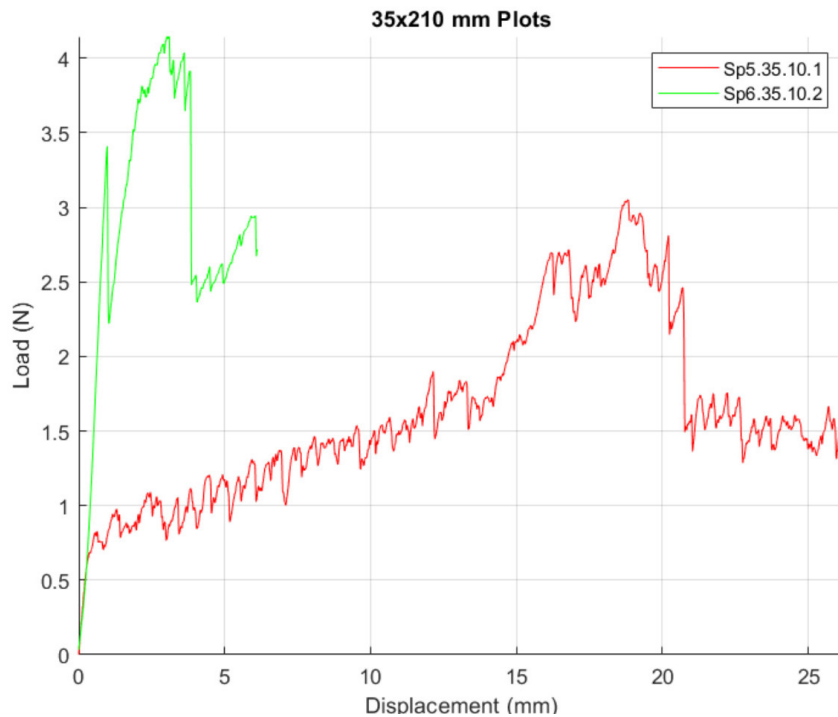


Figure [B.7]: Load-displacement plots for all samples (25 tx 150mm)

Sample	Breaking Force (N)	Elongation (mm)
Sp5.35.10.1	3.0515	18.8173
Sp6.35.10.2	4.1457	3.0424

Table [B.2]: Breaking force and elongation of each wide sample

## Discussion

The narrow samples had a higher average breaking force ( $5.11 \pm 1.345\text{N}$ ) than the wider samples ( $3.60 \pm 0.77\text{N}$ ), though the elongation was much smaller ( $1.19\text{mm}$  and  $10.92\text{mm}$ , respectively). The “stronger” response to tensile loading by the narrower samples is likely due to the number of coarse roots being actively tested.

Though the wide samples have four coarse roots, the width of the samples surpasses that of the grips, so not all four coarse roots are grasped. In fact, because of the sample’s alignment with the center of the clamps, only two of the coarse roots are fully grasped in these samples whereas all three of the narrow samples’ coarse roots are within the tensile clamps during testing.

Recall that the root orientation tests suggest that the coarse roots are the main source of stiffness within the samples. Thus, by not actively distributing the load to all of these roots, the wider samples

are much weaker. This effect is fully on display with the wide samples.

Root elongation is likely determined by fine root density or some other structural components. A close look at the vertices of each cell (**Fig.B.8**) provides insight into how the roots intertwine, as well as the presence of root tips at intersections. This structural analysis reveals that coarse roots are an amalgamation of many fine roots that are bound together by root hairs. The presence of root tips suggests that many of the roots end at vertices. The effects of this are as of yet unknown, but they could have a correlation with mechanical properties.

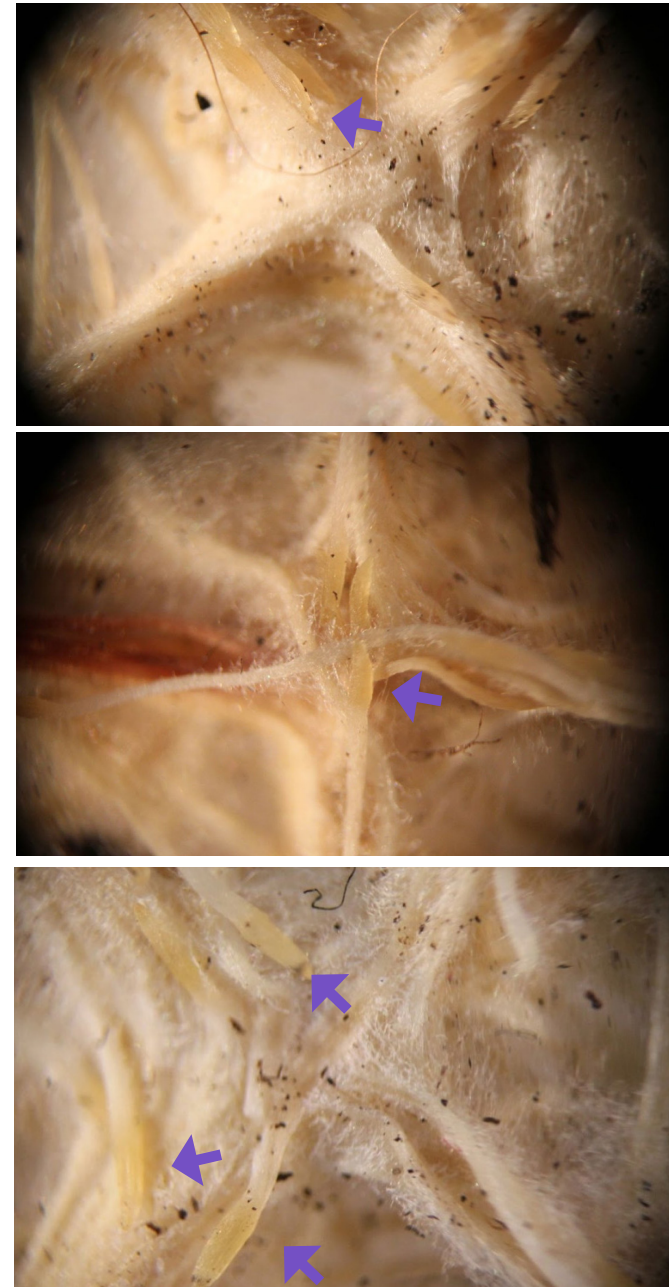


Figure [B.8]: Optical image of grid square vertices. Arrows point to the root tips

## Conclusions

**Figure B.9** shows the root tips accumulated in and around the vertex. It also gives a better understanding of the structure of coarse roots. Though the vertex looks like a junction, it is not strictly a stopping point for many roots. In fact, many roots seem to grow past the junctions in search of more nutrients. The amount of roots passing through here leads to the visible intertwining. Although the lighter areas of the image look like a large, solid root, they are really an agglomeration of roots whose root hairs have become so tangled that the individual roots are not clearly visible anymore.

Both the wide and narrow samples tested in this study have the same structural components seen above, but the number of coarse roots under tension changed. The narrow samples had a higher loading capacity before failure because they had more coarse roots in tension.

The main takeaways from this study are summarized below.

- Coarse roots dictate the magnitude of a sample's breaking force.
- Coarse roots are composed of many fine roots that are held together by a tangling of root hairs.
- Grid cell vertices show that many roots appear to end at the vertex.
- The narrower samples give a more indicative representation of the sample's properties than the wider specimens.

As a result of this study, any following tensile tests will have coupons with the dimensions **25mm x 150mm**. A more exhaustive study on the nature of root intermingling and its effects on mechanical properties is recommended. Understanding the cohesive mechanism of the roots and how to promote this could provide a design parameter that directly impacts the strength of Interwoven components.

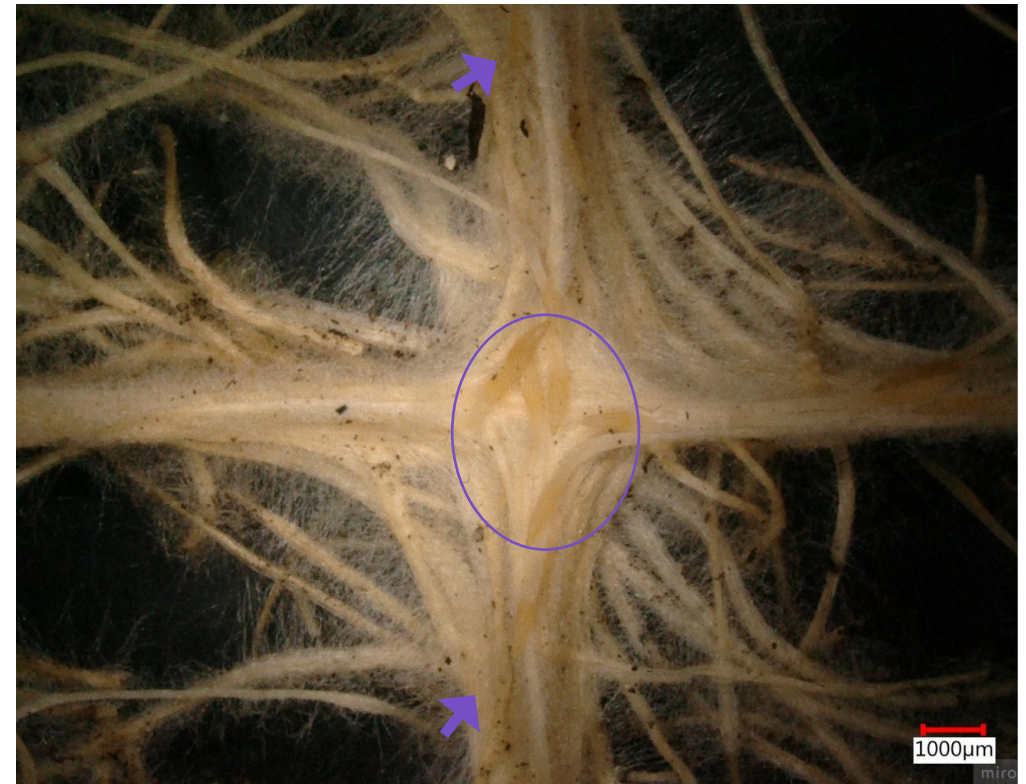


Figure [B.8]: Image of grid square vertex taken with digital microscope. Note the root tip accumulation (purple circle and arrows) and root hairs between fine roots.

## B-2 Tensile Tests on Control Group (3mm-thick grid)

In composite materials, the reinforcement phase is usually made up of stiff fibers, while the matrix holds the fibers together and transfers the load to the fibers. The mechanical properties of composites are often a combination of those of the two phases, depending on the relative amounts of each phase. Increasing the amount of one phase over another comes with trade-offs, but the effects of said trade-offs can be only evident when the properties of both phases are understood.

This study characterizes the benefits of polymer matrices as a strengthening mechanism for Interwoven structures. As such, the individual matrix properties will not be explored.

### *Purpose*

Before making an NFRC from Interwoven structures, the properties of these must be characterized. This section tests the tensile properties of Interwoven root structures.

The tests conducted in B-1 determined the optimal coupon dimensions for tensile testing (25mm x 150mm). All tensile tests henceforth use these dimensions.

Unlike the samples used in the dimensional calibration tests, the template used for these samples had a thickness of 3mm and a tapered shape to promote fine root development (**Fig. B.9**). An example of the samples tested is seen in **Fig. B.10**. For the full details of these templates and the differences between them, refer to the Confidential Appendix.



Figure [B.9]: Template from which samples were taken for testing

## Procedure

Five samples like the one shown below were tested with following the same ASTM D5035 methods as the dimensional calibration tests.

Before pulling each sample, the exact dimensions of each sample were recorded (width, thickness, and length). The width and thickness help determine the cross-sectional area, which will help determine the stress-strain curve. Interwoven structures have variable thicknesses and widths, so an average was taken from three measurements of each dimension.

The length was used define a gauge length that was equidistant from each end of the sample. Before pulling, the coarse roots were aligned vertically in the Zwick's grips.



Figure [B.10]: Control Sample

## Summary of Test Parameters

- *Sample Dimensions:*  
25 x 150mm
- *Template Thickness*  
3 mm
- *Number of specimens:*  
Five
- *Gauge Length:*  
75mm
- *Strain rate*  
15mm/min

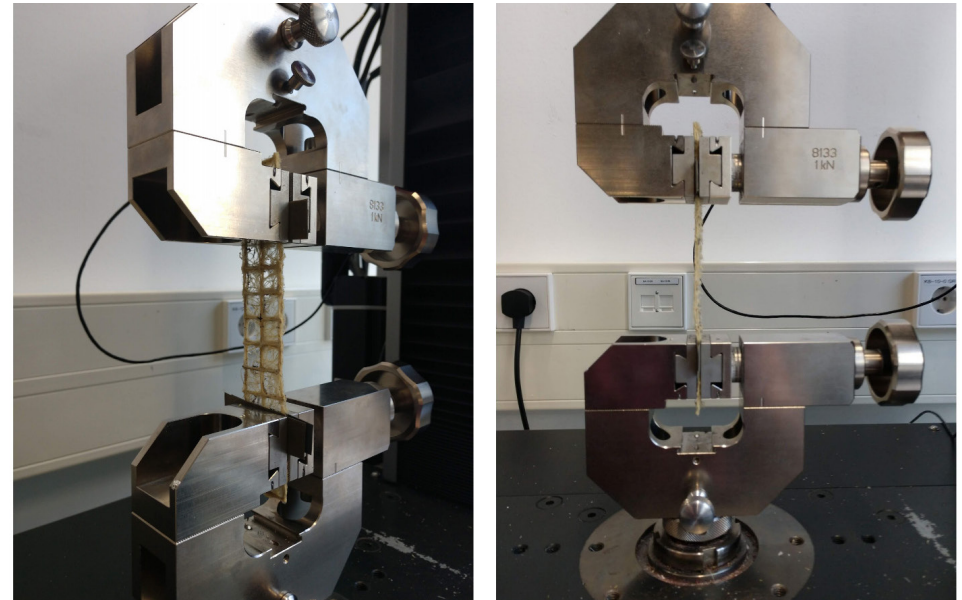


Figure [B.11]:Tensile Test Setup for control group

## Results

The plots in **Fig. B.12** show the load-displacement curves of all five samples. The average breaking force for these samples was  $11.13 \pm 4.426 \text{ N}$  with an elongation of  $0.95 \text{ mm}$ . Although the shape of the graph is relatively uniform throughout the samples, the breaking force values and the slopes of the linear sections are still not lining up much. In theory, samples made from

the same material should have some reproducibility with similarly sloped results, but the variance of these samples was nearly 40%. In fact, the highest breaking force is nearly three times higher than that of the lowest one, as seen in the comparison of all breaking forces in **Fig. B.13**.

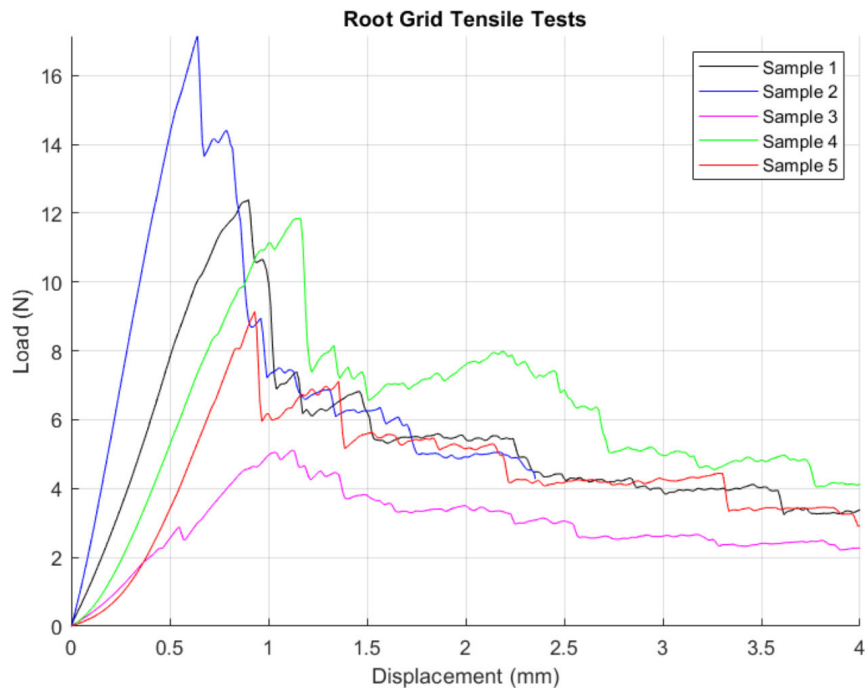


Figure [B.12]: Load-Displacement curves for control group

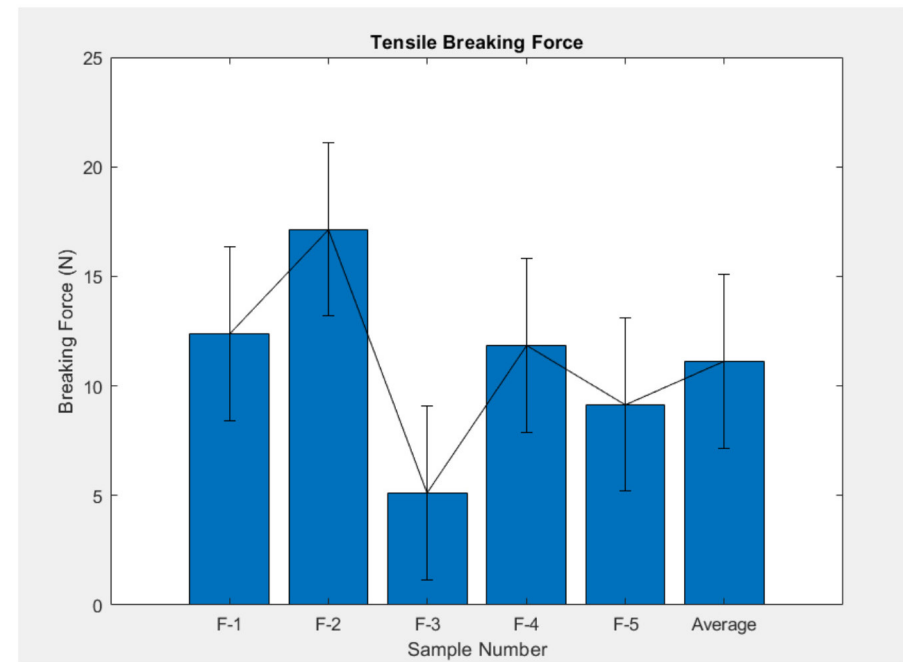


Figure [B.13]: Breaking force of each sample (and average)

## Microscopic Analysis

The consistent disparities between test results suggest that the structure and/or other dimensional parameters play a role on the tensile properties. Recall that load-displacement curves cannot be easily compared because there is no dimensional normalization like there would be in stress-strain curves. This is due to the non-uniform cross sectional area that loads act on when a sample is pulled.

Microscopic analysis was performed to estimate the cross-sectional area of a sample. To do this, the samples that were pulled in this test were cut at various

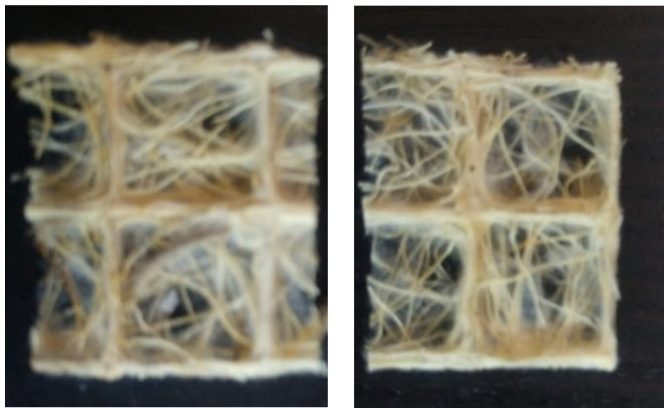


Figure [B.14]: Sectioned sample



Figure [B.15]: Two cross sections observed

points along the length of the sample, as in **Fig. B.14**. Depending on the location of the cut, one of two types of cross sections were created (**Fig. B.15**). If the cut was in the middle of a square, the cross section showed three “columns”, but if it occurred along the edge of a square, a horizontal “bar” was seen. Both cross sections were then studied with a DHX Keyence® digital microscope.

The cross section was held normal to the microscope with a clip, from which the root density was measured based on brightness differences. The digital microscope has a function to calculate measures the relative amounts of two phases differentiated by brightness values. An example of the measured area is seen in **Fig. B.16**. The fiber density within the sample cross sections is used to calculate the effective area upon which the load acts.

Three measurements were taken on each of the five samples. Two measurements only accounting for longitudinal columns and one measurement for transverse bars. The resulting area was given as a percentage (with any areas not including the fibers taken to be porosity). The results are seen in the following page.

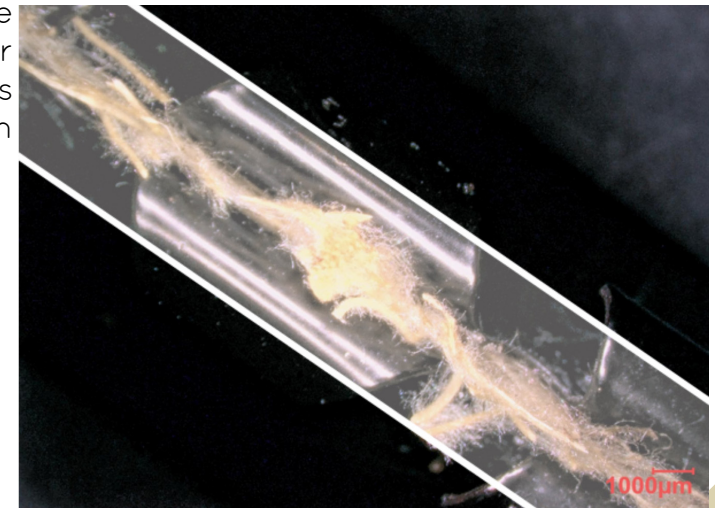


Figure [B.16]: Column Cross section. White area was the section from which the fiber percentage was calculated

The measured root density for each cross section are seen in **Fig. B.17**. The average fiber density at the cross-section of the samples was **79.60 ± 8.77%**. Despite the bar cross sections having a higher density (**89.00 ± 5.96%**) than the columns (**76.20 ± 5.72%**), their contribution to the load is considered to be less direct, though it is not fully understood. The average root density was used to convert the load-displacement curves to stress-strain curves.

The dimensional parameters of each sample (width and thickness) taken before testing were used to calculate a rectangular area following  $A = \text{width} \times \text{thickness}$ . Then, using the volume fraction above, the effective cross sectional area for each sample was determined using  $A_{\text{effective}} = w \times t \times 0.796$ .

**Figures B.18** and **B.19** display the resulting stress strain curves and calculated moduli, respectively. Despite the normalization factor, the slopes

of the curves are still very different. This is significant because, in materials science, the linear part of a stress-strain curve is a material constant known as Young's Modulus, or the elastic modulus. This constant should, in theory, be the same (or very similar) for all samples made from the same material. It also serves as an estimation of a material's relative stiffness - the higher the modulus, the stiffer a material's behavior.

Since the linear-elastic region of each sample was different, the elastic modulus for each of these was calculated using a range of 20-50% of the tensile strength (highest peak). Within this range, the modulus was used by finding the slope of the line with a simple slope-intercept formula (in this case, with stress/strain). The average elastic modulus for these samples was **0.29 ± 0.13 MPa**. The coefficient of variance is very large, at 42.67% because Interwoven is a structure and not a homogeneous engineering material.

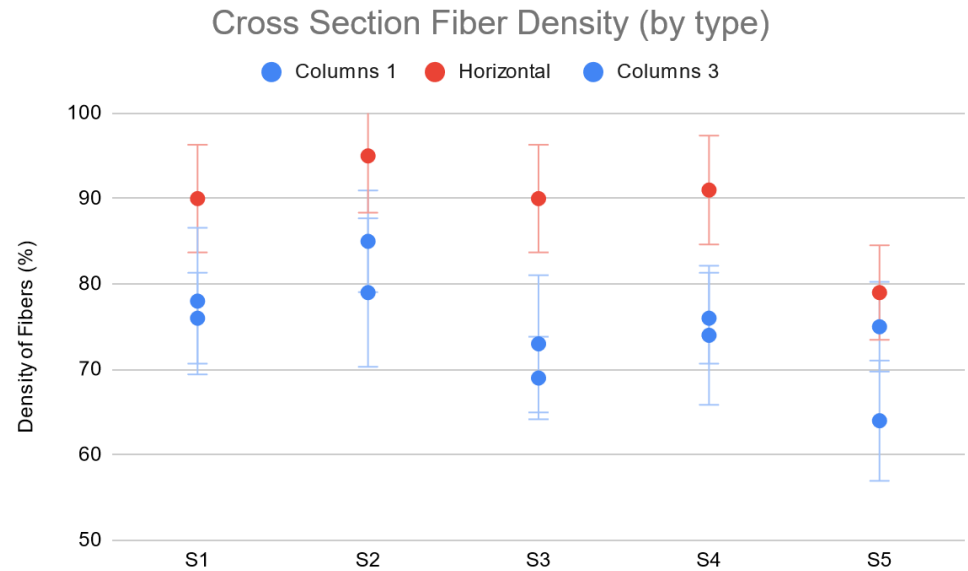


Figure [B.17]: Measured cross-sectional root density per sample, per type.

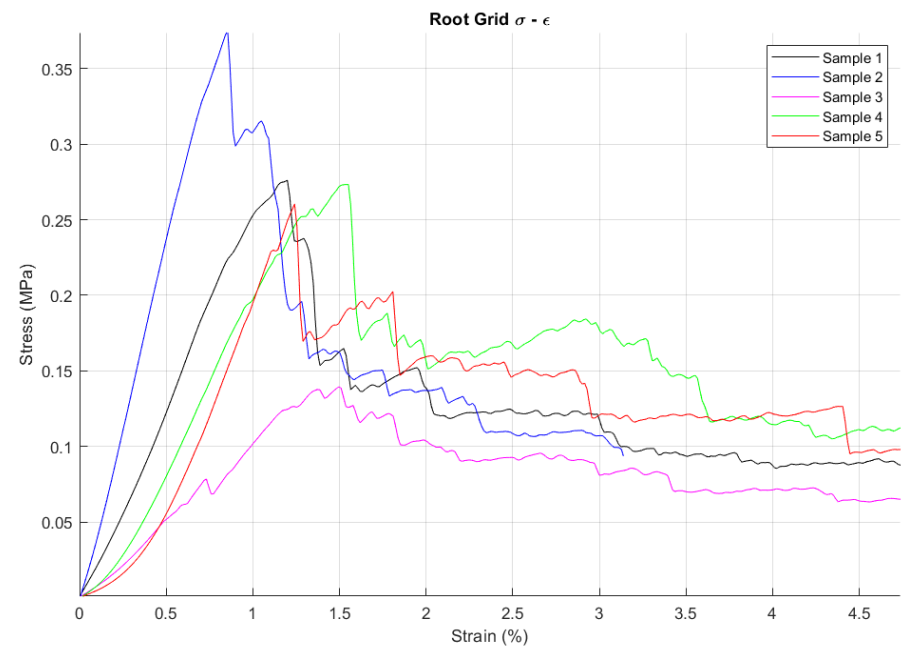


Figure [B.18]: Stress-strain curves calculated using  $A_{\text{effective}}$

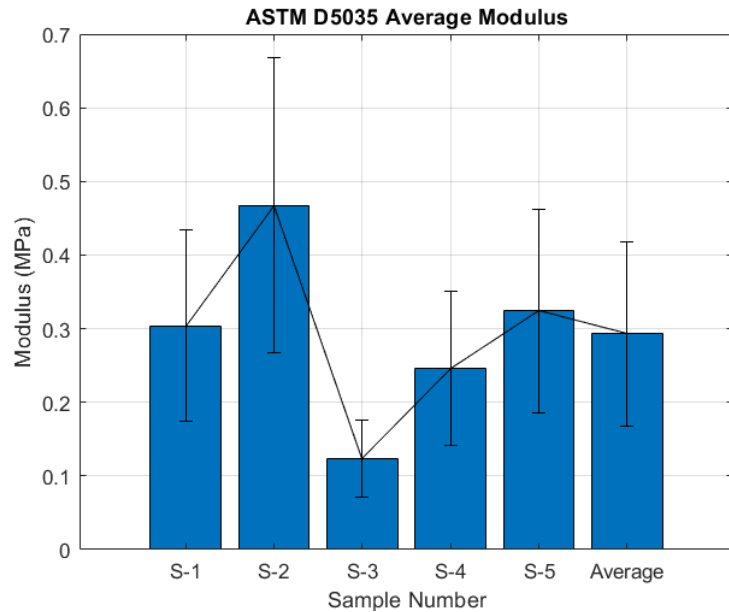


Figure [B.19]: Calculated modulus for each sample.

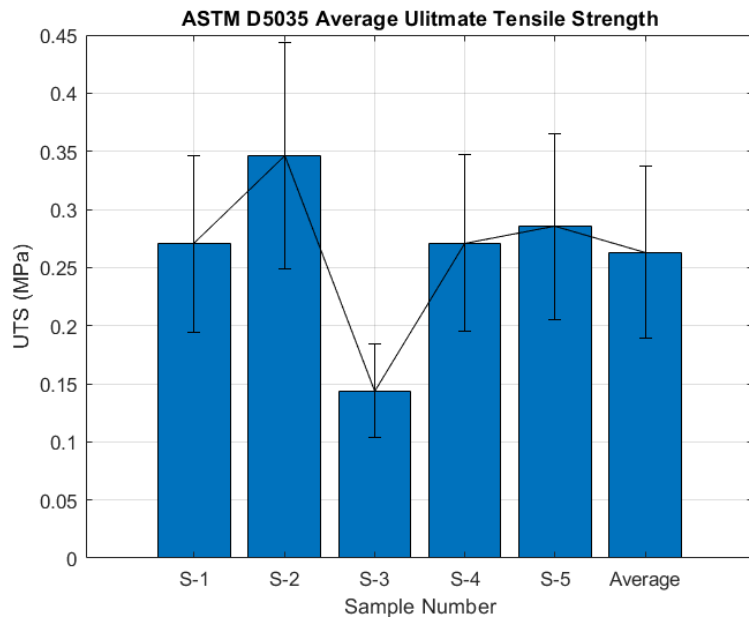


Figure [B.20]: Ultimate Tensile Strength of each sample

The ultimate tensile strength (UTS) is defined as the maximum stress carried by sample within the tensile test. It also signifies a turning point in a material's response to stress. Beyond the UTS, the cross sectional area of the sample begins to narrow locally until failure is reached (Callister and Rethwisch 2013, figure 6.5 and 6.11). The individual UTS values for each sample are shown in **Fig. B.20**. The average ultimate tensile strength was  **$0.26 \pm 0.07$  MPa**. This value was quite close to that of the elastic modulus, but the variance was lower, at only **28.04%**.

To gain further insight into correlations between structural and mechanical

properties, the number of root tips found per vertex on each of the tested samples were quantified with the same digital microscope.

**Figure B.21** shows an example of one of the micrographs used to quantify this. The number of root tips in a vertex (seen in the red circles) is an estimation, given that only the top layer is observed and there are surely many more root tips obscured by the complex interactions between roots that occur at this point. Though it may not be indicative of the total number of roots ending at a vertex, this surface level analysis provides a first look at a possible correlation between

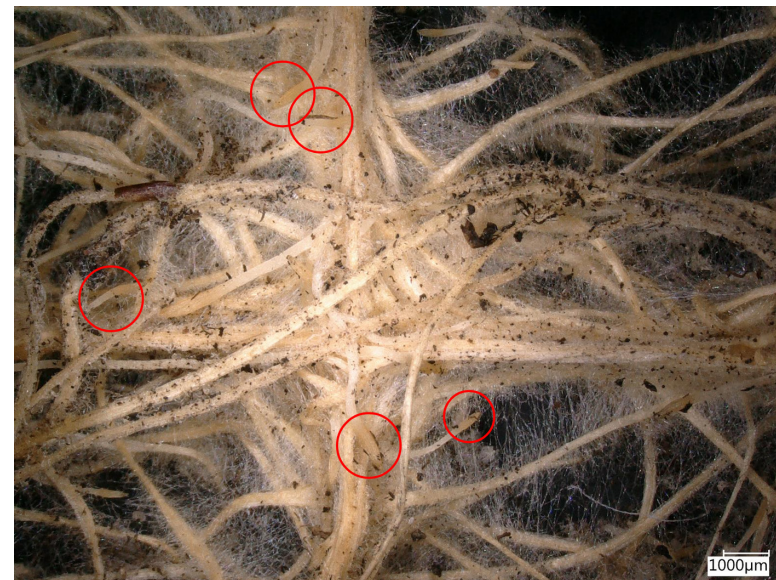


Figure [B.21]: Micrograph from Sample 2 used to count the number of root tips present in a vertex.

the complex structure of Interwoven samples and their performance.

The process for quantifying the root tips is by no means rigorous or complete, but an attempt is made at being consistent.

**Procedure:**

Given the inconsistent nature of Interwoven structures, each vertex is unique, so there is no clear definition for the beginning or end of a vertex. Instead, a constant magnification of 20x is kept and the center of the vertex is placed in the center of the microscope. The number of visible roots is then quantified counted.

**Fig. B.22** shows the average number of root tips per vertex. Sample 2 had the highest average with 12.2 roots. While samples 1,3, and 5 were all close with an average of about 6, sample 3 had the lowest average out of all the samples.

The sample with the most root tips per vertex, Sample 2, is also the sample with the highest elastic modulus and UTS values. Sample 3, (the one with the least root tips) also corresponds to the lowest elastic modulus and UTS. This trend is also evident for UTS values in other samples and, to a lesser extent, the elastic moduli, where Sample 5 breaks the pattern. **Table B.3** is a comparison of mechanical properties ordered from highest root density to lowest, where the aforementioned correlation is seen.

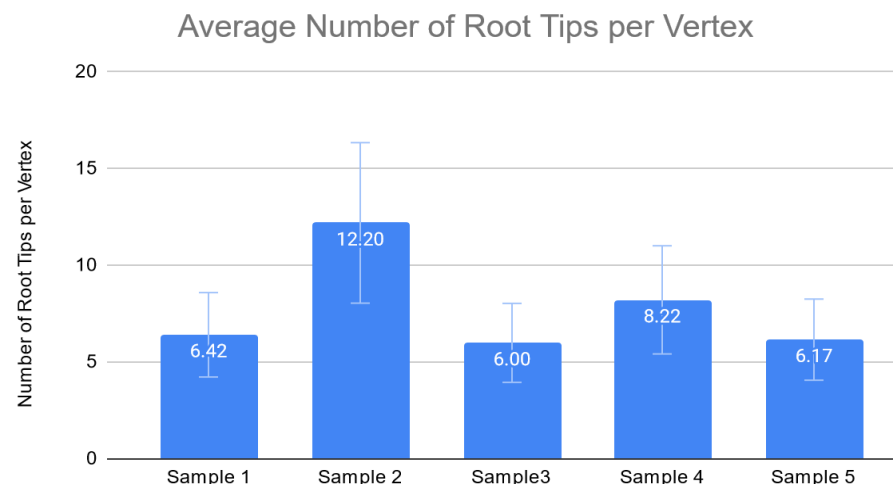


Figure [B.22]: Average vertex root tip density per sample

**Root Tip Density vs. Mechanical Properties**

Sample	Modulus (MPa)	UTS (MPa)	Root Density
Sample 2	4.678*10 <sup>(-1)</sup>	3.461*10 <sup>(-1)</sup>	12.20
Sample 4	2.458*10 <sup>(-1)</sup>	2.708*10 <sup>(-1)</sup>	8.22
Sample 1	3.040*10 <sup>(-1)</sup>	2.703*10 <sup>(-1)</sup>	6.42
Sample 5	3.244*10 <sup>(-1)</sup>	2.853*10 <sup>(-1)</sup>	6.17
Sample 3	1.236*10 <sup>(-1)</sup>	1.436*10 <sup>(-1)</sup>	6.00

Table [B.3]: Comparison of root density vs. mechanical properties

## Discussion

An example of a typical stress-strain curve for metals was used to describe the material properties that can be derived from said curves in the opening section of Chapter 4. Turning the load-displacement curves for Interwoven samples into a stress-strain curve is therefore very important to being able to compare Interwoven to other materials. The effective cross-sectional area of Interwoven tensile coupons was calculated to estimate the stress-strain curves and attempt to normalize the curves.

Note that the stress-strain curves are only estimations. The calculated cross section only faithfully describes the measurements taken from the samples, but the area varies for each cell according to the growth of the roots. The estimation may be one of the reasons that the normalization was not as effective as expected, but another explanation for this lies more on the structure of the samples. Much like textiles that are made up of yarns from a specific fiber, Interwoven is a complex structure composed of many interweaving roots, so the material properties are derived from the roots. The perceived elastic modulus from the samples is thus not truly the intrinsic material property - it remains a measure of the response for that specific sample alone. The elastic modulus will have

to be derived from single root samples in future sections.

The quantified root tips-per-vertex point toward a correlation between the perceived modulus and the number of root tips (and thus, the number of roots) present. The number of root tips present in each vertex vary because the samples are composed of many short roots, rather than one continuous root, along the length of the structure. The short roots become tangled and hold onto each other as a load is placed on the sample. A closer study relating the number of roots to mechanical properties should be carried out. Once the relationship between these is better established, it should be possible to find a corresponding parameter that better controls the preferred mechanical properties.

## Conclusions

The root grid tensile tests serve as a starting point for understanding Interwoven samples as a potential composite reinforcement. The average perceived modulus for these samples was **0.29 MPa** with a corresponding ultimate tensile strength of **0.26 MPa**. Microstructural analysis revealed that fine roots are intertwined in layers and held together by their tangled root hairs to create coarse roots. The coarse roots then become the main microstructural component of the macrostructure - the tensile test coupon. The details of how a load is transferred throughout the coupon

## B-3 Grid Cell Tests (Extended)

*What are the effects of coarse root density?  
Does the density of root tips at vertexes impact  
tensile properties?*

Appendix B-1 and B-2 tested tensile coupons with a gridded pattern composed of 1cm cells. Using the dimensions for ASTM D5035, these coupons had three coarse roots along the width (25cm). It was postulated that strength and the number of coarse roots along the width of the sample were related.

### Purpose

This section will test this theory by changing the size of the cells in each sample, effectively changing the number of longitudinal coarse roots. This parameter becomes important for making composites since the cell size influences the percentage of the root fibers present over a specific area. **Figure B.23** explains the differences between cell size (the length of a square in the grid), vertices (intersection of cells), and grid (sample made up of multiple cells).

### Procedure

To test the effects of cell size on mechanical properties, ASTM D5035 samples (25 x 150mm) were cut from templates with three different cell sizes: 1cm, 2cm, and 0.5cm (**Fig. B.24**). Before preparing the samples, the grids were taken to a DHX Keyence® microscope, where the average root tip density within each cell was quantified using differences in brightness. The root density measurements give insights about differences in fine root formation caused by the templates. **Figure B.25** shows an example of this with a 2cm cell, and the figures on the next page are the sections of the 2cm and 0.5 cm grid cells that were measured, respectively.

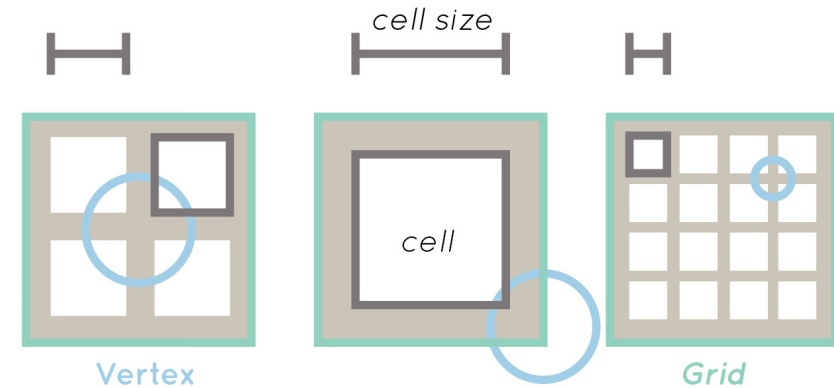


Figure [B.23]: Cell Terminology used here

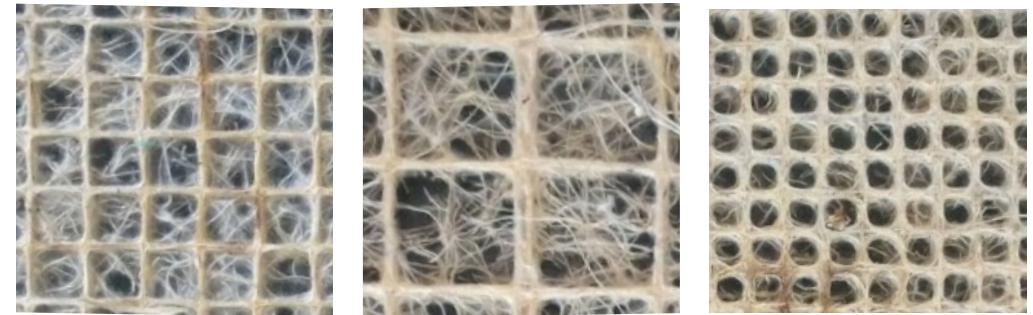


Figure [B.24]: Three cell sizes tested: (1) 1cm cell, (2) 2cm cell, (3) 0.5cm cell

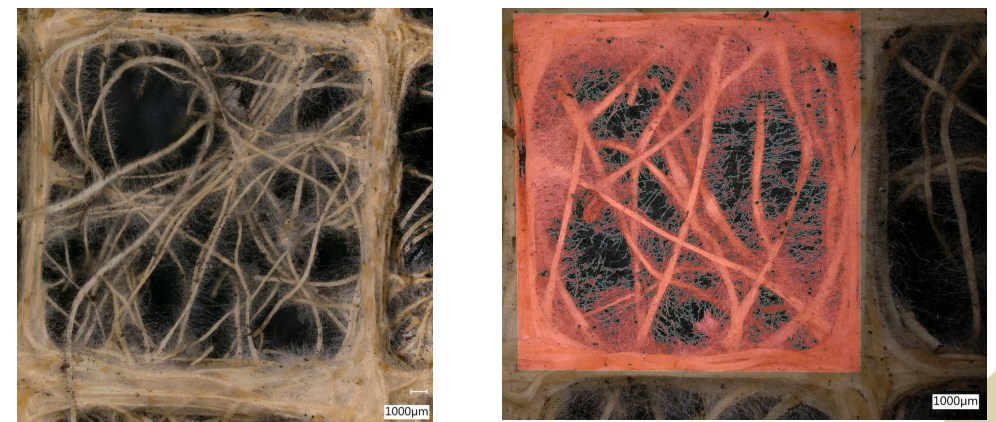


Figure [B.25]: Fiber root density measured on a 1cm cell



Figure [B.26]: Fiber root density measured on a 2cm (left) and 0.5cm cell (right). Note the rounded edges of the 0.5cm cell.

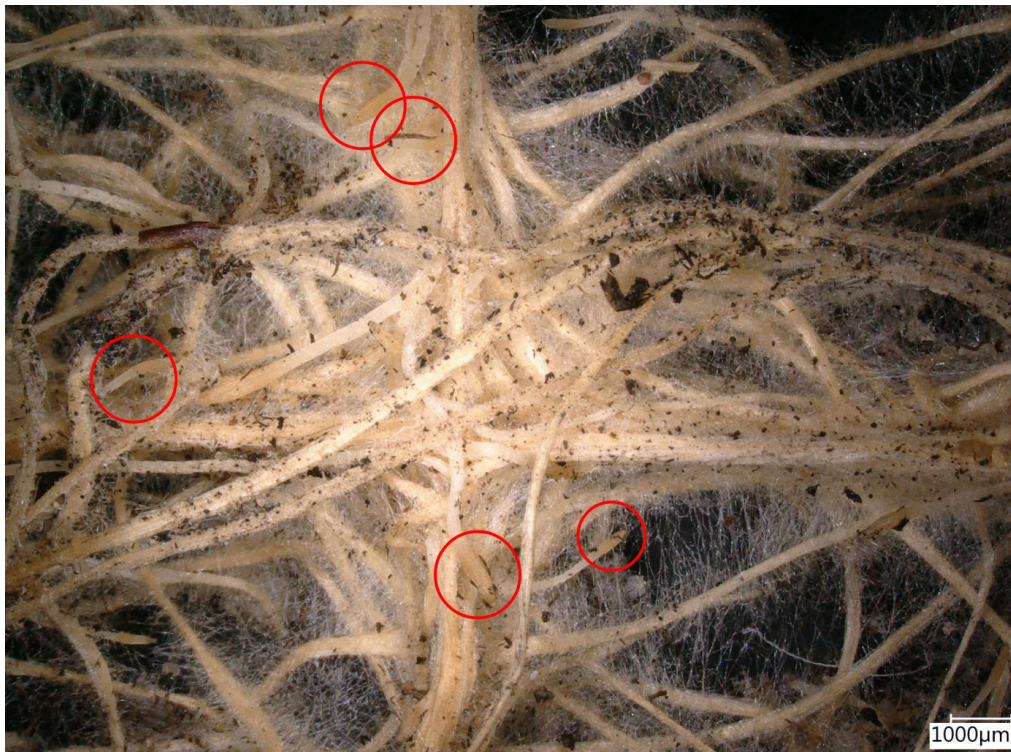


Figure [B.27]: Root tip density on a 1cm cell vertex.

**Figure B.27** is an example of a root tip density analysis being performed on a 1cm cell. This analysis is performed to further evaluate the correlation between the interwoven structure and the measured tensile properties first seen in the control group's tests (Appendix B-2).

process will not be explained again. However, a summary of the parameters used for testing is provided here, along with a sample of each dimension

#### Summary of Test Parameters

- *Sample Dimensions:*  
25 x 150mm
- *Template Thickness*  
3 mm
- *Number of specimens:*  
3 x 1cm cell size  
3 x 2cm cell size  
3 x 0.5cm cell size
- Gauge Length:*  
75mm
- *Strain rate*  
15mm/min

Since the tensile test procedure is the same version of the ASTM D5035 standard used in the calibration tests and control group, (Appendix B-1, B-2), the details of the



Figure [B.28]: ASTM D5035 samples for (top) 1cm cell, (mid) 2cm cell, and (bottom) 0.5cm cell-sized grids.

## Results

At first glance, it is clear that the fine root density within each cell differs with size. However, the 2cm cells had the most visible fine root hairs, but the lowest overall root density within the cell with  $72.25 \pm 7.41\%$ . As expected, the smallest grid size had the highest root density with  $79.75 \pm 5.5\%$ . The 1cm cells had  $78.75 \pm 7.14\%$ . The differences between these values was not large, but the root density was considered representative of the cross sectional area of the samples (as was done in the control group tests of Appendix B-2), so these percentages were used to calculate cross-sectional area and derive stress-strain curves. The average modulus and tensile strength of each cell size were computed. The sample with the modulus closest to the average of each size was plotted against that of the other sizes to compare results (Fig. B.29).

### Stress-Strain Curves

The stress-strain plots in figure Fig. B.30 include a representative curve from each sample group based on proximity to the average values of the modulus, which are summarized by the bar graph in Fig. 3.5.8. The group with 2cm cells had the steepest modulus with  $0.324 \pm 0.051$  MPa, followed by 0.5cm samples at  $0.196 \pm 0.086$  MPa, which is only slightly higher than the 1cm group's average,  $0.182 \pm 0.046$  MPa.

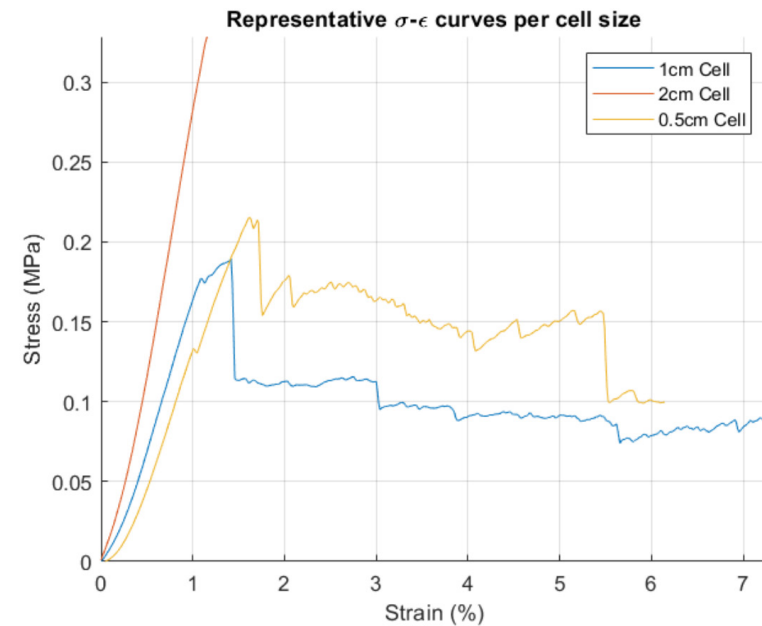


Figure [B.29]: Representative Stress-Strain Curves for each cell size

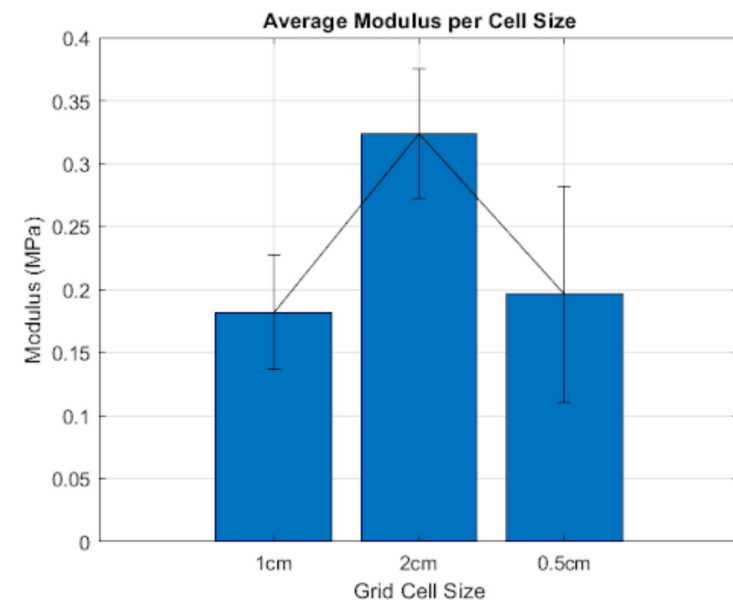


Figure [B.30]: Average moduli per cell size

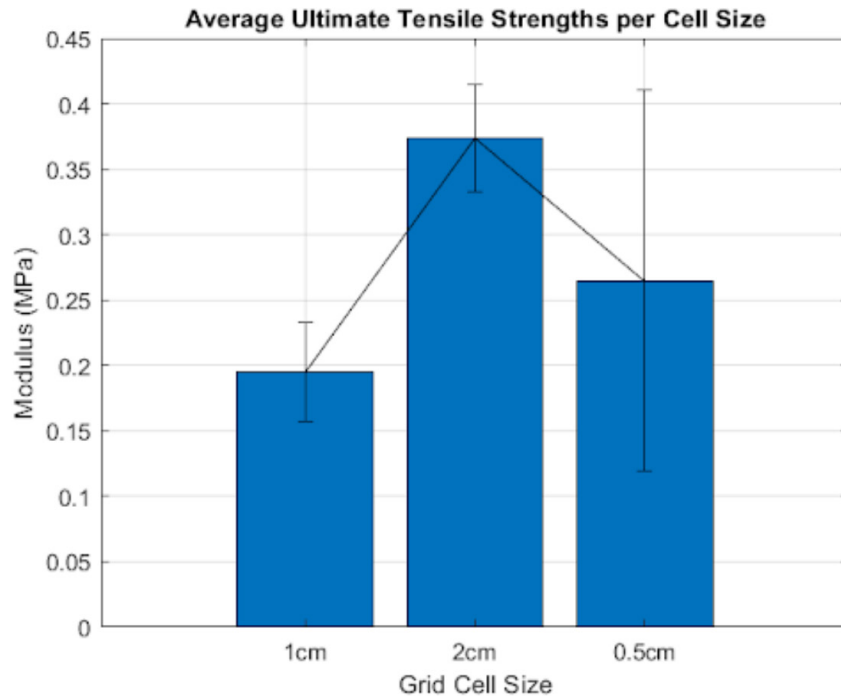


Figure [B.31] Average tensile strength per cell size

### Average Tensile Strength

The ultimate tensile strength averages per group followed the same trend as the moduli (Fig. 3.5.9). 2cm grid cells yielded the strongest samples with an average UTS of **0.374 ± 0.041 MPa**, 0.5cm cells were next (**0.265 ± 0.146 MPa**), and 1cm cells had the lowest UTS (**0.195 ± 0.038 MPa**).

### Vertex Root Tip Density

One final correlation found with the samples was the number of root tips present at the vertexes. The root tip density reflected the same trend presented by the two previous bar graphs. Below is a visual summary. On average, 2cm cells had **16.13 ± 5.13** root tips at each vertex. The next densest vertexes were found in 0.5cm cells, which had **3.88 ± 1.97**, and 1cm cells had an average of **3.84 ± 1.92**. The difference in root tip density was hardly

evident in the last two groups, but one key difference between them was also how the roots looked in the cell. The smaller cells had roots turning corners around a small diameter, which gave the small squares a more circular look, whereas the 1cm samples only had slightly rounded edges. This effect is even less evident in the 2cm cells.

### Conclusion

The tensile properties of ASTM D5035 coupons with varying grid cell sizes (1cm, 2cm, and 0.5cm) were tested. The largest cell size exhibited the highest elastic modulus and UTS. A correlation between root tip density and mechanical properties was identified through digital microscopy. The strongest samples also had the highest number of roots per vertex, suggesting root tip density is a better indicator of tensile properties than the number of coarse roots along the sample's width.

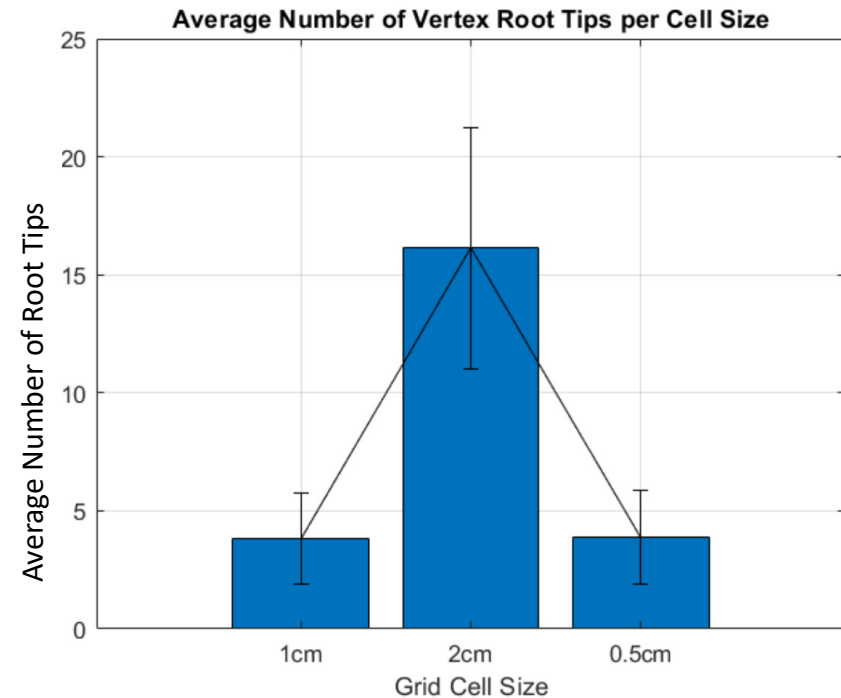


Figure [B.32]: Average number of root tips per cell size

## B- 4 Tensile Tests on Single Roots with a DMA

It has been established that Interwoven samples are structural members and not material samples. These members are composed of many individual roots that tangle and weave into each other.

### Purpose

The mechanical behavior of individual roots and their interactions remain unexplored. Analyzing the interactions at an individual level poses a challenge, but testing the mechanical behavior is possible with specialized equipment, and doing provides insight into the “actual” elastic modulus of the material, which, in theory, is much less varied than the that of the tests performed thus far.

### Procedure

Testing individual roots is possible with the help of a dynamic mechanical analyzer (DMA), which has a very small tensile tester with many parameters. The equipment used for this test was a DMA

Q800 from TA Instruments in tensile mode. The parameters used for testing are summarized below.

#### Summary of Test Parameters

- *Sample Dimensions:*  
at least 20 mm long
- *Number of specimens:*  
Eight (8) individual roots
- *Gauge Length:*  
at least 10 mm
- *Strain rate*  
10% of gauge length

The standard test method for tensile properties of single textile fibers, ASTM D3822, states that the gauge length should be at least 10mm and the strain rate should be 10% of that (ASTM International, 2020b). An example of the gauge length on a loaded fiber is seen in **Fig. B.33**. The value of the gauge length varied per sample because the lower section of the stage is set manually. Thus, before each test, the gauge length was measured and the strain rate used was 10% of the measured

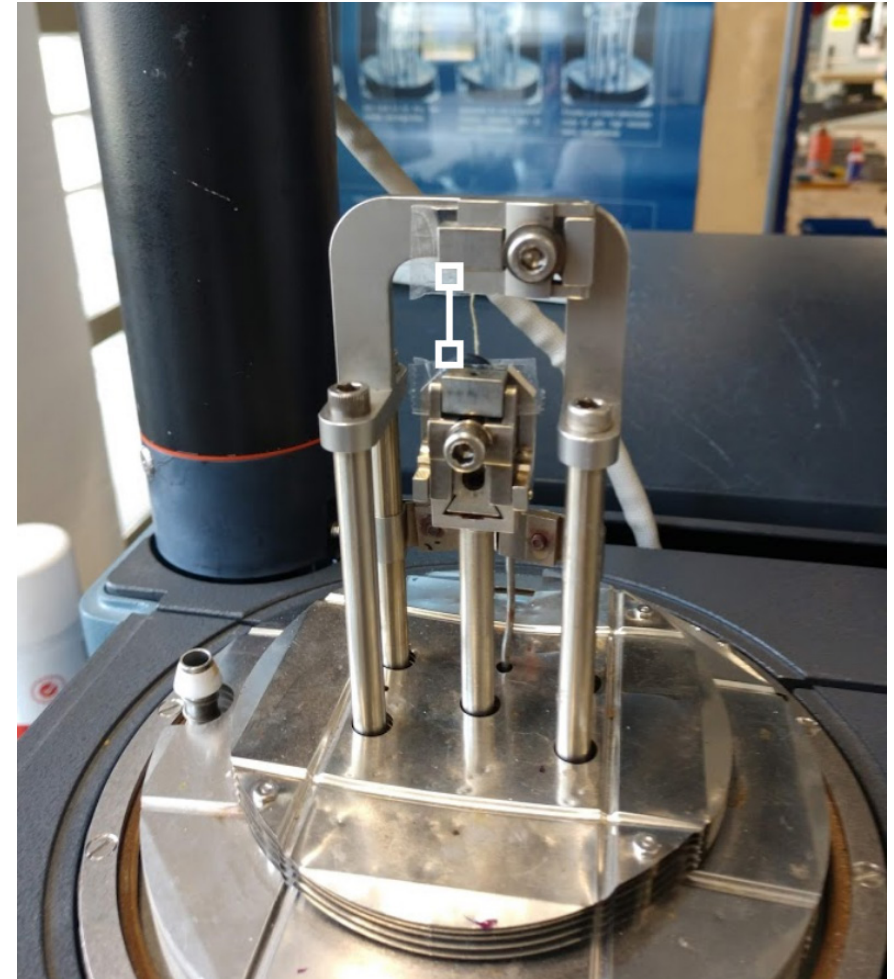


Figure [B.33]: image of root mounted onto DMA Q800 with gauge length in white.

value. However, before testing, the diameter of the root being tested was measured with a digital caliper whose precision goes to 0.001mm.

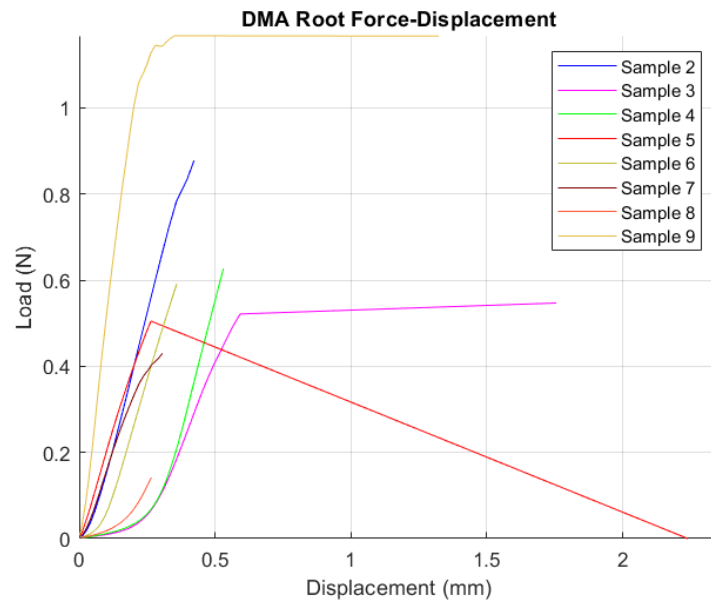


Figure [B.34]: Load Displacement Root Curves

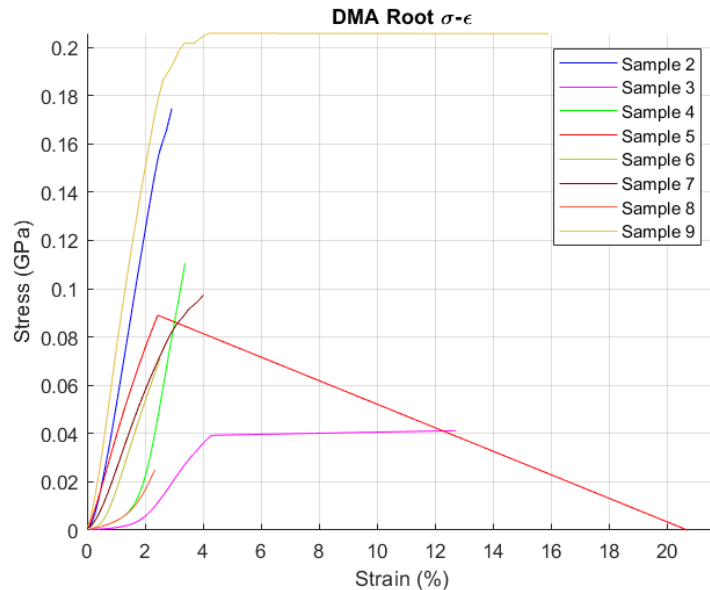


Figure [B.35]: Stress-Strain Root Curves

A total of nine samples were tested, but one was discarded as an outlier that had a breaking force more than two orders of magnitude higher than the other samples.

As was the case in previous tests, the initial data response was recorded in a load-displacement curve. The slopes of the linear portion of the curves varied a lot, but there were similarities. All samples started with a gradual increase in force, after which a sharp change to a much steeper slope was observed. The extent of the gradual slope varied per sample, but the ones with the largest extension

before reaching the linear-elastic region (samples 3, 4, and 8) were also some of the weakest samples.

The discrepancies between samples were somewhat reduced in the stress-strain curves. For the conversion of graphs, the roots were treated as cylinders, so the cross sectional area was calculated by using the diameter that was calculated prior to each test (Fig. B.36). The average modulus was  $E_{avg} = 46.10 \pm 24.01$  MPa. The variance in modulus between samples exceeded that of any of the structural samples tested at 52.07%.

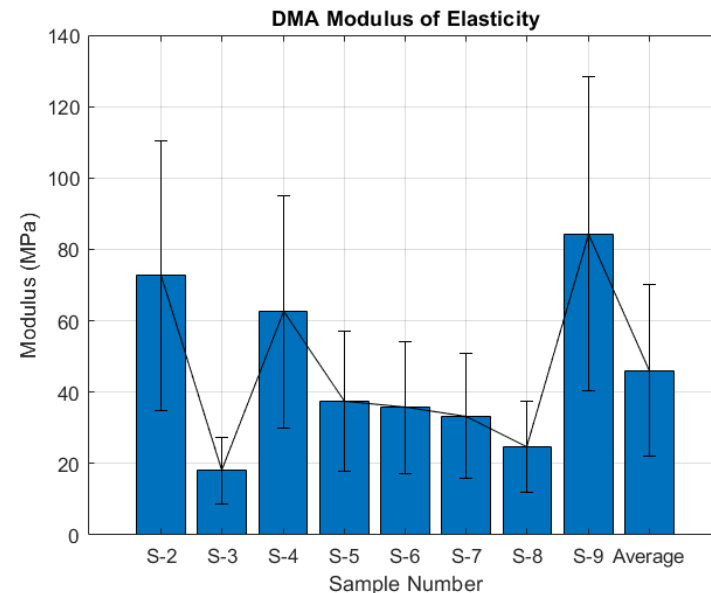


Figure [B.36]: Individual Modulus of elasticity for each root tested

## Microstructural Analysis

After tensile tests, the structure of the root was studied under the digital microscope. **Fig B.36** shows a closeup of the area surrounding the fracture surface and the length of a root, respectively. The length of the root shows many lines going along its length. Recall from the root anatomy that roots are composed of various types of tissue that help them anchor the plant, absorb water

and nutrients, and transport those to other parts of the cell (refer to Chapter 1). Nutrient transportation is done by vascular tissues that run throughout the root, which is likely what is seen in the image. The image depicting the area near the fracture surface also shows the many root hairs that grew to increase the root surface area.

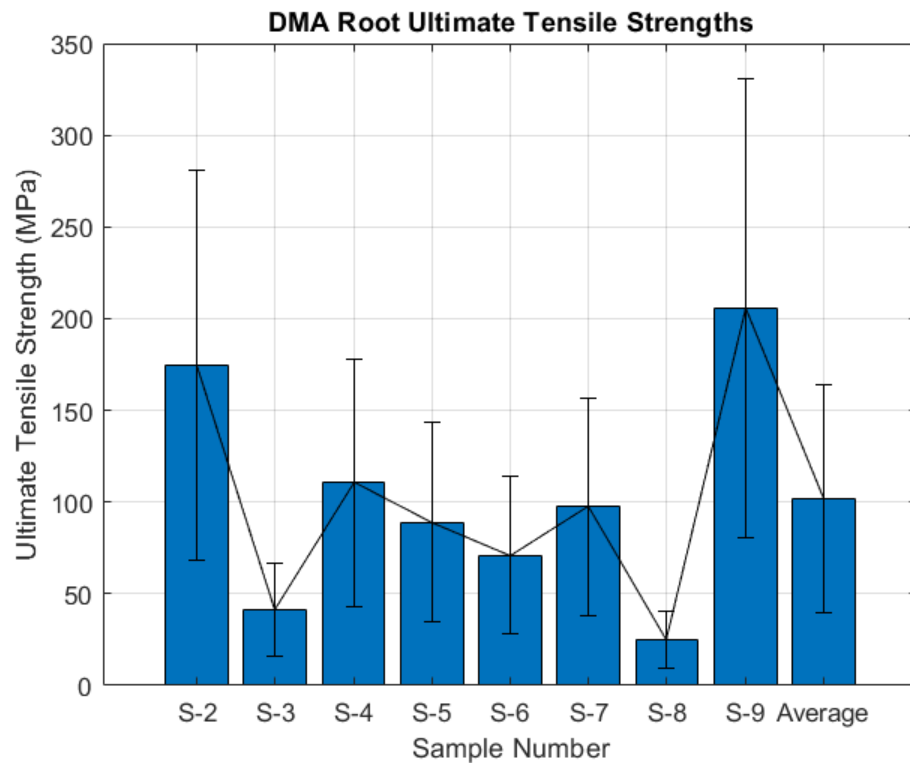


Figure [B.37]: Individual UTS for each root tested

The ultimate tensile strength of the samples was just as varied. The average was  $UTS_{avg} = 101.83 \pm 61.98$  MPa. The sample with the highest UTS (205.78 MPa) was also the one with the highest modulus - sample 9. Sample 8 had the lowest UTS (24.00 MPa), but the lowest modulus was seen in sample 3 (18.1 MPa).



Figure [B.38]: Area near root fracture surface



Figure [B.39]: Longitudinal axis of an oat root

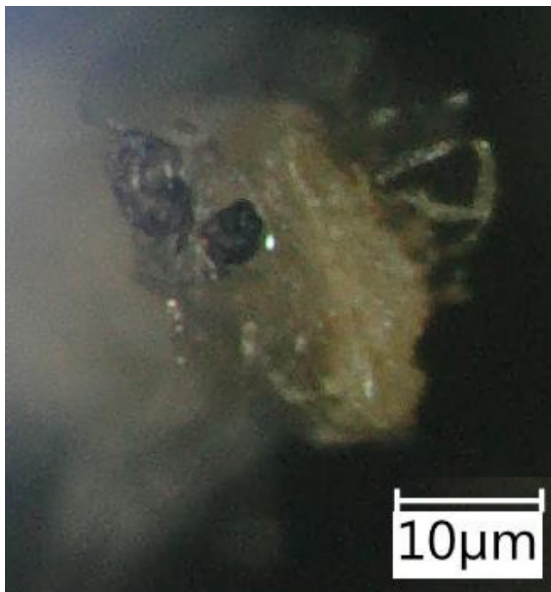


Figure [B.40]: Cross sectional view of fractured root

The fracture surface provides some insights into the mechanisms that lead to the root's fracture. The cross section is not perfectly flat nor planar. A line goes down the middle showing a slightly raised surface, which could indicate some plastic deformation before fracture. The dark particle at the top left of the fracture is likely a remnant of soil from the original sample.

**Figure B.40** below is the cross section of a typical monocot root, such as those tested here. The endodermis is an external membrane-like layer that protects the root and facilitates nutrient absorption while the xylem and phloem are the vascular components that transport nutrients to and from the rest of the plant, respectively.

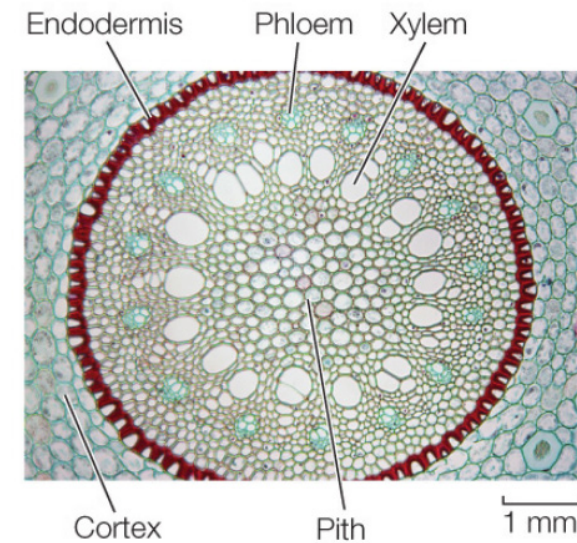


Figure [B.41]: cross section of a monocot root (Hillis et al., 2013)

## Discussion

Individual roots are the structural units that make up the structures designed with the Interwoven method. At the beginning of this test, it was assumed that the root was therefore an individual material, meaning that it would have a somewhat homogeneous tensile response with a somewhat consistent elastic modulus, but the results were not as expected.

## Tensile Tests

Half of the tested samples had somewhat consistent values for modulus and UTS, but the other four were on either extreme of the range of values. With such a spread of results, it is evident that the root is not the material tested within the Interwoven structure, it is a structural unit made up of other structures that contribute to the mechanical properties. The microstructural analysis, paired with biological sciences, provides more insights about this.

## Microstructure

The heterogeneity in the roots' response to tensile loading are a result of the structure of the individual roots. The oat root is made up of various tissues with their own properties, and the tubes that make up the vascular system of the root provide some of the structure. This tissue is evident in the lines seen along the length of the root.

Individual roots are not homogeneous in nature either. Even though the same structures are present, the layout may differ in other roots according to the health of the plant. A macroscopic example of unhealthy roots is seen in the image below. The discoloration seen across the vertex in the image indicates

the varying degrees of health seen in the samples. Just like any other living organism, the roots of plants will vary in health, and the effects of this may go unnoticed until tested. This may account for the results seen within the sample size of this study. A more expansive study is necessary to normalize the differences in root health.



Figure [B.42]: Example of varying root health. Arrow points at unhealthy section

## Result Comparison

The tensile properties of individual roots proved to be much higher than that of the Interwoven structure. The average tensile modulus of root fibers (**46.10 ± 24.01 MPa**) was more than two orders of magnitude larger than the Interwoven samples with 2 cm cells, which had the next highest modulus at **0.32 ± 0.051 MPa**. The same trend is seen for the UTS of the two aforementioned samples - **101.83 ± 61.98 MPa**, compared to **0.374 ± 0.0409 MPa**. **Table B.4 and B.5** compare all of the samples tested, ranked in descending order.

Although they have the strongest tensile properties of the samples tested thus far, the root fibers also exhibit the largest deviation. A look at another popular natural fiber used for reinforcement, hemp, shows a similar trend. Shahzad tested individual hemp fibers from a bundle using two methods of defining the cross-sectional area, one assuming the cylindrical nature of the fiber, and another assuming

a more polygonal shape, and calculated a tensile strength of  $277 \pm 191$  MPa (a 68.95% variance) (Shahzad, 2013). Five years earlier, Ashori reported a higher tensile strength at 690MPa in a table comparing the mechanical properties of natural fibers with those of synthetic fibers used for reinforcement (Ashori, 2008). This table is reproduced in the next page.

Unlike synthetic fibers, the mechanical properties of natural fibers are less consistent, due in part to the small area of the fibers and the increased possibility of defects within that area. Some of these defects could be related to the presence of different tissues in the fibers, as is evidenced in the microstructure of the oat root fibers tested here.

Modulus Values per Test Group			
Group	Average Modulus (MPa)	Standard Deviation	Variance (%)
Root	<b>4.610*10<sup>1</sup></b>	± 24.01	52.07
Agar(Ind.)	<b>2.705*10<sup>0</sup></b>	± 0.571	21.11
Agar (Bulk)	<b>1.3125*10<sup>0</sup></b>	± 0.554	42.22
2 cm Cell	<b>3.235*10<sup>(-1)</sup></b>	± 0.051	15.89
Control	<b>2.931*10<sup>(-1)</sup></b>	± 0.125	42.68
0.5 cm Cell	<b>1.964*10<sup>(-1)</sup></b>	± 0.0859	43.74
1 cm Cell	<b>1.822*10<sup>(-1)</sup></b>	± 0.046	24.97

Table [B.4]: Comparison of all moduli thus far

UTS Values per Test Group			
Group	Average Modulus (MPa)	Standard Deviation	Variance (%)
Root	<b>1.018*10<sup>2</sup></b>	± 61.98	60.86
2 cm Cell	<b>3.74*10<sup>(-1)</sup></b>	± 0.041	10.94
0.5 cm Cell	<b>2.65*10<sup>(-1)</sup></b>	± 0.146	55.04
Control	<b>2.63*10<sup>(-1)</sup></b>	± 0.074	28.04
1 cm Cell	<b>1.95*10<sup>(-1)</sup></b>	± 0.038	19.51

Table [B.5]: Comparison of all UTS values

Fiber	Density (g/cm <sup>3</sup> )	Elongation (%)	Tensile strength (MPa)	Young's modulus (GPa)
<i>Fibers (reinforcements)</i>				
Cotton	1.5–1.6	7.0–8.0	287–800	5.5–12.6
Jute	1.3	1.5–1.8	393–773	26.5
Flax	1.5	2.7–3.2	3451035	27.6
Hemp	1.5	1.6	690	70
Ramie	1.5	1.2–3.8	400–938	61.4–128
Sisal	1.5	2.0–2.5	511–635	9.4–22.0
Coir	1.2	30.0	175	4.0–6.0
Viscose (cord)	–	11.4	593	11
Soft wood (kraft)	1.5	–	1000	40
E-glass	2.5	2.5	2000–3500	70.0
S-glass	2.5	2.8	4570	86.0
Aramide (normal)	1.4	3.3–3.7	3000–3150	63.0–67.0
Carbon (standard)	1.4	1.4–1.8	4000	230.0–240.0

Table [B.6]: Mechanical properties of natural fibers compared to conventional polymers (Ashori, 2008)

**Fig.B.43 and B.44** compare all the samples tested in one graph. However, because the results for the single root were much higher in magnitude, another graph is included without it, for reference.

The large difference between the mechanical properties of a single root and those of the structure is likely due to the interaction of roots in the structure. In DMA tests, the entire load from the tester is

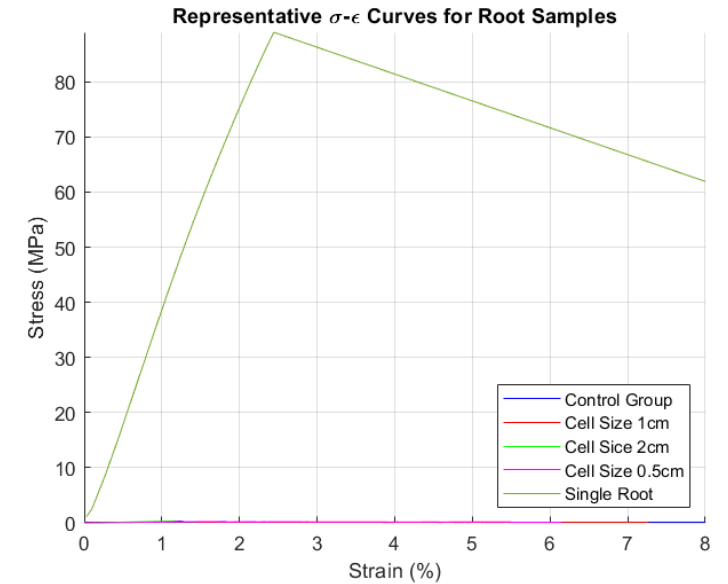


Figure [B.43]: Representative Load Displacement Curves

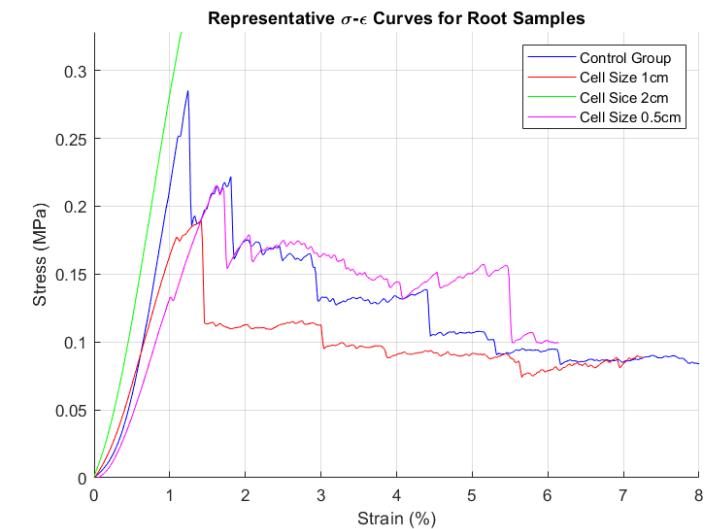


Figure [B.44]: Representative Stress-Strain Curves

evenly distributed throughout the root as it is pulled from both sides. Interwoven samples, on the other hand, do not pull one single root from both sides. They pull a series of connected roots from one end, and the load is distributed along an unevenly tangled network of roots that deform together for some time before breaking. Evidently, the load distribution throughout this network is inefficient considering the magnitude of tensile properties seen for Interwoven samples.

## Conclusions

Structural members designed with the Interwoven method are composed of many individual roots that are tangled together in a network. When a load is placed on the structure, it is distributed along the network of roots in a way that is inefficient. A single root can withstand up to **101.83 ± 61.98 MPa** of tensile stress, but even the most effective Interwoven structure tested thus far can only withstand **0.37 ± 0.04 MPa**.

The mechanical properties of roots vary greatly because of variations in root diameter,

defects present along the cross section, and the different tissues that make up the microstructure of the root. This study shows that, despite being the unit that makes up Interwoven structures, roots are not a homogeneous material. They are also a complex structure made up of tissues that serve various functions in plant life, and fully understanding the microstructure and root interactions during load distribution are key to optimizing the mechanical properties of Interwoven designs.

## B-5 Root-Agar Tests

As mentioned in section 3.5, Interwoven-[agar-agar] NFRPMCs will be produced to strengthen 1cm cell grids.

### Procedure

A 0.8%wt agar-water matrix is used to prepare ASTM D3039M samples to execute the standard test methods for Tensile Properties of Polymer Matrix Composite Materials. Due to the many possibilities of polymer matrix composites (PMCs), the standard provides guidelines for deciding on sample dimensions rather than precise dimensions (D30 Committee, 2017).

The guidelines in the standard were mainly fulfilled by the sample dimensions for testing textiles (ASTM D5035 samples), so the parameters were left the same to facilitate comparison within this study. The only parameter in the standard that could not be fulfilled was that of using a 1cm thickness because agar shrinks into a film that was thinner than this. Finally, ASTM D3039M samples are meant to be manufactured flat, and that was tested here in two different methods described below.

### Sample Preparation

The composition of agar was determined in Chapter 2. A matrix composition of 0.8wt% agar (8g agar:1L water) was chosen due to its mixture of malleability and structural integrity. To prepare this matrix, 8 grams of agar-agar powder were added to 1L of water and brought to a boil. Once all of the powder was dissolved and the solution started to thicken, it was allowed to cool down slightly. The solution was poured over a mold with clamped roots once it had no more steam coming out from it, but before it started to solidify. This infuses the roots like in **Fig. 3.5.11**.

If left alone for enough time, agar-agar dries out and the original gel made when mixed with water becomes a stiff flake. This means that, when left to dry for long enough, any shape that the agar-agar was cast into will shrink into a flake. Recall in the tinkering chapter that the first agar-root composite grid shrunk and warped as a result of this. The warping is not desirable for tensile testing, so the Interwoven grids used to produce ASTM D3039M samples were clamped down throughout the drying process (which takes about 5 days in ambient temperature, and 6 hours in a humidity chamber at 30°C and 50% humidity).

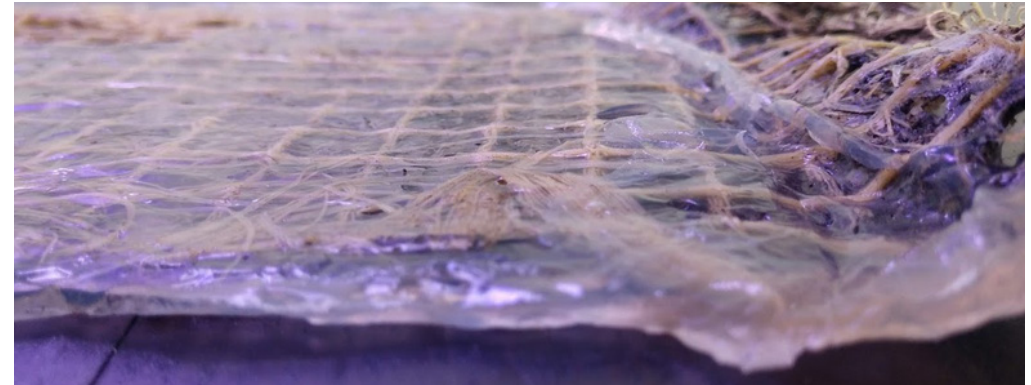


**Figure 3.5.11:** Unclamped Interwoven grid infused in agar matrix

## Clamping Mechanism

The two clamping methods can be described as bulk clamping and individual clamping. The principle behind both of these is the same and it involves holding the Interwoven grid in tension while the agar dries completely (**Fig.3.5.12**).

Bulk clamping used a large clamp to hold down the edges of the entire Interwoven grid (**Fig.3.5.13**), whereas individual clamps were 3D printed to produce samples with the exact dimensions for tensile testing (**Fig 3.5.14**).

### Bulk-Clamped Samples

Using the clamping mechanism seen above, the agar gel was poured on top of an Interwoven grid with 1cm cells. This cell size was used to compare directly with the “control” group of tests seen earlier in this chapter. Once poured, the top of the mold (seen in the first image) was added and weights were placed on top of the samples to evenly distribute the agar-agar and keep the inner sections of the grid flat as they dried

The resulting bulk clamp and tensile coupons are seen on the following page (**Fig. 3.5.15**). Note from the bulk composite that the fibers of the grid are not distributed evenly throughout. The samples taken from this bulk grid were chosen from areas that were most consistent, but some sections had holes in the agar matrix. Another observation to note is that the bulk grid was smooth and slightly curved (likely due to internal stress caused by the shrinkage), but the individual coupons are less smooth. The cause for this is unclear, but it is likely that, when cutting the samples into individual coupons, the internal stresses were no longer evenly distributed throughout the root fibers and the samples deformed slightly.

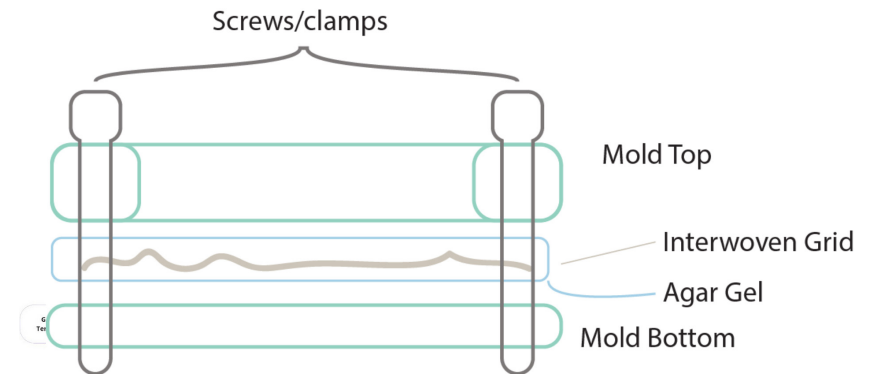


**Figure 3.5.12:** Clamping Mechanism



**Figure 3.5.13:** Bulk Clamp

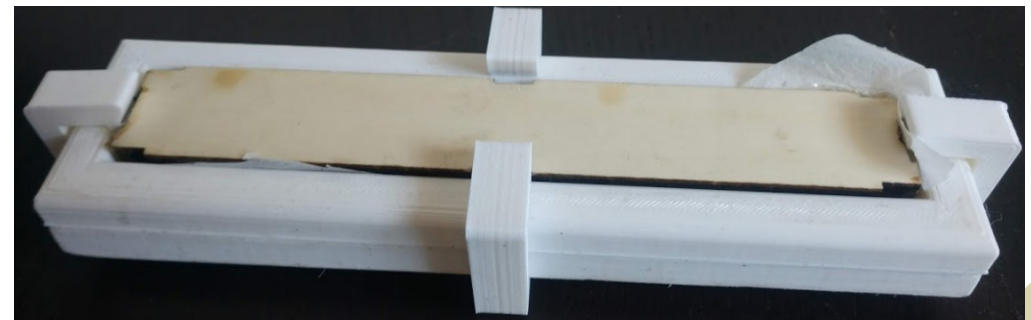


**Figure 3.5.14:** Individual Clamp



**Figure 3.5.15:** Bulk Composite and tensile coupons

### Individually-Clamped Samples

The 3D printed clamp/mold for individual samples is seen in the previous page. Each mold had 4 clamps to hold the edges of the roots in place and prevent shrinkage while a laser-cut top was added to provide even pressure throughout the sample. Sample preparation here was similar to that of the bulk samples, except that most of the cutting took place before pouring the agar. Samples were cut from a large grid, but in this case, they were left slightly oversized on each side so that the clamps could hold down the roots. The opening at the top has the sample dimensions, 25 mm x 150mm. Once the roots are clamped into place, the agar is poured on top (just enough to cover the roots) and the top is pressed lightly on it so that any excess agar is pushed up and out. The samples are then left to dry at room temperature (about 5 days). The resulting samples are seen in **Fig 3.5.16**.

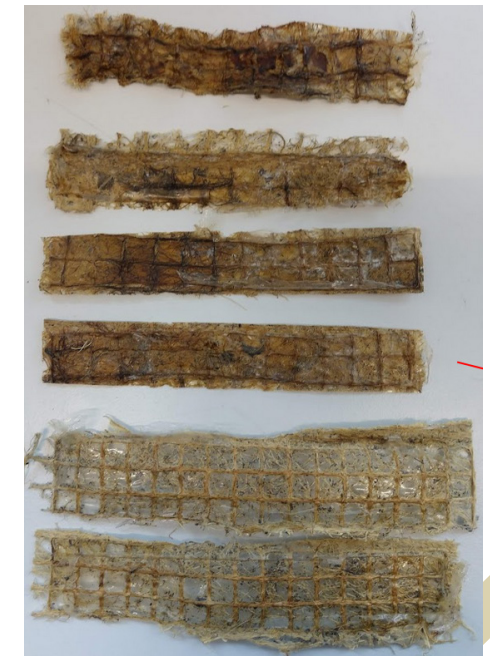


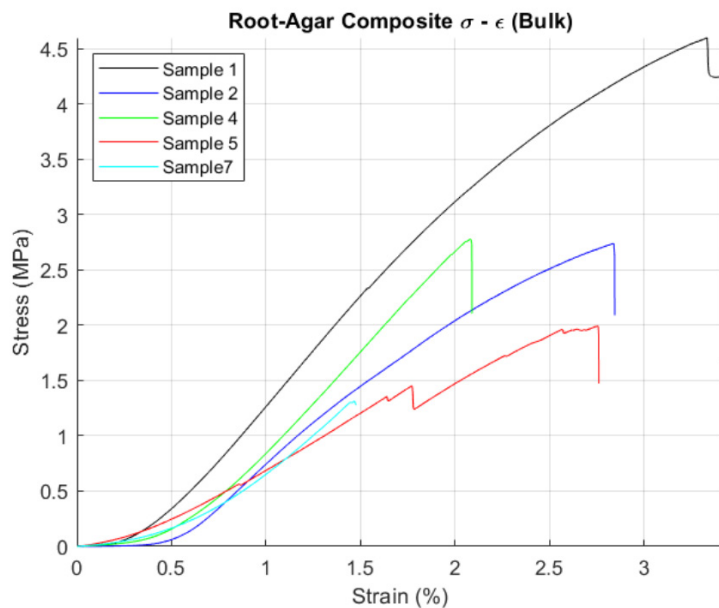
**Figure 3.5.16:** Individual Clamp samples

## Testing Parameters

- **Sample Dimensions:** 25 x 150mm
- **Number of samples:** 7 (per group)
- **Sample Thickness:** varied (standard asks for 1mm)
- **Strain rate:** 15mm/min (standard asks for 0.01\*strain min<sup>-1</sup>)
- **Gauge length:** 75mm

## Results

Once the agar matrix was fully dried, it flattened the cross section of the sample, so it was assumed that the porosity seen in the pure root samples was filled. As such, the cross sectional area of the composite samples was calculated by multiplying the average measurements of thickness and width based on three separate measurements for each dimension.. These values were then used to convert force-displacement curves the stress-strain curves seen below. Though 7 samples were tested, two of them were discarded because the modulus was less than half of the average of the rest of the samples.



## Bulk-Clamped

The linear region for these samples was very small, so the slope was determined by picking two points from the most linear sections of each graph. The average elastic modulus of the set was **1.3125  $\pm$  0.5541 MPa**. As expected of Interwoven structures, the modulus was not the same throughout the different samples.

## Individually-Clamped

These samples were stiffer than bulk samples and the modulus was higher, with an average value of **2.7047  $\pm$  0.5711 MPa**. Individual clamping molds doubled the experienced modulus of elasticity and halved the variance (only 21.1%).

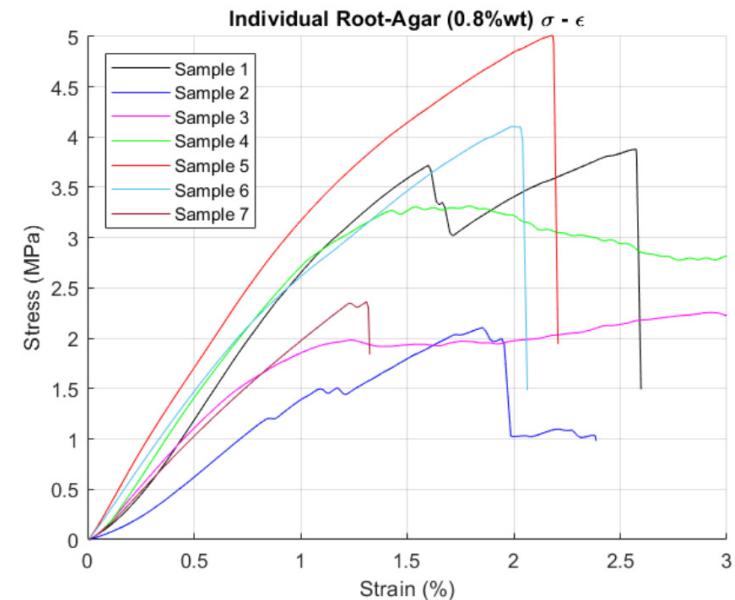
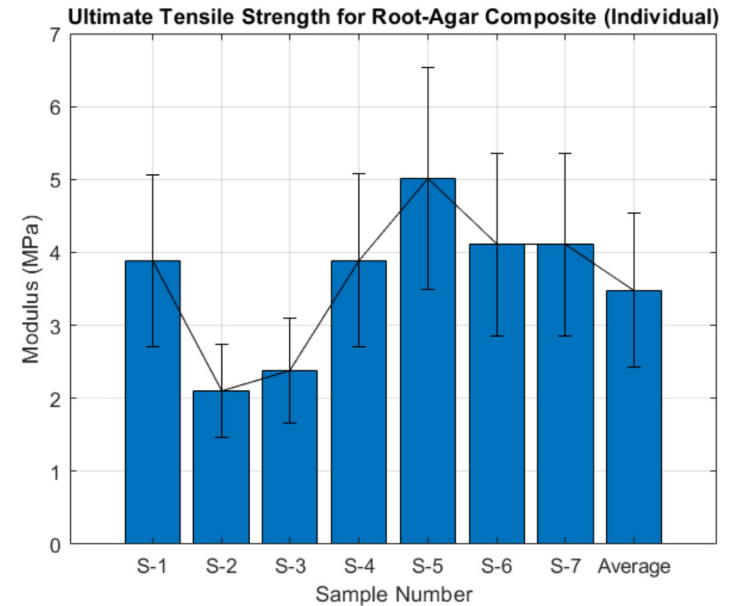
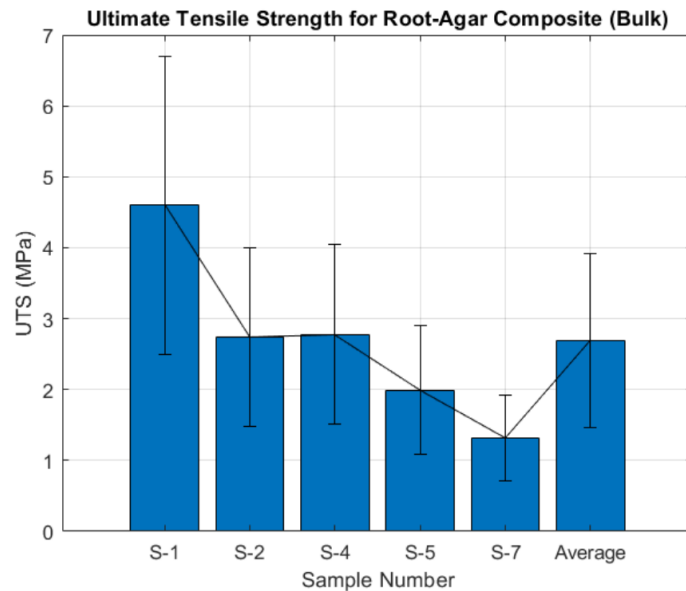


Figure 3.5.17: Stress-strain curves for Bulk (left) and Individual clamp samples (right)



**Figure 3.5.18:** Average UTSs for Bulk (left) and Individually clamped samples (right)

### Average Tensile Strength

The average tensile strength of both composite groups was considerably higher than that of any other Interwoven structures. The average for the bulk samples UTS was **2.69 ± 1.228 MPa**, which is one order of magnitude higher than the next strongest structure (2cm cell grids). A summary of all tensile properties across the samples can be found in **Tables 3.5.1 and 3.5.2**.

While the average tensile strength of individually-clamped samples did not double that of the bulk samples, it was still considerably higher than that of the bulk samples, with a value of **3.4788 ± 1.0566 MPa**. **Figure 3.5.18** shows the spread of UTS values between both data sets, and **Table 3.5.2** compares UTS of all data sets in the study in descending order.

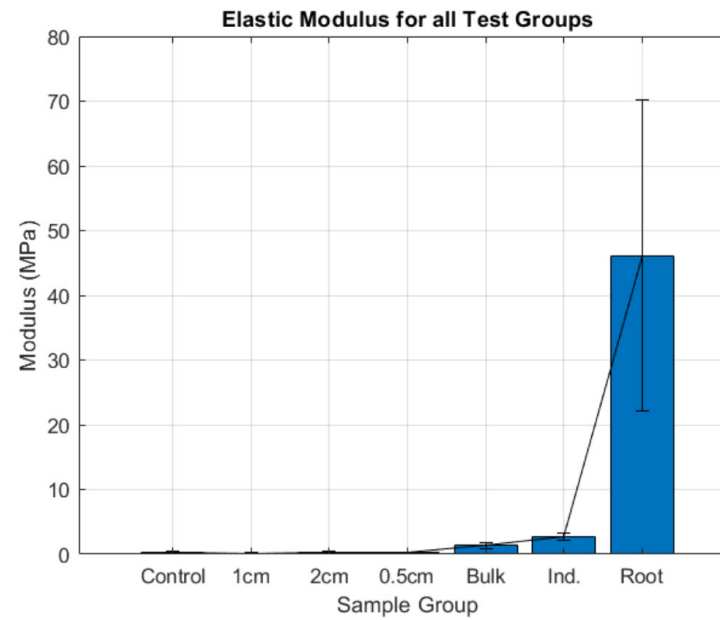
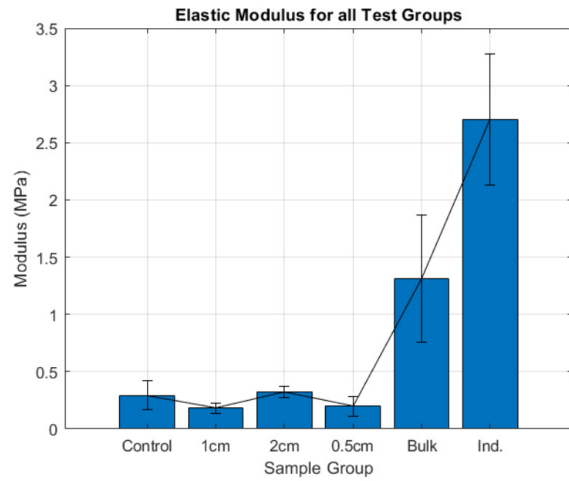
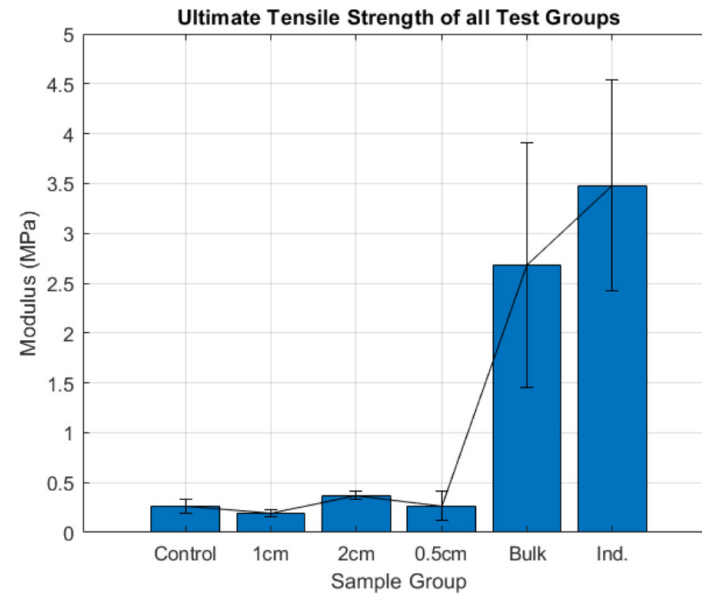
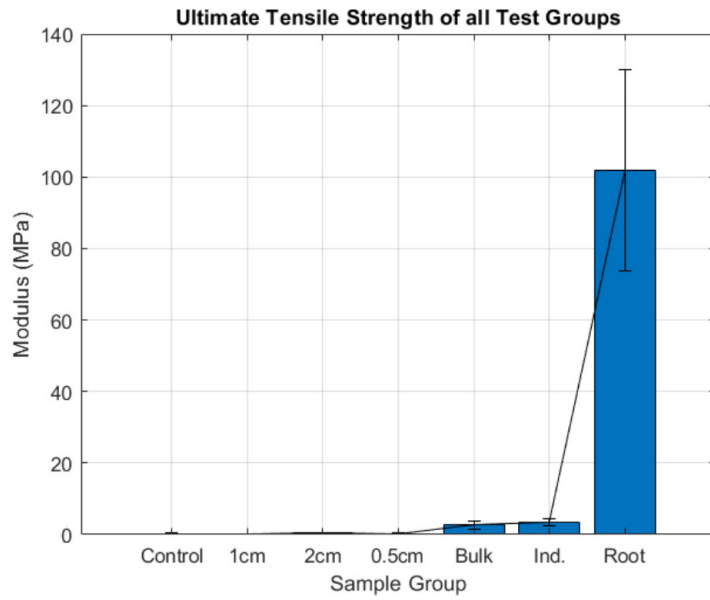
## Comparison Across All Sample Sets

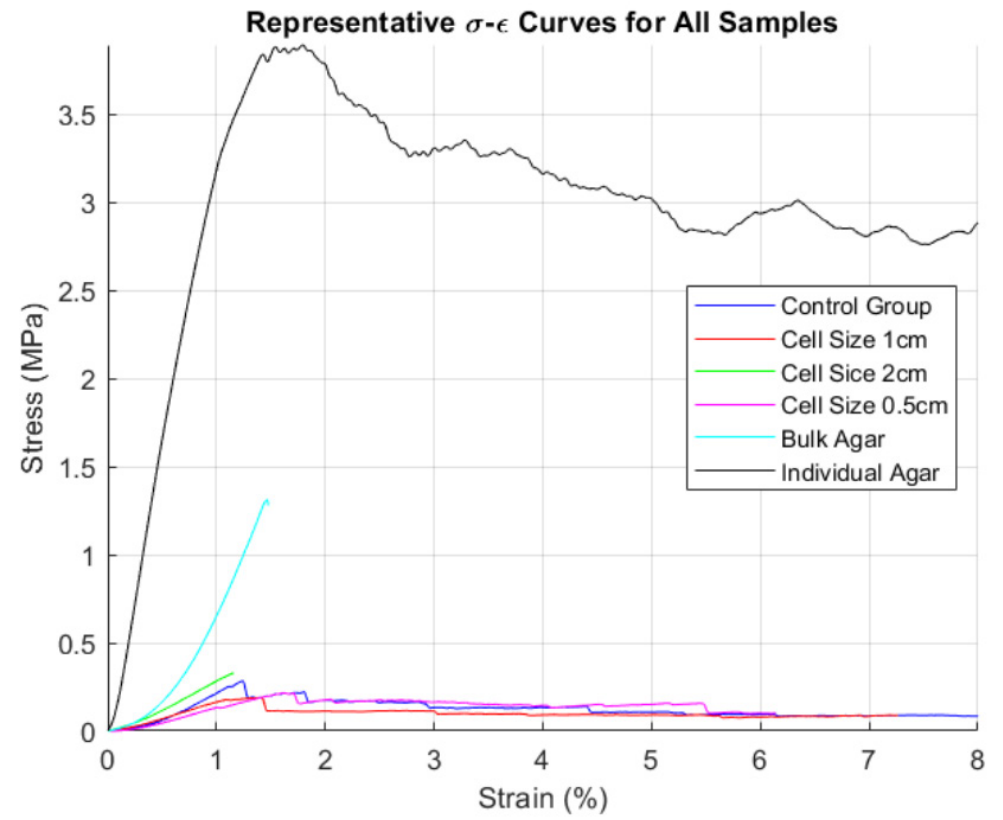
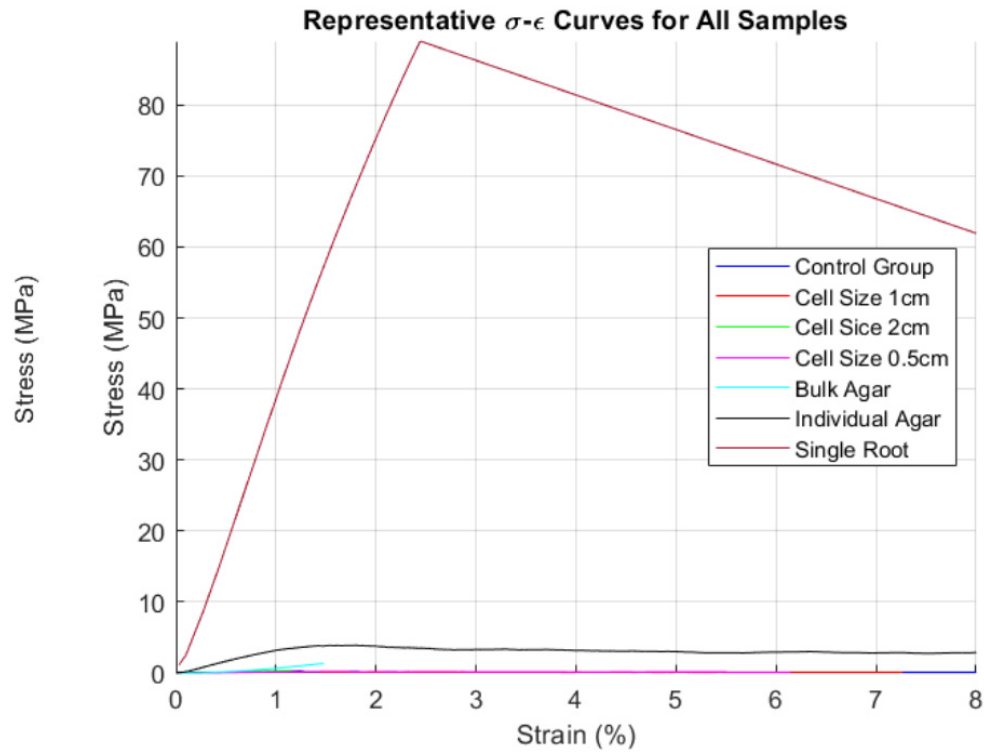
Modulus Values per Test Group			
Group	Average Modulus (MPa)	Standard Deviation	Variance (%)
Root	$4.610 \cdot 10^1$	$\pm 24.01$	52.07
Agar(Ind.)	$2.705 \cdot 10^0$	$\pm 0.571$	21.11
Agar (Bulk)	$1.3125 \cdot 10^0$	$\pm 0.554$	42.22
2 cm Cell	$3.235 \cdot 10^{(-1)}$	$\pm 0.051$	15.89
Control	$2.931 \cdot 10^{(-1)}$	$\pm 0.125$	42.68
0.5 cm Cell	$1.964 \cdot 10^{(-1)}$	$\pm 0.0859$	43.74
1 cm Cell	$1.822 \cdot 10^{(-1)}$	$\pm 0.046$	24.97

Table 3.5.2: Comparison of all Elastic Moduli Tested

Modulus Values per Test Group			
Group	Average Modulus (MPa)	Standard Deviation	Variance (%)
Root	$4.610 \cdot 10^1$	$\pm 24.01$	52.07
Agar(Ind.)	$2.705 \cdot 10^0$	$\pm 0.571$	21.11
Agar (Bulk)	$1.3125 \cdot 10^0$	$\pm 0.554$	42.22
2 cm Cell	$3.235 \cdot 10^{(-1)}$	$\pm 0.051$	15.89
Control	$2.931 \cdot 10^{(-1)}$	$\pm 0.125$	42.68
0.5 cm Cell	$1.964 \cdot 10^{(-1)}$	$\pm 0.0859$	43.74
1 cm Cell	$1.822 \cdot 10^{(-1)}$	$\pm 0.046$	24.97

Table 3.5.2: Comparison of UTS from test groups





# Appendix E: Project Brief

Characterizing Interwoven: Testing and Modeling Root-Based Textiles \_\_\_\_\_ project title

Please state the title of your graduation project (above) and the start date and end date (below). Keep the title compact and simple. Do not use abbreviations. The remainder of this document allows you to define and clarify your graduation project.

start date 22 - 02 - 2021 \_\_\_\_\_ 20 - 07 - 2021 \_\_\_\_\_ end date

## INTRODUCTION \*\*

Please describe, the context of your project, and address the main stakeholders (interests) within this context in a concise yet complete manner. Who are involved, what do they value and how do they currently operate within the given context? What are the main opportunities and limitations you are currently aware of (cultural- and social norms, resources (time, money,...), technology, ...).

Interwoven is a plant-root textile developed by Amsterdam-based artist, Diana Scherer. In collaboration with Elvin Karana of the Industrial Design Engineering faculty in TU Delft, its potential as an alternative material for product design has been explored. Previous Master Graduation projects conducted by Jiwei Zhou and Damienmarc Ford did this by following the Materials Driven Design Method (MDD) developed by Professor Karana. Despite these precedent projects, there is not yet enough characterization data to provide a holistic view of Interwoven materials' properties.

The MDD method maps out the properties that are afforded to a designer when using a specific material in a design. With this as a starting point, the designer becomes aware of all the properties associated with the material - both the properties experienced through direct interaction, and properties derived from empirical data. While the former influence a user's experience, the latter parameters affect the performance of the material. In the case of Interwoven, this includes parameters like the pattern and orientation of the plant roots, the morphology and shape of elements that make up the structure, the media in which the roots are grown, and the mechanical loading with respect to root orientation. This project will use the MDD method to establish a combination of empirical and experiential techniques to fully define what the Interwoven materials are capable of. This includes the use of the Materials Lab within Applied Labs to cultivate and test the root-based material with the available equipment - tensile strength machines and microscopes.

Interwoven materials are still novel, but most of the existing data on them is available through the Materializing Futures section of SDE. This means that, although there is still much to be defined, the work from previous years creates a solid foundation from which to start. For example, it is known from both works mentioned earlier that Interwoven textiles are brittle and need reinforcement as a bio-composite. Plant-specific parameters such as root density and a binding medium for the composite (such as using agar or pectin) impact the mechanical properties and still need further optimization. Similarly, it is known that the same fragility and perceived delicateness of the material invokes a positive response in users who liken the experience of interacting with Interwoven to a nostalgic and calming experience. Jiwei's work sets a stronger foundation of the technical characterization, as she developed a composite (refer to image 1 in the next page) that is co-created with the growth of the roots by including porous structures in the product. This adds structural strength to the material and establishes another possible parameter for improving the feasibility of using this material in a more quotidian fashion.

Despite the information available from previous projects, this data is still quite limited. When compared to materials that have been characterized by specific standards, Interwoven is atypical, which means that correlations must be extrapolated and deduced from similar systems such as natural fibers or textiles.

space available for images / figures on next page

introduction (continued): space for images



image / figure 1: Compression tests of Interwoven textile with embedded PLA structures



image / figure 2: Optical microscopy setup for analysing mechanical response

**PROBLEM DEFINITION \*\***

Limit and define the scope and solution space of your project to one that is manageable within one Master Graduation Project of 30 EC (= 20 full time weeks or 100 working days) and clearly indicate what issue(s) should be addressed in this project.

The aim of the project is to develop an overview of the relationship between the Interwoven materials' performance and the parameters under which the material was grown. The material performance is separated into the mechanical performance and the experiential performance, as defined below:

- (1) The mechanical performance and limitations - defined by traditional technical characterization techniques.
- (2) The experiential performance - how users respond to the material, based on interactions defined by the MDD method.

Interwoven is a plant-root textile whose properties are still not fully understood. In collaboration with the Materializing Futures section of the SDE department at TU Delft's IDE faculty, a series of bio-composites have been produced with these Interwoven materials. A continuation of previous works will complete the characterization of the material on both levels of performance defined above.

Throughout the project, the Material Driven Design (MDD) method will be used in combination with material characterization techniques to arrive at a series of design guidelines for those interested in using Interwoven materials in future designs. The main issues to address here are optimization of parameters related to growing/developing the Interwoven material, such as the angles of loads in relation to root orientation, the choice of matrix (resin) to bind the roots, etc. The final product of this design will be a set of design guidelines showcased with the design of a product that uses this material in a fitting context, thus fulfilling all four steps of the Material Driven Design method: (1) understanding the material, (2) envisioning a materials experience, (3) manifesting said vision, and (4) designing a materials product/concept.

**ASSIGNMENT \*\***

State in 2 or 3 sentences what you are going to research, design, create and / or generate, that will solve (part of) the issue(s) pointed out in "problem definition". Then illustrate this assignment by indicating what kind of solution you expect and / or aim to deliver, for instance: a product, a product-service combination, a strategy illustrated through product or product-service combination ideas, .... In case of a Specialisation and/or Annotation, make sure the assignment reflects this/these.

This assignment will study the mechanical and experiential characteristics of novel root-based composites, Interwoven. Since its properties are not yet fully understood and they differ according to certain parameters, a set of guidelines for working with Interwoven will be prepared and demonstrated with a product that puts said guidelines to use.

The expected result of the project is a product that demonstrates the capabilities and/or limitations of designing with Interwoven materials. The product will be presented alongside a comprehensive set of guidelines detailing the parameters that yield certain mechanical or experiential properties from the root-based natural composite.

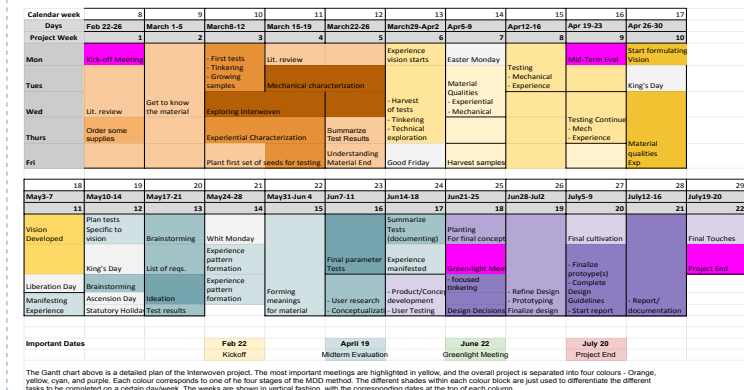
The guidelines will be based on the characterization of the mechanical and experiential properties of Interwoven. Technical characterization will explain the constitutive response of these materials by linking the structural parameters mentioned in previous sections to mechanical test results. A complete structural characterization will be achieved by combining microscopy and fracture analysis with mechanical tests performed in intervals (and analysed with the microscope) to monitor instantaneous changes in the material's behavior. Identifying the parameters tied to brittleness, failure, and fracture will provide a road map to addressing them or finding alternatives that improve the mechanical response of Interwoven materials.

Experiential characterization, on the other hand, will identify the characteristics that users associate with the material, such as "weakness" or "fragility", as well as how these perceptions change when certain parameters are altered. The correlations between the quantified characteristics from above and the perceived characteristics are combined to shape unique user experiences that could only be elicited by such a novel material.

**PLANNING AND APPROACH \*\***

Include a Gantt Chart (replace the example below - more examples can be found in Manual 2) that shows the different phases of your project, deliverables you have in mind, meetings, and how you plan to spend your time. Please note that all activities should fit within the given net time of 30 EC = 20 full time weeks or 100 working days, and your planning should include a kick-off meeting, mid-term meeting, green light meeting and graduation ceremony. Illustrate your Gantt Chart by, for instance, explaining your approach, and please indicate periods of part-time activities and/or periods of not spending time on your graduation project, if any, for instance because of holidays or parallel activities.

start date 22 - 2 - 2021 end date 20 - 7 - 2021



The Gantt chart above is a detailed plan of the Interwoven project. The dates of important meetings are highlighted in pink and listed at the bottom. The overall project is separated into four colours - Orange, yellow, cyan, and purple. Each colour corresponds to one of the four stages of the MDD method. The different shades within each colour block are just used to differentiate the different tasks to be completed on a certain day/week. The weeks are shown in vertical fashion, with the corresponding dates at the top of each column. Starting in week 3, there is a repeating set of "tests" every two weeks, denoted by the Nth round of testing. This is assuming that it takes two weeks for the roots to grow to a state where they can be tinkered with, but the number of tests is subject to change in practice.

While the main structure of the planning mirrors the MDD method, there are still sections that have milestones more typical of a design project, such as ideation, user research, product/concept development, etc. The seven white cells denote public holidays in which no work will be done on the project. This seemingly extends the 20 week period, but the number of work days is still limited to 100.

### MOTIVATION AND PERSONAL AMBITIONS

Explain why you set up this project, what competences you want to prove and learn. For example: acquired competences from your MSc programme, the elective semester, extra-curricular activities (etc.) and point out the competences you have yet developed. Optionally, describe which personal learning ambitions you explicitly want to address in this project, on top of the learning objectives of the Graduation Project, such as: in depth knowledge a on specific subject, broadening your competences or experimenting with a specific tool and/or methodology, ... . Stick to no more than five ambitions.

This project will serve as a culmination of my education up until this point. Before coming to TU Delft, I completed an MSc in Materials Engineering, and the main reason I studied at IDE was to gain the understanding needed to make desirable products from the materials that I learned to make in my previous master. Learning the MDD method and working through it with the skills that I have learned throughout my time as an IPD student will serve as a stepping stone for my future endeavors. In my time here, I have learned to develop products with an end-user in mind, but now I wish to more explicitly apply my knowledge of materials science to product design. This is exactly where the MDD method comes into play, as it is a direct bridge between my previous and current studies. Thus, the main personal goal that I want to address with this project is to become more familiar with this method as well as better creating that bridge between studies so that I have somewhere to start when I eventually pursue a PhD.

With that being said, it is not the only goal to come out of this project. Below is a list of some of the personal objectives that I hope to clear with this project.

1. Gain hands-on experience and knowledge with the MDD method.
2. Extending my knowledge of mechanical testing and characterization to include natural materials and using said knowledge to clearly define the constitutive behavior of a novel material such as Interwoven.
3. Learning to work with a natural material that is grown along with the decision-making process.
4. Develop my prototyping and modeling skills.
5. Improving my ability to document and communicate a research-based project with other stakeholders, thus enhancing both my technical and interpersonal skill set.

### FINAL COMMENTS

In case your project brief needs final comments, please add any information you think is relevant.